

Timelike Compton Scattering with RG-K Sp24 8.477 GeV Dataset towards CLAS Approved Analysis

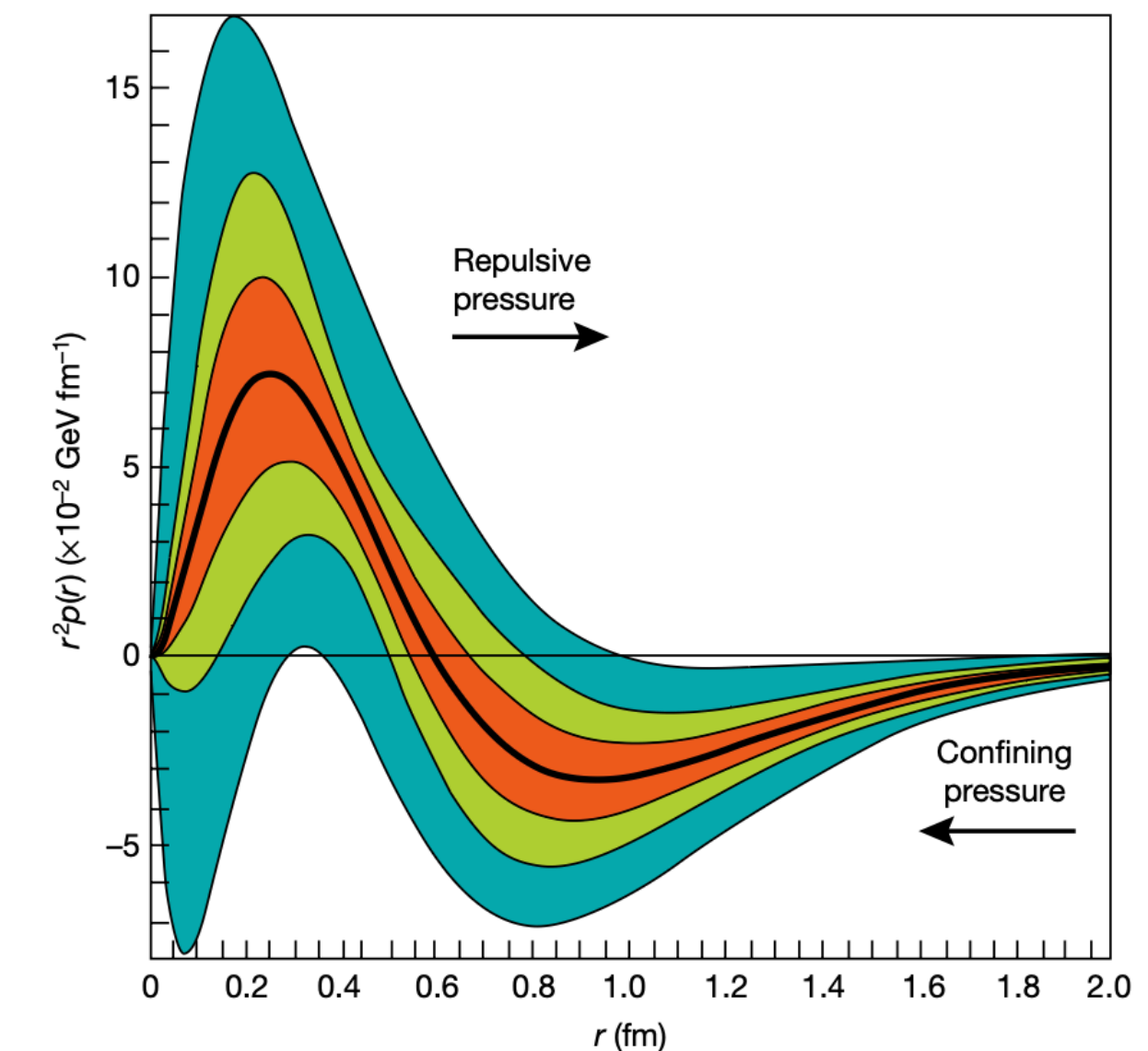
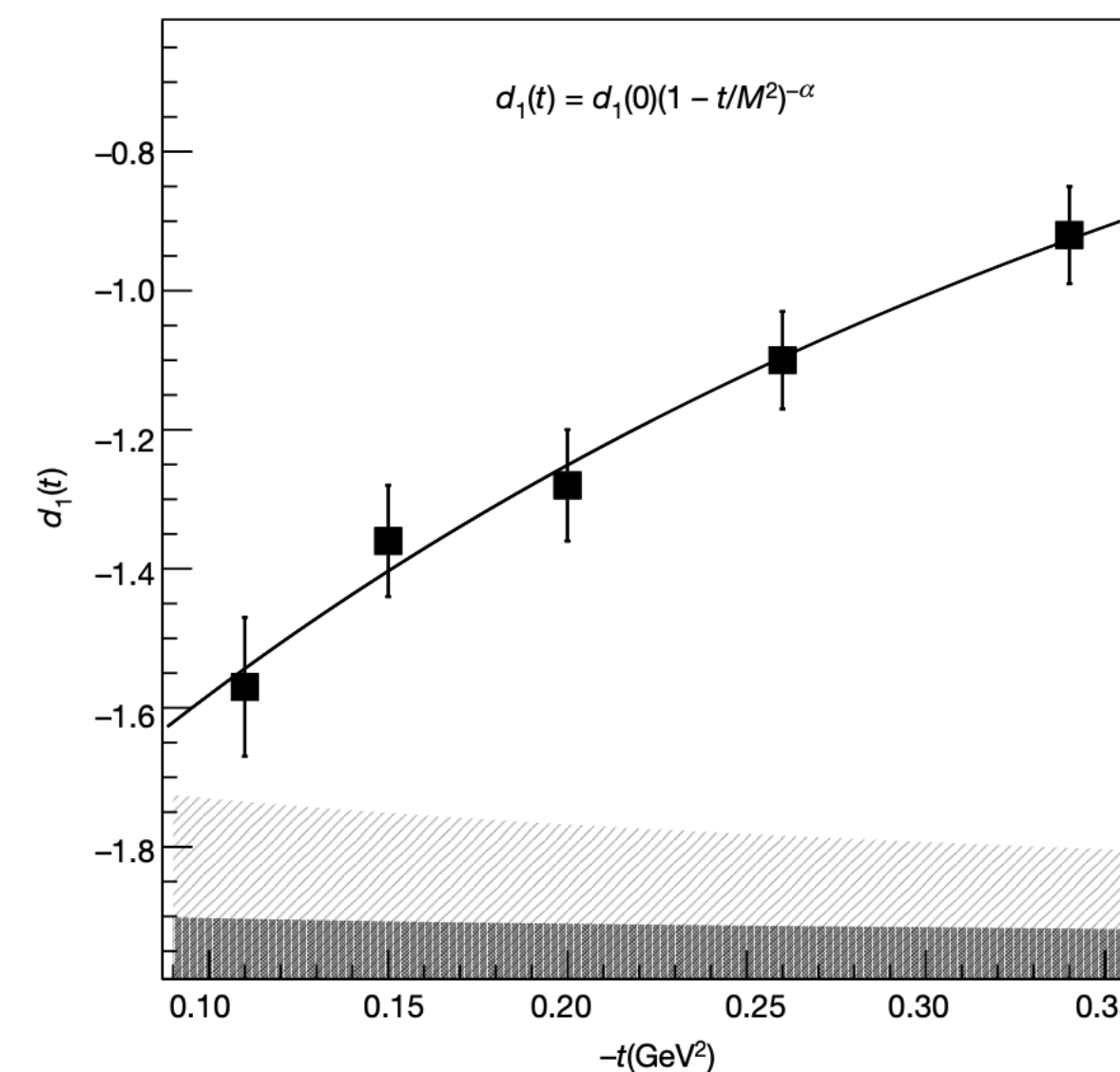
M. Kerr, L. Elouadrhiri, V. Burkert

June 30, 2026 | CLAS Collaboration Meeting

Mechanical Properties of the Proton

- Generalized parton distributions (GPDs) contain three-dimensional information on nucleon structure
 - Chiral even GPDs**, $H, E, \tilde{H}, \tilde{E} \rightarrow$ DVCS (“golden channel”), **TCS**
 - $H \rightarrow$ best probed with unpolarized target (RG-A/B/K @ CLAS12)
 - $\tilde{H} \rightarrow$ best probed with longitudinally polarized target (RG-C @ CLAS12)
 - $E \rightarrow$ best probed with transversely polarized target (RG-H @ CLAS12)
 - Chiral odd GPDs**, $H_T, E_T, \tilde{H}_T, \tilde{E}_T \rightarrow$ DVMP
- Using GPDs H and E , we can probe gravitational form factors (GFFs), which encode nucleon mechanical properties
 - “D-term” \rightarrow pressure and shear forces of quarks in nucleon arising from EMT, via GPD H

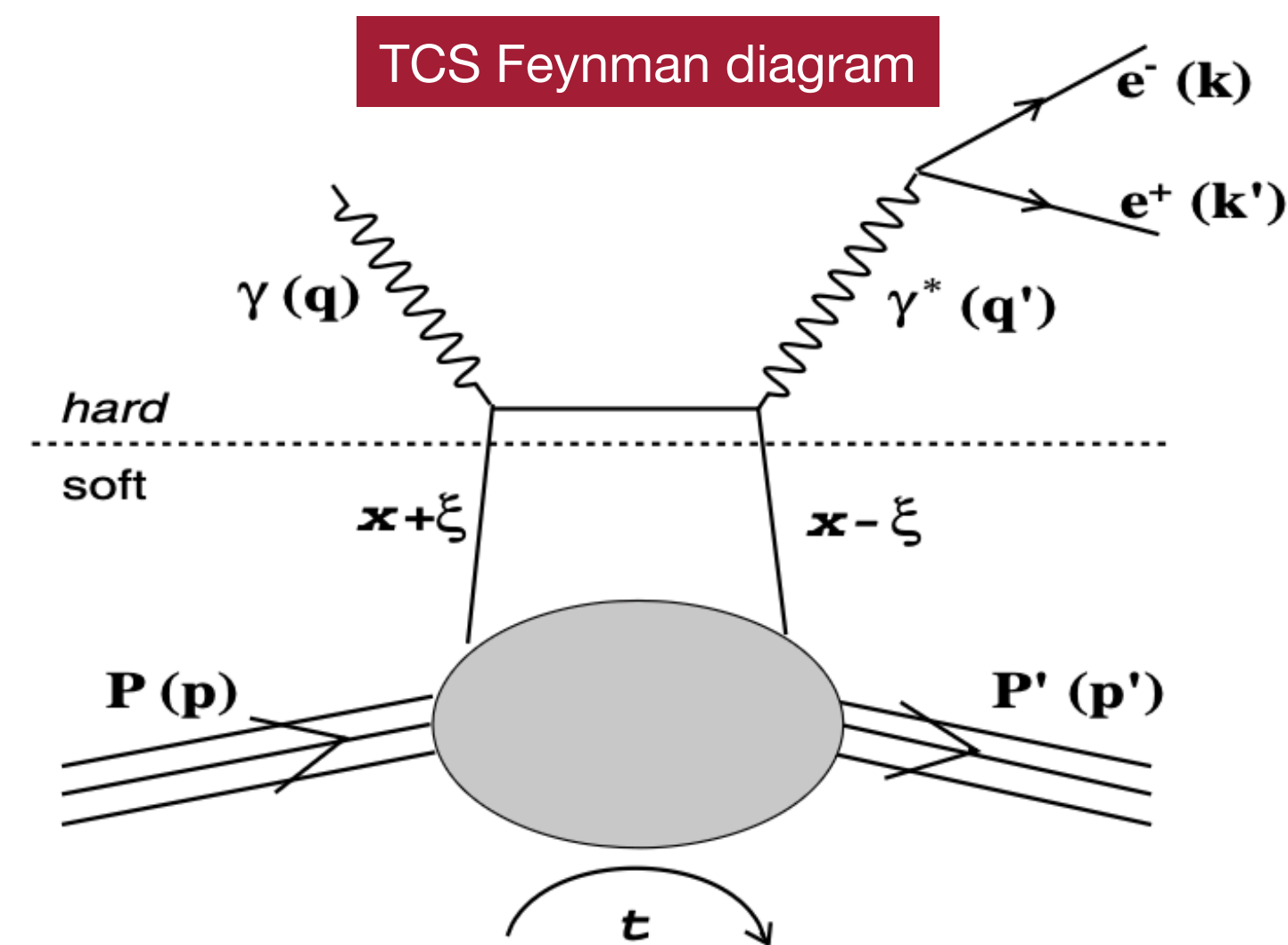
		Quark Polarization		
		Unpolarized (U)	Longitudinally Polarized (L)	Transversely Polarized (T)
Nucleon Polarization	U	H		$2\tilde{H}_T + E_T$
	L		\tilde{H}	\tilde{E}_T
	T	E	\tilde{E}	H_T, \tilde{H}_T



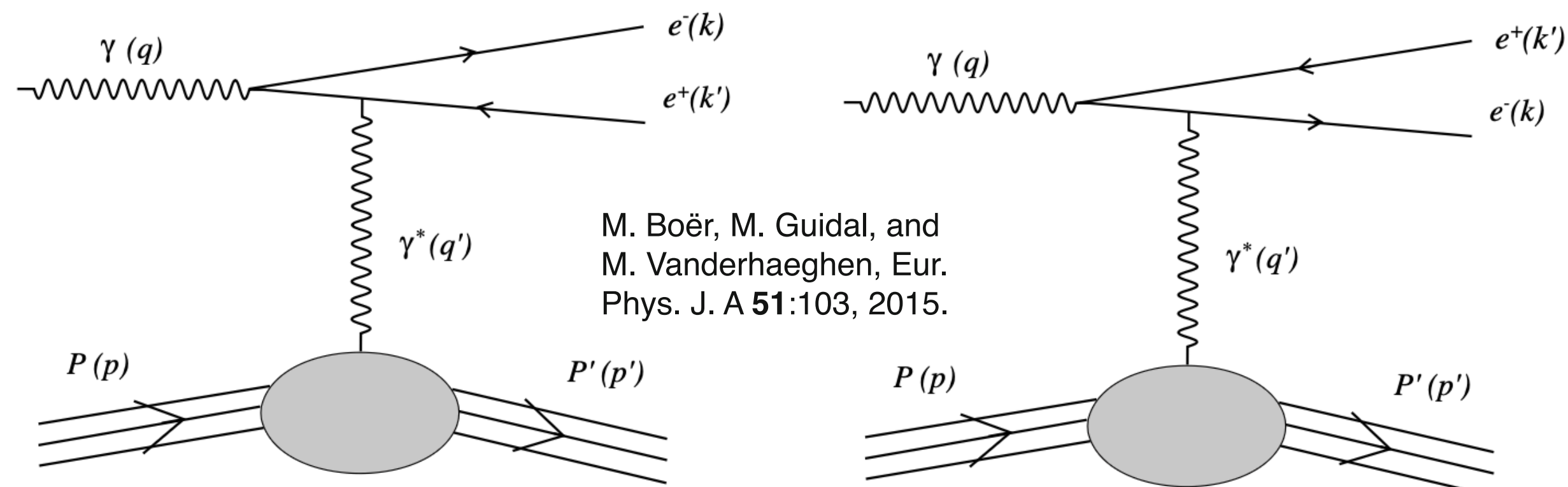
TCS Background

- TCS channel is time-reversed DVCS
 - ▶ Contributions to total $\gamma p \rightarrow e^- e^+ p$ cross section from TCS, BH, interference terms
 - ▶ Lower statistics than DVCS \rightarrow more EM couplings
 - ▶ Interference term provides access to GPDs (by way of CFFs) through:
 1. **Photon polarization asymmetry**, $A_{\odot U}$ (analogous to DVCS BSA) \rightarrow imaginary component of CFF \mathcal{H}
 2. **Forward-backward asymmetry**, A_{FB} \rightarrow real component of CFF \mathcal{H}
- Studying with new high statistics RG-K Sp24 data \rightarrow extraction of higher level physics: CFF components, D-term, and gravitational properties

$$\sigma(\gamma p \rightarrow e^- e^+ p) = \sigma_{TCS} + \sigma_{BH} + \sigma_{INT}$$



BH Feynman diagrams



Previous CLAS/CLAS12 TCS analyses:

- R. Parnuzyan. *Timelike Compton Scattering*. PhD thesis, Yerevan Physics Institute, 2010.
- P. Chatagnon. *Nucleon Structure studies with CLAS12 at Jefferson Lab: Timelike Compton Scattering and the Central Neutron Detector*. PhD thesis, Université Paris-Saclay, 2020. + **P. Chatagnon et al. (CLAS Collaboration), Phys. Rev. Lett. 127, 262501, 2021.**
- K. Gates. *Timelike Compton Scattering from a longitudinally polarised target with CLAS12 at Jefferson Lab*. PhD thesis, University of Glasgow, 2024.

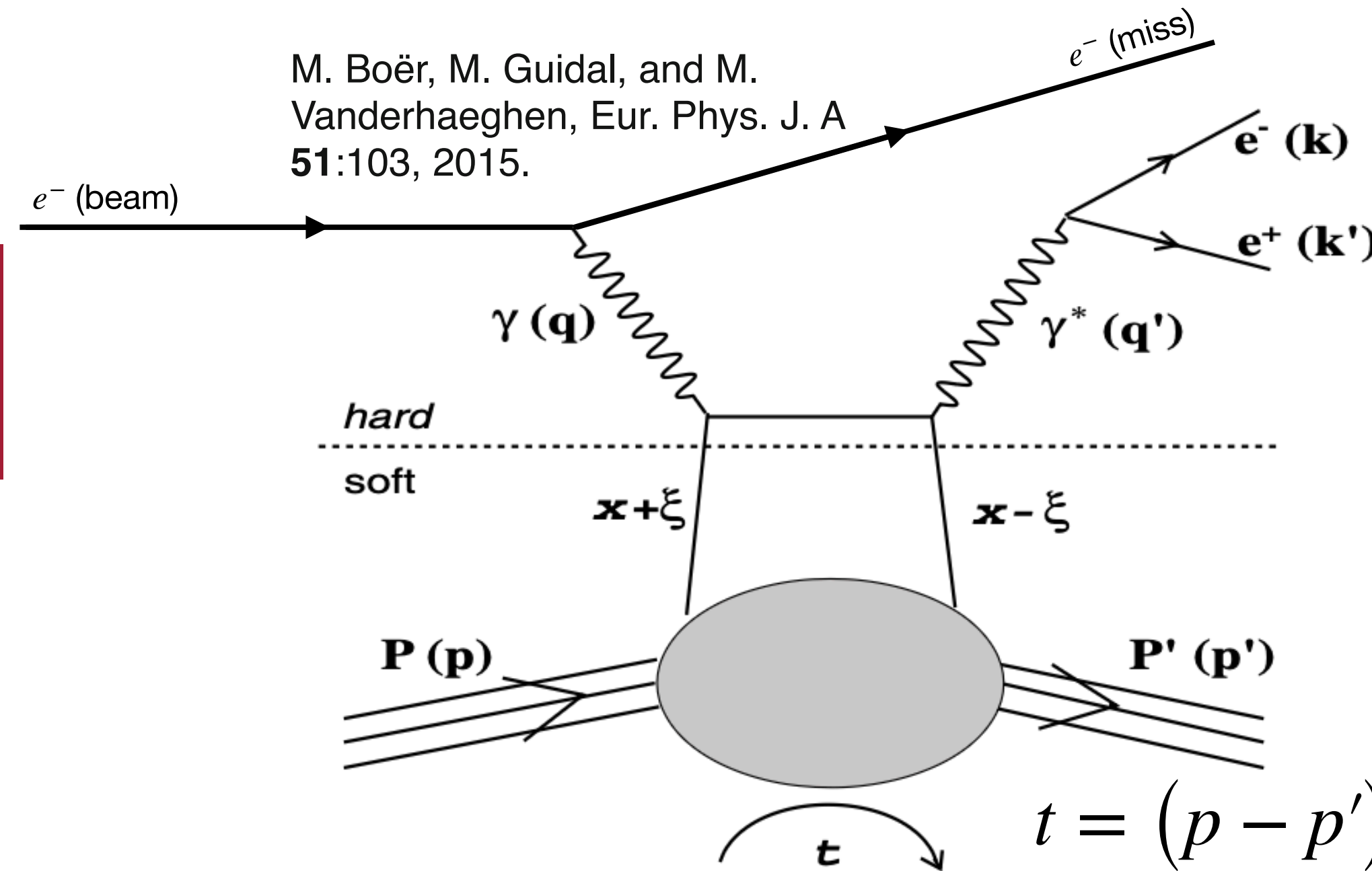
Kinematic Definitions for TCS

TCS process at CLAS12:

1. (Quasi)real photon (q) is emitted from the electron beam ($beam$) and interacts with the target proton (p)
2. Timelike virtual photon (q') emitted, which decays into a dilepton pair (k, k')
3. The electron and positron from this dilepton pair are detected, as well as the scattered proton (p')
4. Following the emission of q , the beam line electron continues to travel down the beam line and is not detected in the final state ($miss$)

$$Q^2 = 2E_b E_X (1 - \cos \theta_X)$$

Unlike most deep processes, the initial emitted photon, $q = beam - miss$, is (quasi)real, so $Q^2 \approx 0 \text{ GeV}^2$



$$Q'^2 = (k + k')^2, M_{e^-e^+} = \sqrt{Q'^2}$$

The mass squared of the dilepton pair constitutes Q'^2 , which must be sufficiently virtual $\rightarrow Q'^2 > 1 \text{ GeV}^2$

Mandelstam variable t

$$s = (p + q)^2$$

Mandelstam variable s (COM energy)



$$\tau = Q'^2 / (s - m_p^2)$$

Analogous to DVCS x_B



$$\xi \approx \tau / (2 - \tau)$$

Analogous to DVCS ξ

RG-K Status Update

- Focus is on RG-K Sp24 data, which has significantly higher statistics than RG-K Fa18 and therefore is more suited to analysis of lower statistics channels such as TCS
- Sp24 data (“pass 3” and “pass 4”) started cooking at the start of April, and is effectively completed
 - Passes 1 and 2 from RG-K Fa18 are at 7.546 GeV and 6.535 GeV, respectively
 - Pass 3 → 6.395 GeV
 - Pass 4 → 8.477 GeV (**highest statistics RG-K run period**)
- Preliminary analysis shown here is using RG-K Sp24 8.477 GeV
 - Closely following methodology used in RG-A analysis where appropriate
- No QADB yet for RG-K Sp24; no quality cuts/corrections yet for preliminary look.

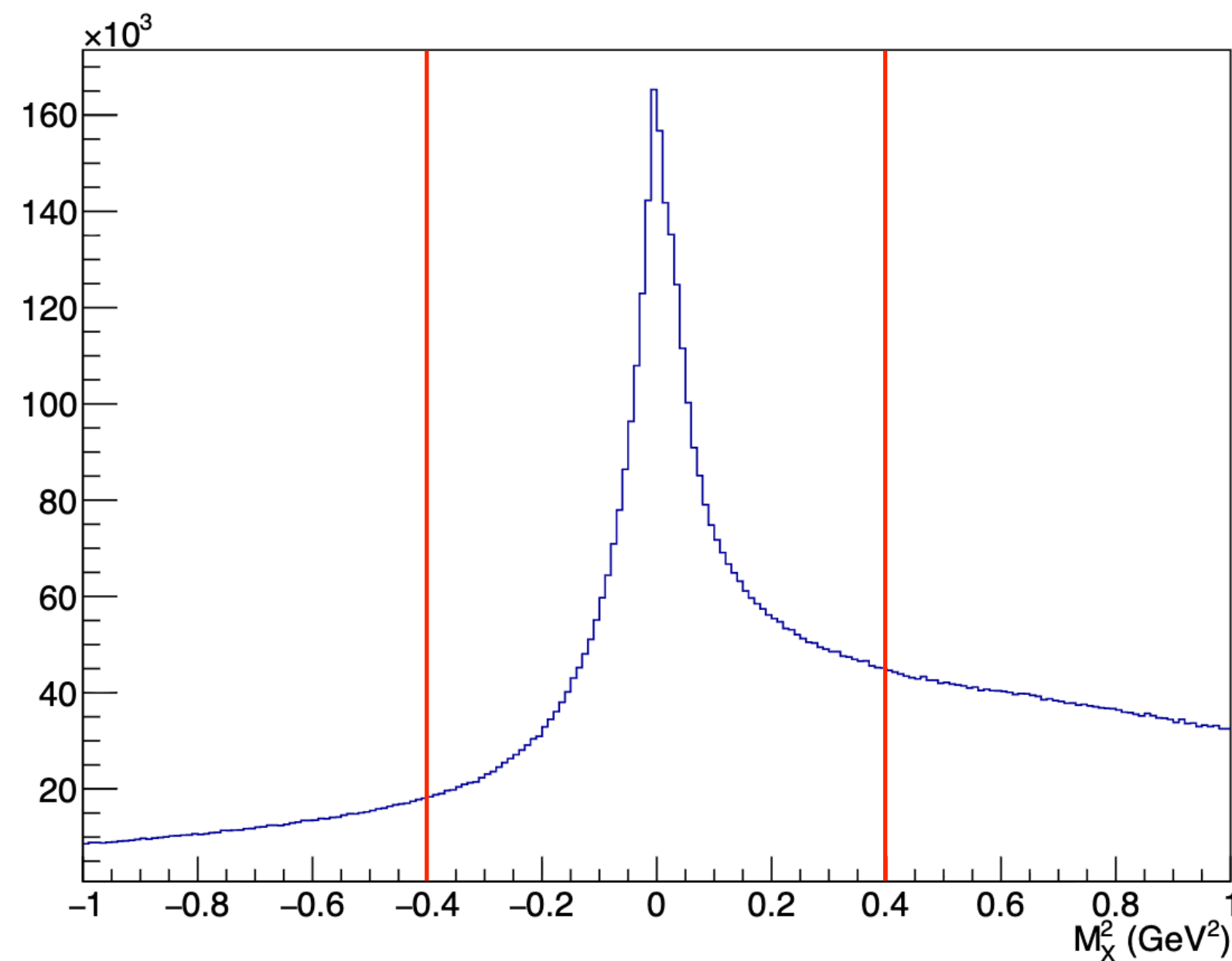
2	pass1_8477_1	rgk-ra-pass1_all_8477_1	19668,19669,19670,19671,19676,19677,19678	rgk-ra-pass1_8477_1-19668x7	251620	Running 99%
59	pass1_6395_37	rgk-ra-pass1_6395_37	19316-19319,19321-19323,19541,19543-19550,19604-19608	rgk-ra-pass1_6395_37-19316x21	252011	Running 70%

Very few remaining RG-K Sp24 runs remaining to be cooked as of 2026/06/22

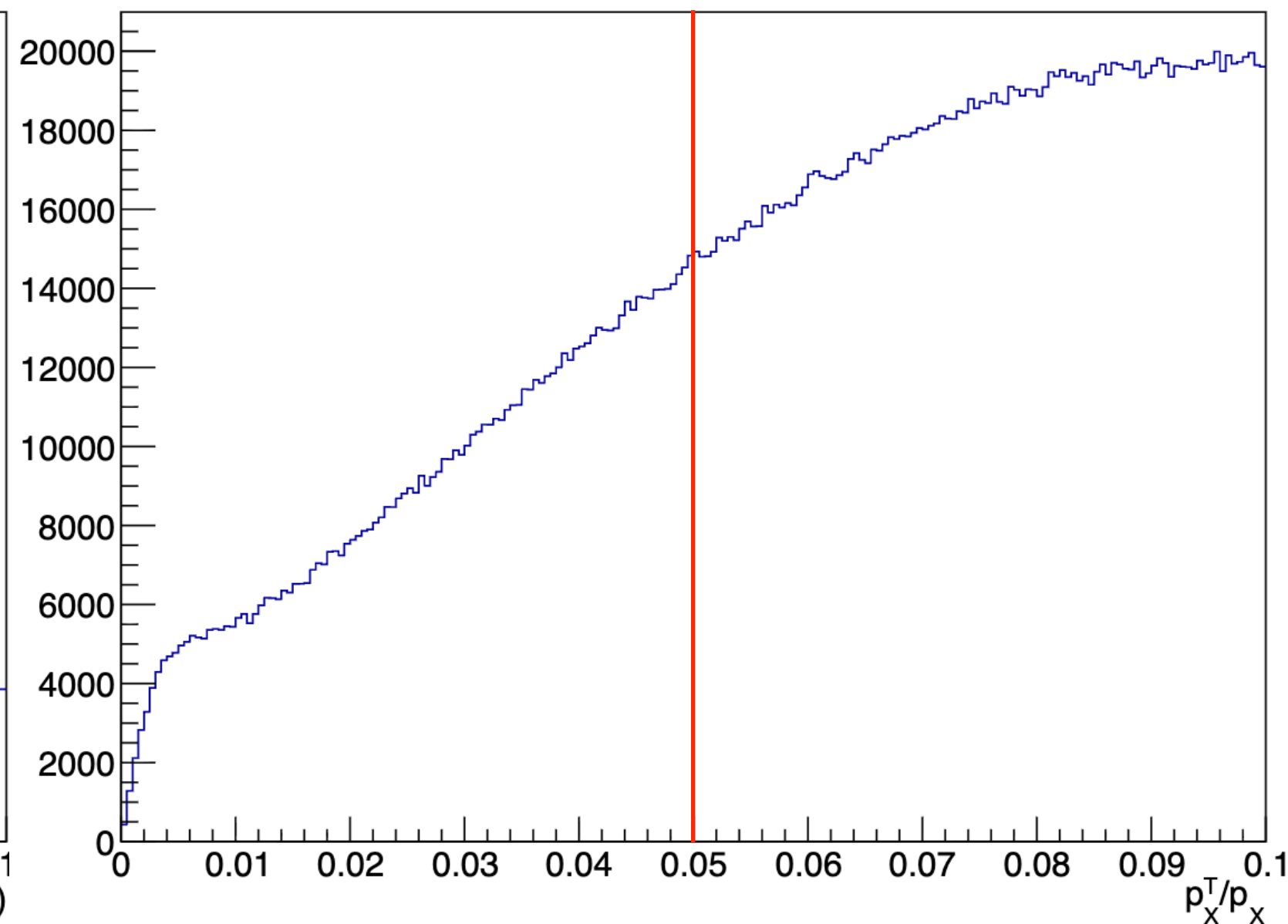
https://clasweb.jlab.org/wiki/index.php/Run_Group_K#tab=RGK_DATA_Processing_FALL_2023_2F_SPRING_2024

Selection of Events and Exclusivity Cuts

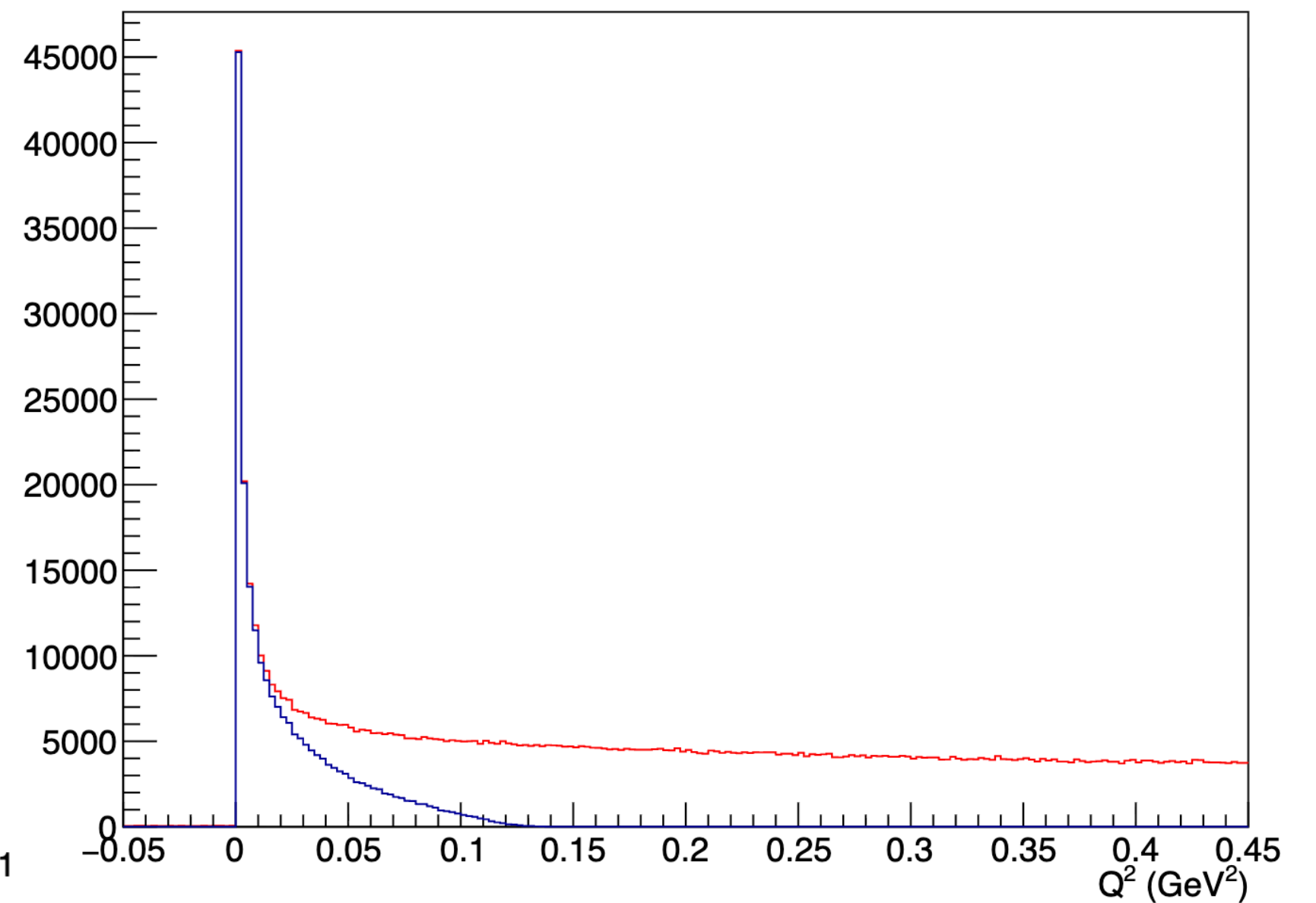
- TCS final state events filtered from RG-K TCS skim with e^-e^+pX (using built-in EventBuilder PID for all three particles)
- Applying same exclusivity cuts as in RG-A analysis for initial first look
 1. $|M_X^2| < 0.4 \text{ GeV}^2$, to remove any events with excess missing mass beyond undetected beam electron
 2. $p_{T,X}/p_X < 0.05$, to remove any events with excess missing momentum *not* going down the beamline
- Following these cuts, Q^2 distribution should resemble a sharp peak at $\approx 0 \text{ GeV}^2$



Missing mass distribution for RG-K Sp24 8.477 GeV data

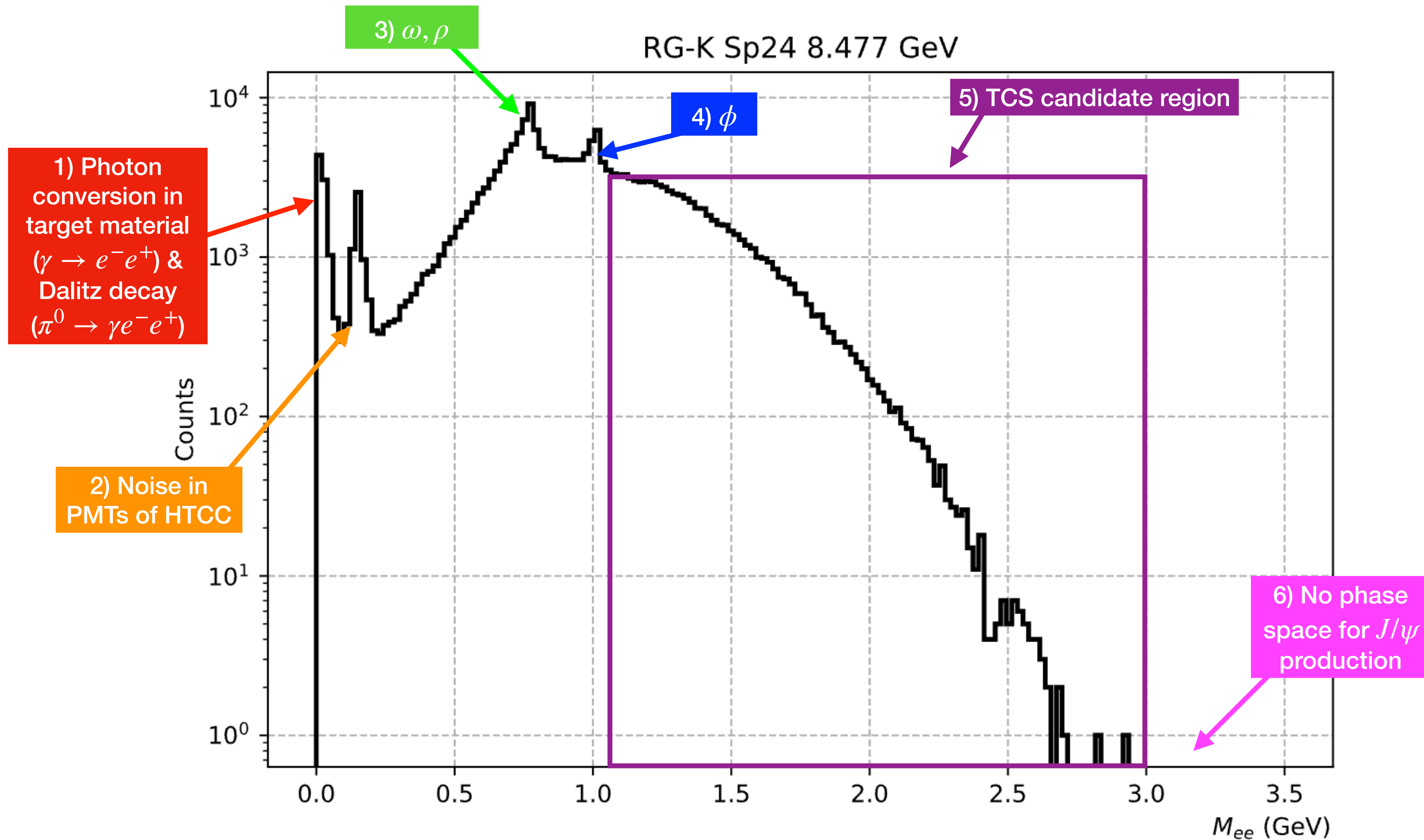


Missing transverse momentum to missing momentum ratio distribution for RG-K Sp24 8.477 GeV data

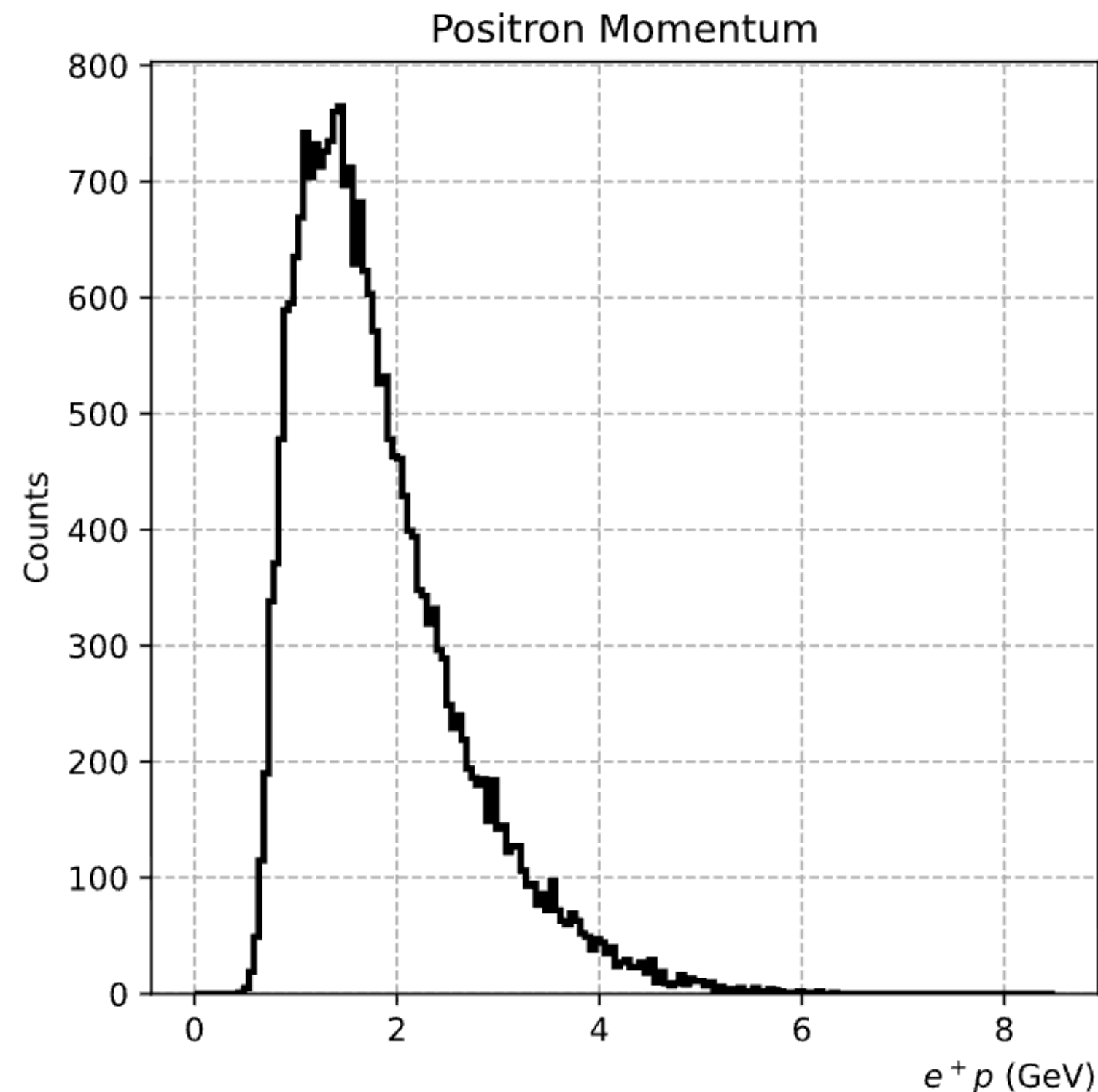
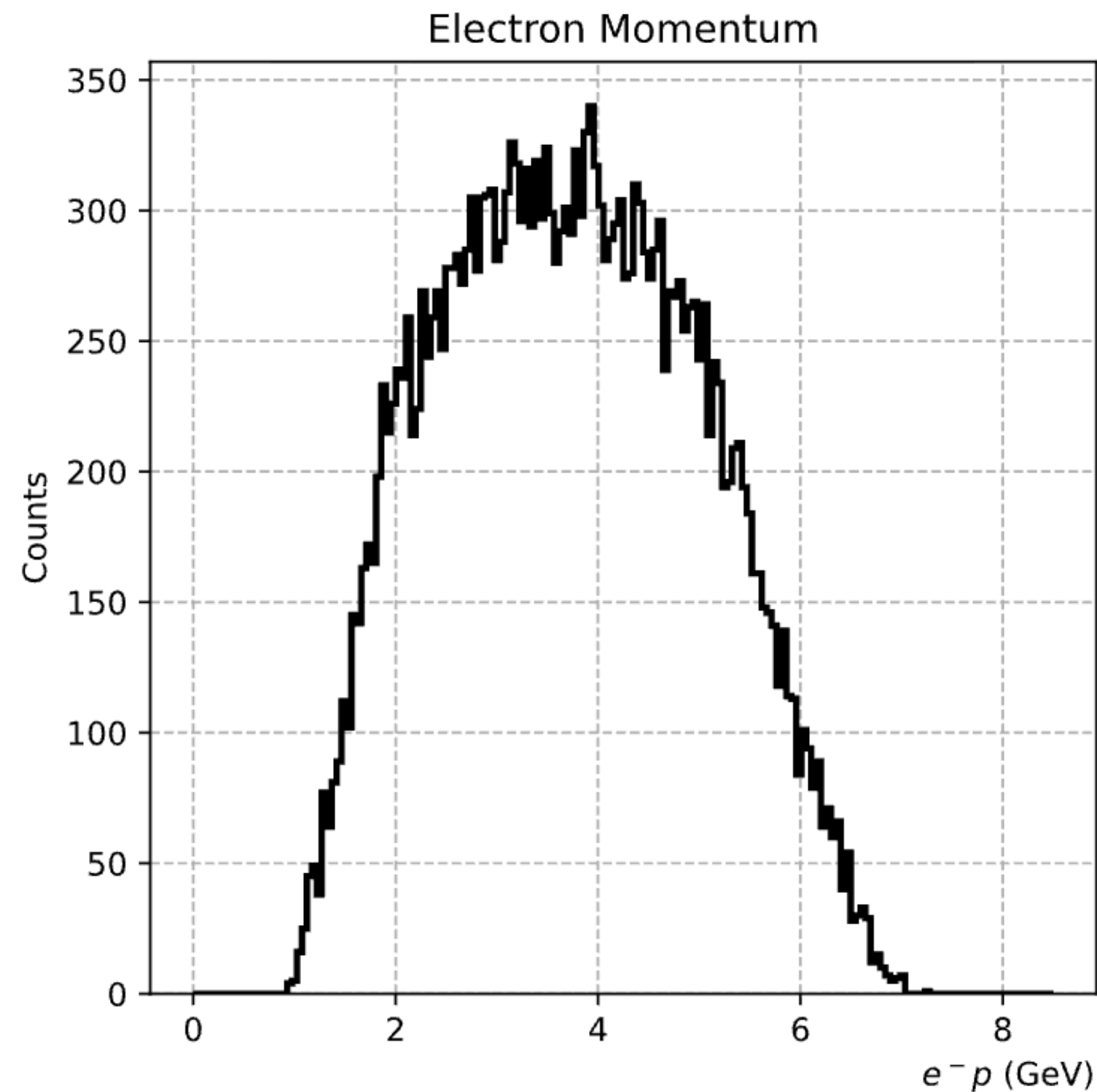


Q^2 (from quasi-real photon) distribution for RG-K Sp24 8.477 GeV data after only M_X^2 cut, and both exclusivity cuts

M_{ee} Distribution



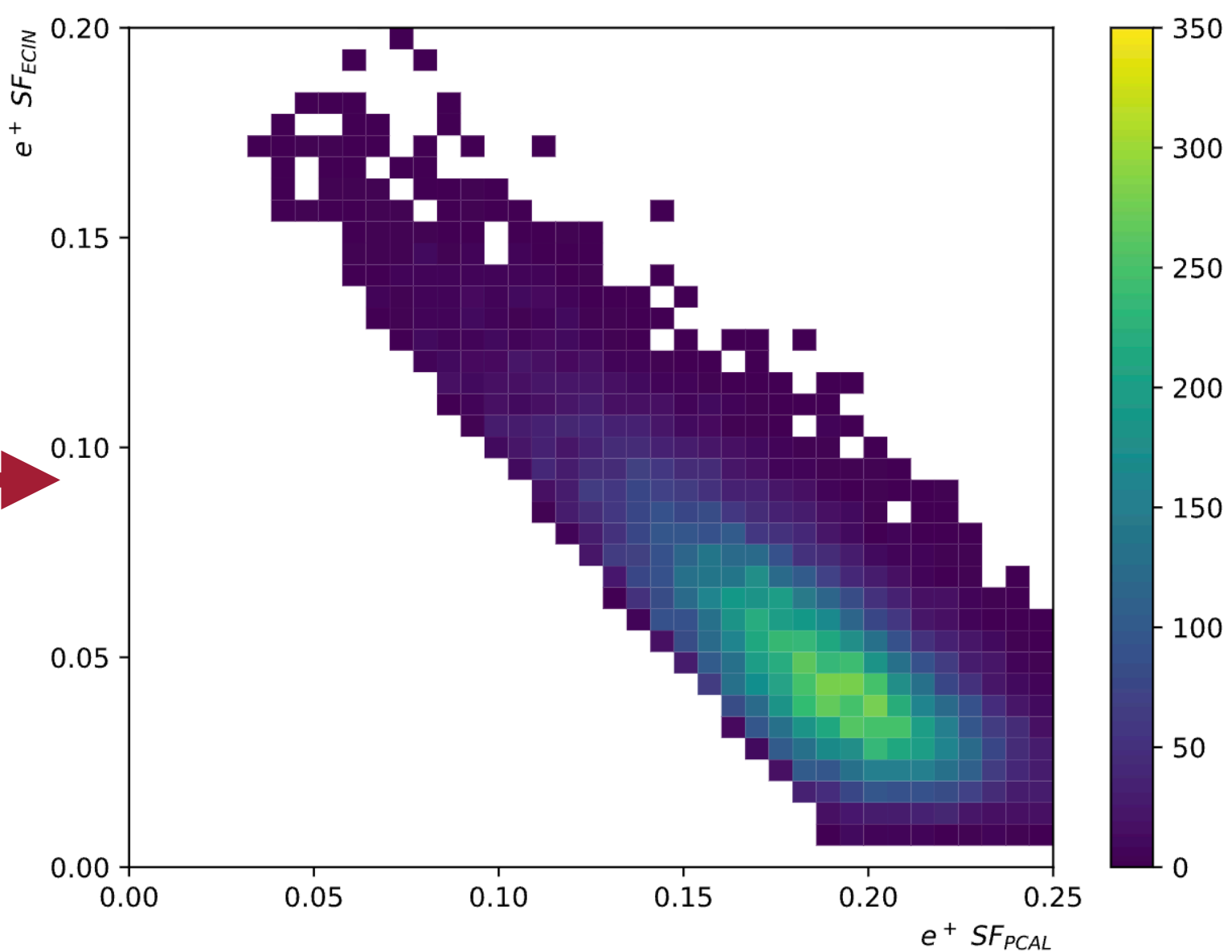
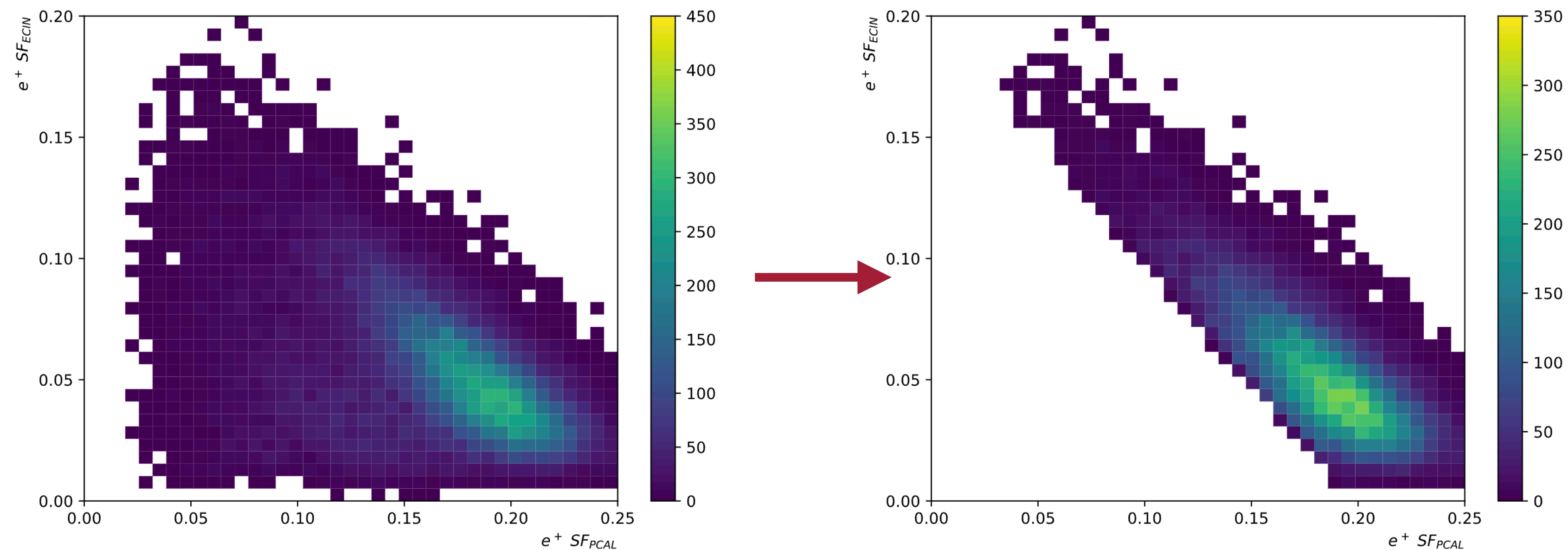
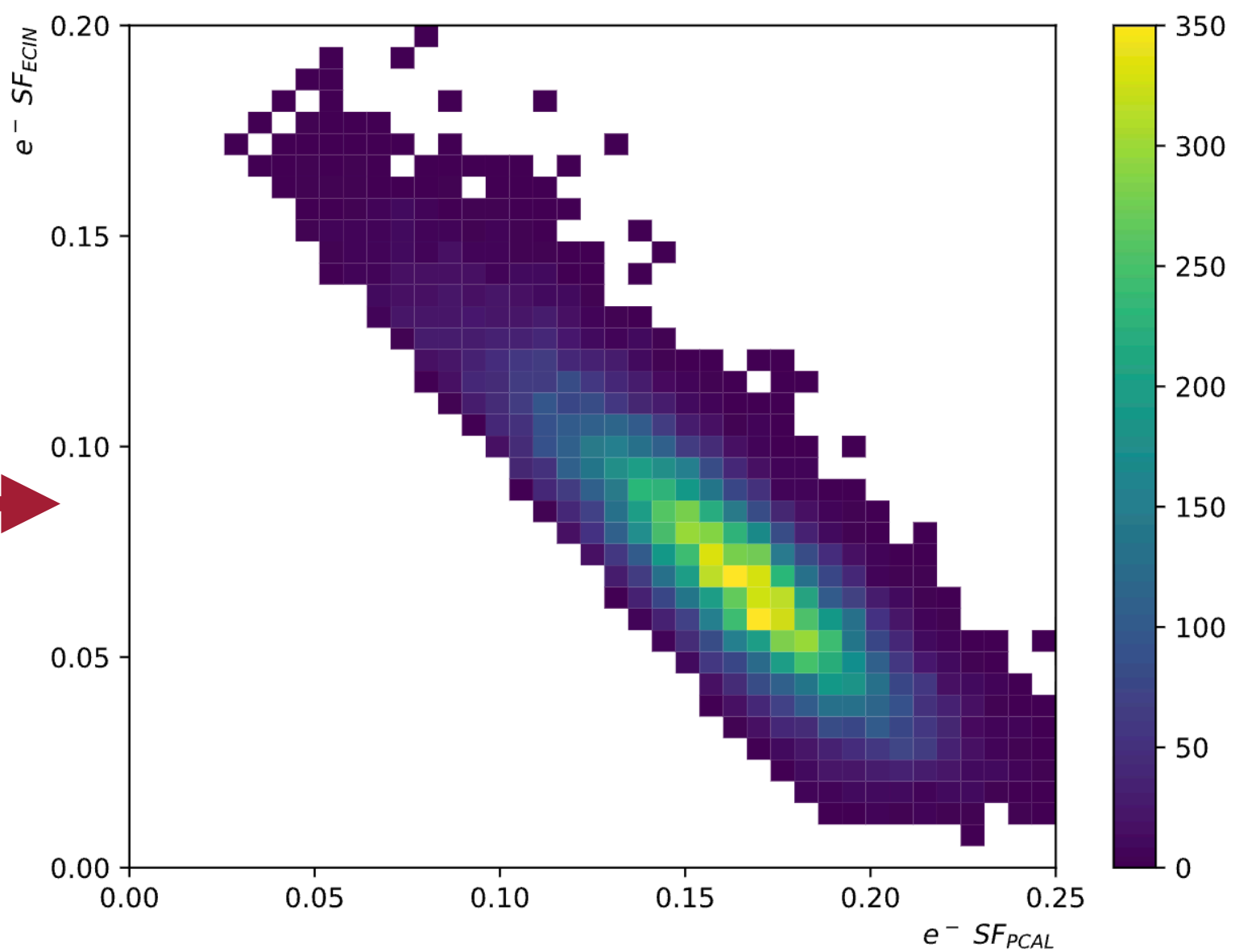
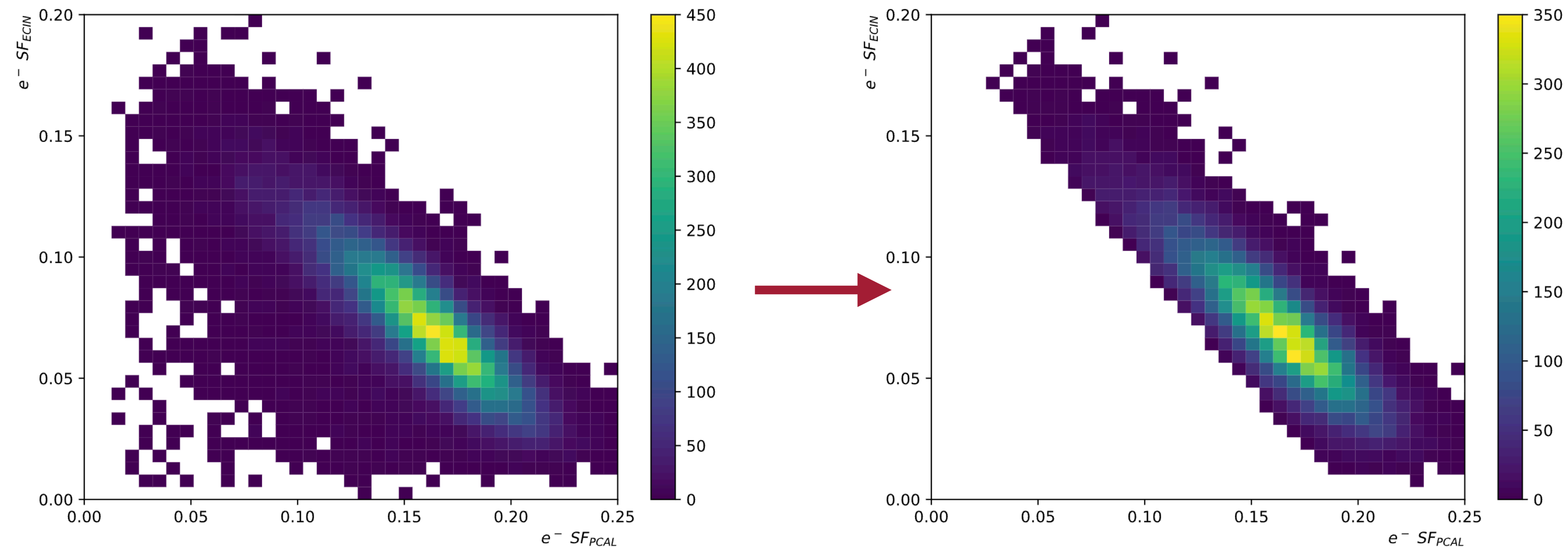
Additional Lepton PID



Electron and positron cuts following complete set of exclusivity, PID, and kinematic cuts \rightarrow extremely few positrons with momentum above the HTCC threshold, no bump in electron counts above HTCC threshold

- Previous CLAS12 TCS analyzers observed charged pion contamination in lepton samples beyond HTCC efficiency threshold of ~ 4.9 GeV
- In RG-K Sp24 8.477 GeV dataset, both electron and positron distributions have events above HTCC efficiency threshold of 4.9 GeV \rightarrow potential misidentification of charged pions as leptons
- Applied cuts based on partial sampling fractions as a first pass at additional PID \rightarrow cleans up with additional PID cuts on partial sampling fractions and kinematic cuts without full MVA approach

Additional Lepton PID

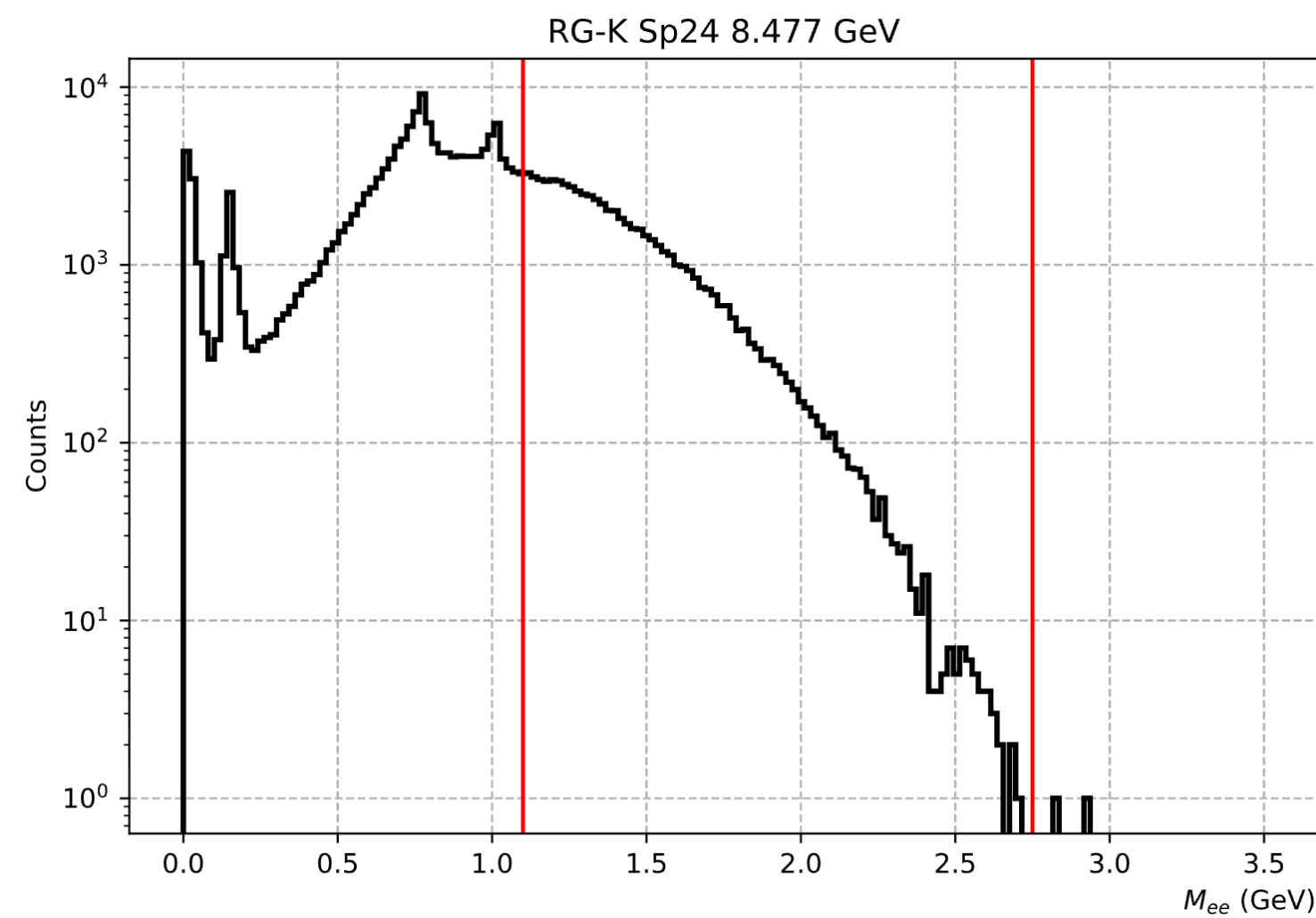


$$SF_{ECIN} = -SF_{PCAL} + 0.2,$$
$$SF_{layer} = E_{layer}/p$$

- Pions more likely to deposit energy throughout ECAL layers, while electrons/positrons more likely to deposit most of their energy in PCAL
- Diagonal cut on partial SF from PCAL vs partial SF from ECIN, discarding events below line as pion contamination

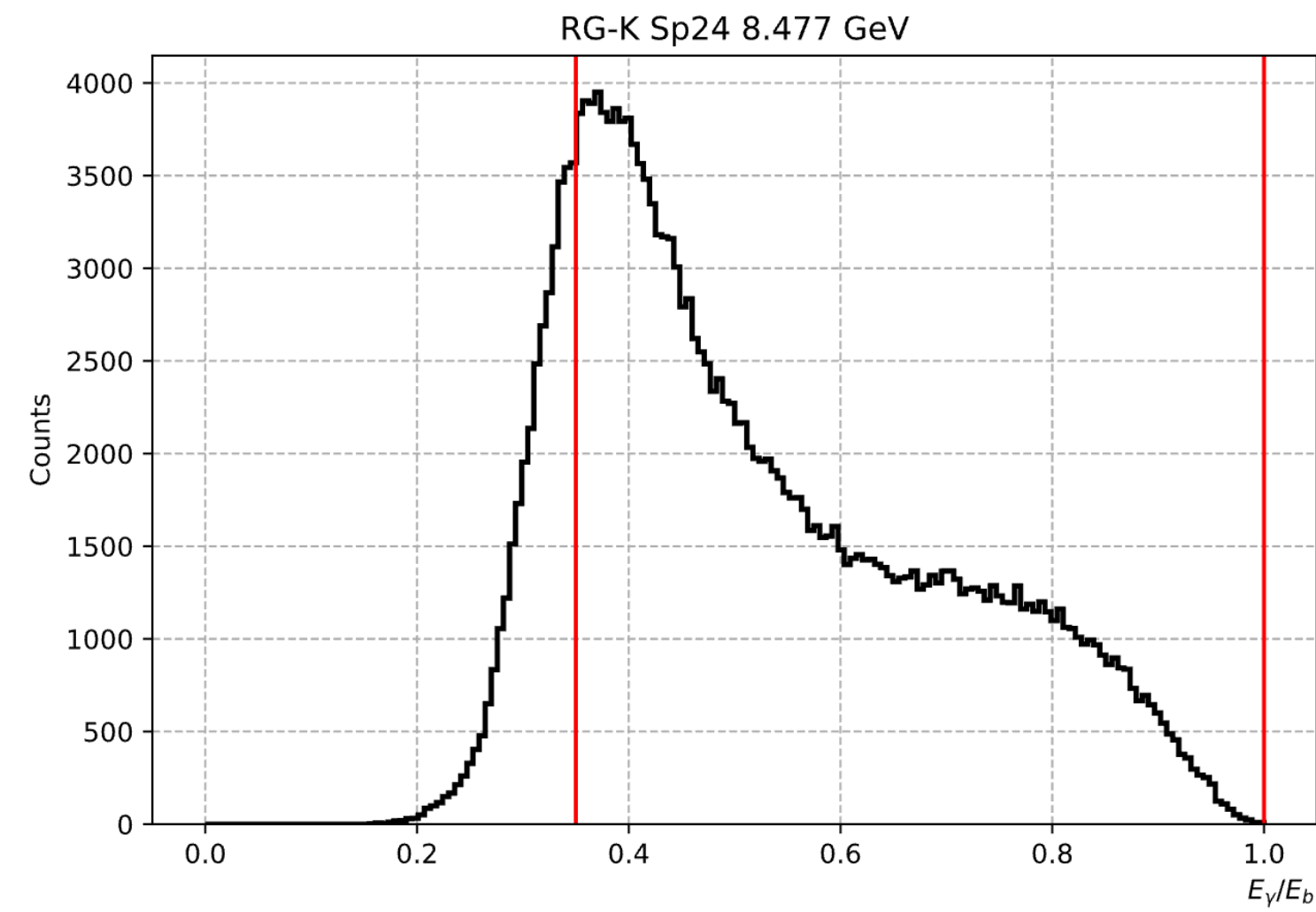
Kinematic Cuts

M_{ee}



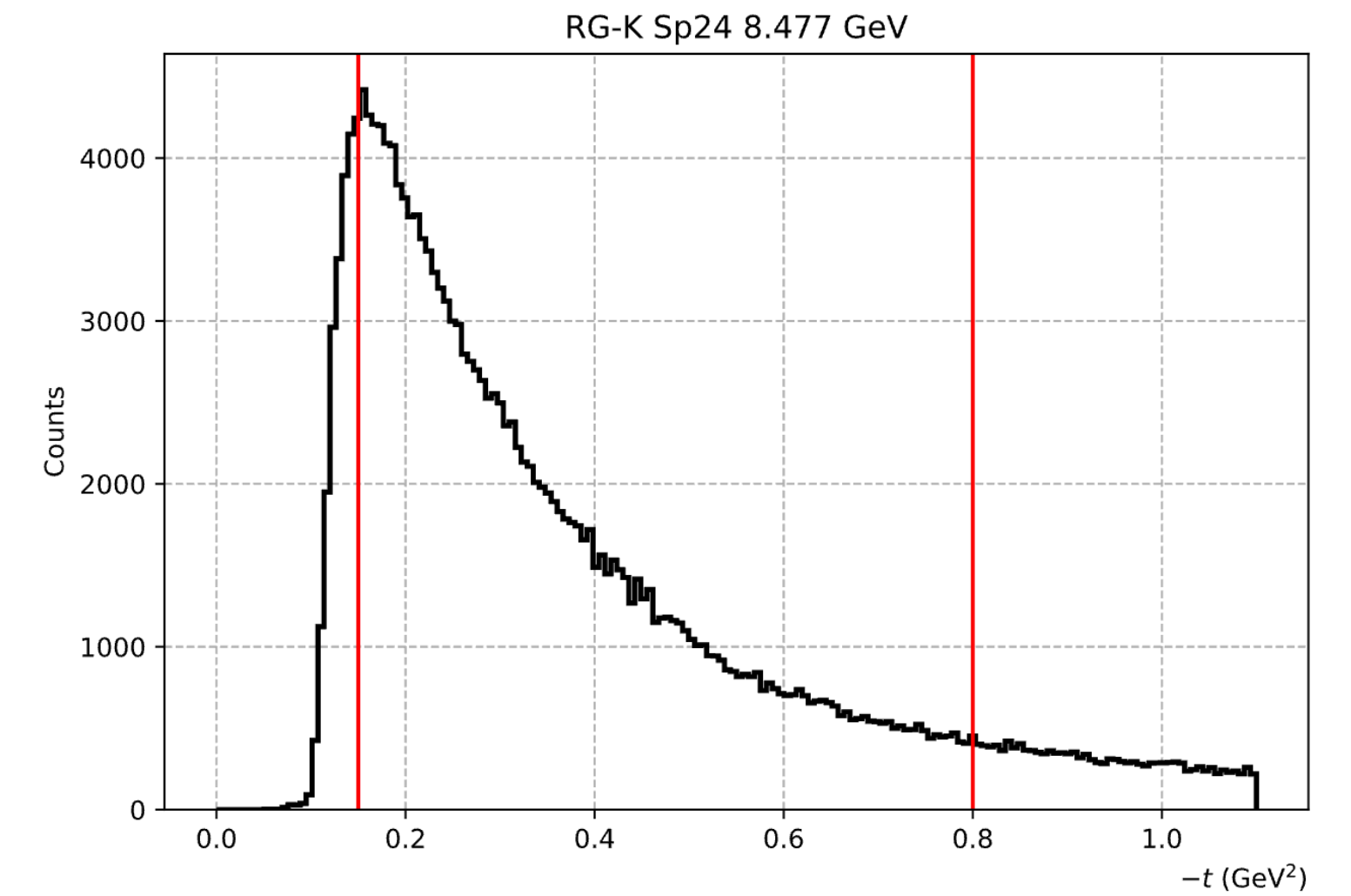
- $M_{ee} \geq 1.1$ GeV
- Expanding M_{ee} kinematic range to include lower range, with minimum at 1.1 GeV to avoid ϕ peak
- Very few events with $M_{ee} > 2.5$ GeV

E_γ



- $0.35 \leq E_\gamma/E_{beam} < 1.0$
- Cutting on E_γ/E_{beam} ratio instead of E_γ for transferability between RG-K run periods with different beam energies
- RG-A E_γ range of 4.0 GeV to 10.6 GeV corresponds to $\sim 0.35 - 1.0 E_\gamma/E_{beam}$

$-t$



- $0.15 \text{ GeV}^2 \leq -t < 0.8 \text{ GeV}^2$
- Same range as was used in RG-A analysis

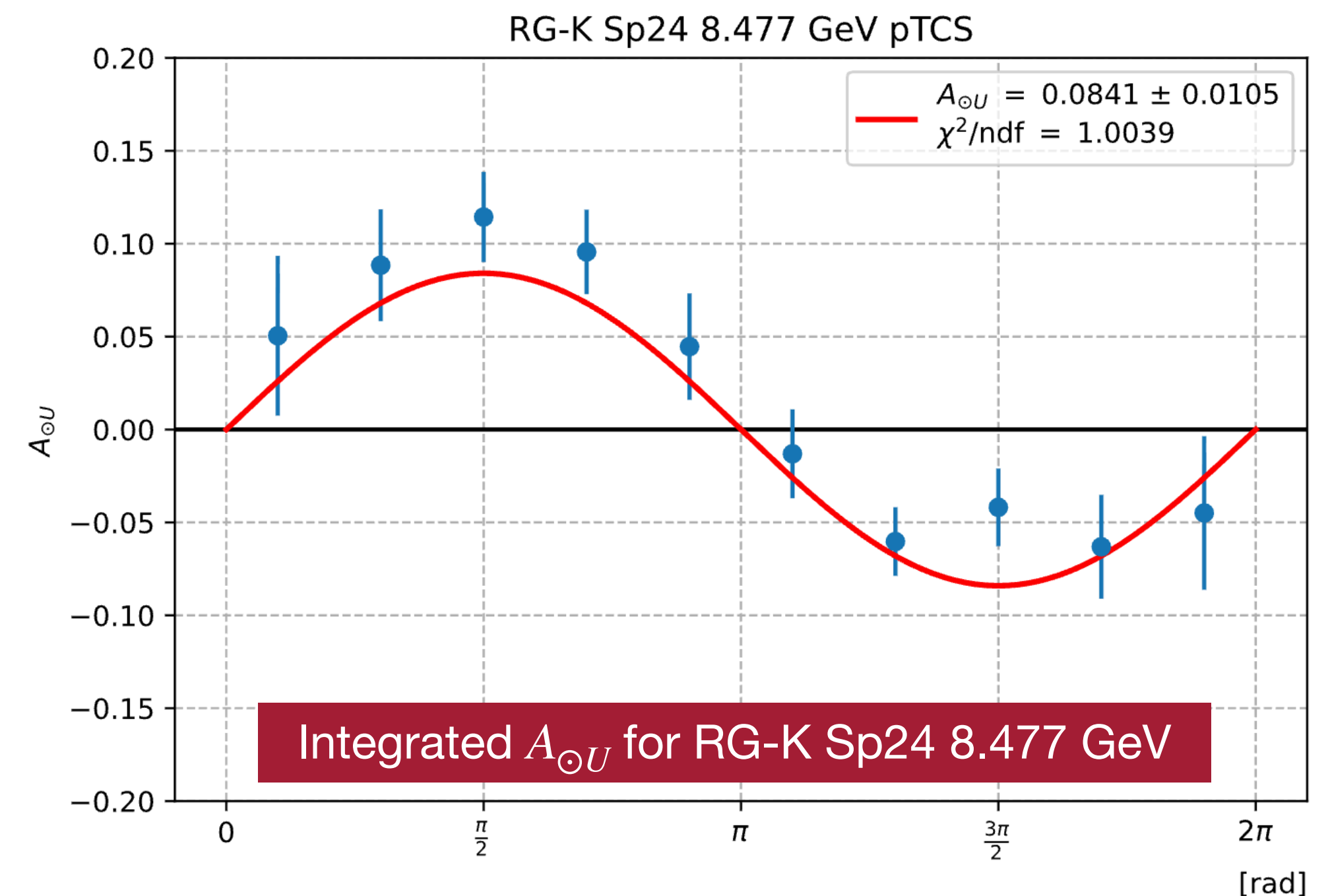
Photon Polarization Asymmetry

- The photon polarization asymmetry, $A_{\odot U}$, is constructed similarly to a beam spin asymmetry, but the polarization considered is of the circularly polarized photons emitted from linearly polarized electron beam, not the electrons
- Electrons with positive (negative) helicity emit right (left) handed circularly polarized photons \rightarrow following convention of BSA with \pm

$$A_{\odot U} \sin \phi = \frac{1}{P_b} \frac{N^+ - N^-}{N^+ + N^-} \text{ with } N^\pm = \sum_{\text{events}} Pol_{transf}^* , \text{ and } \sigma_{A_{\odot U}} = \sqrt{\sum_{\pm} \left(\frac{\partial A_{\odot U}}{\partial N^\pm} \delta N^\pm \right)^2}$$

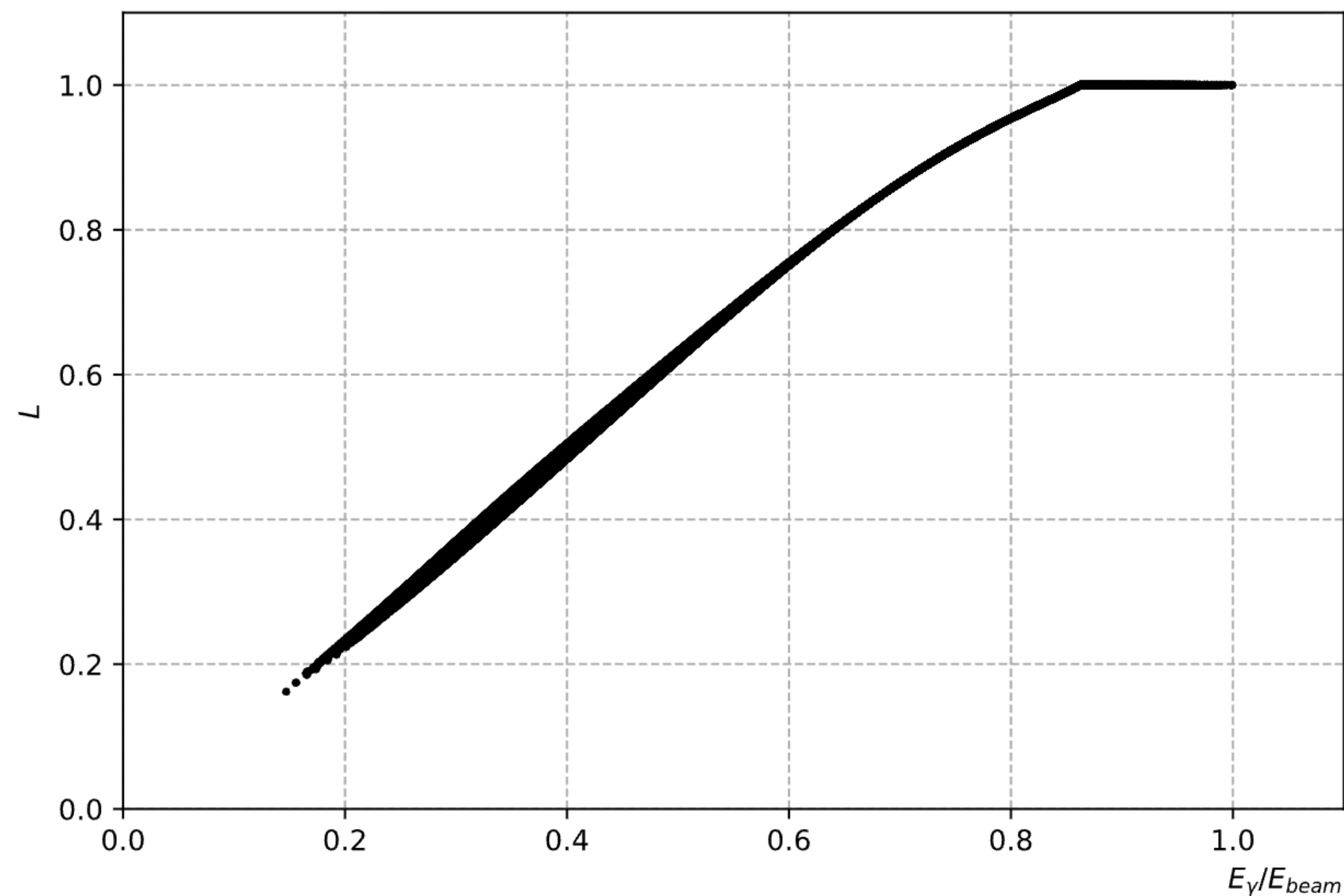
*Plan to also incorporate acceptance into counts (as done for RG-A analysis)

- 1D, 2D, 3D binning in M_{ee} , $-t$, ξ across $M_{ee} \in [1.1 \text{ GeV}, 3.0 \text{ GeV})$, $-t \in [0.15 \text{ GeV}^2, 0.80 \text{ GeV}^2)$, $\xi \in [0.0, 0.40)$
- Fitting using χ^2 and MLE methods:
 - χ^2 method fits $A_{\odot U} \sin \phi$ to distribution using 10 bins in ϕ
 - MLE method fits unbinned in ϕ for more accurate and stable fit
 - Each event has PDF $f(h_i, PolTranf_i, \phi_i; A_{\odot U}) = 1 + h_i PolTranf_i P_b A_{\odot U} \sin \phi_i$ where h_i is the beam helicity of the event
 - Sum PDF of all events in particular bin to get log-likelihood, $\ln \mathcal{L}(A_{\odot U}) = \sum f_i$
 - Minimize normalized negative log-likelihood, $N - \ln \mathcal{L}(A_{\odot U})$, to determine asymmetry amplitude (N is number of events in a particular bin)

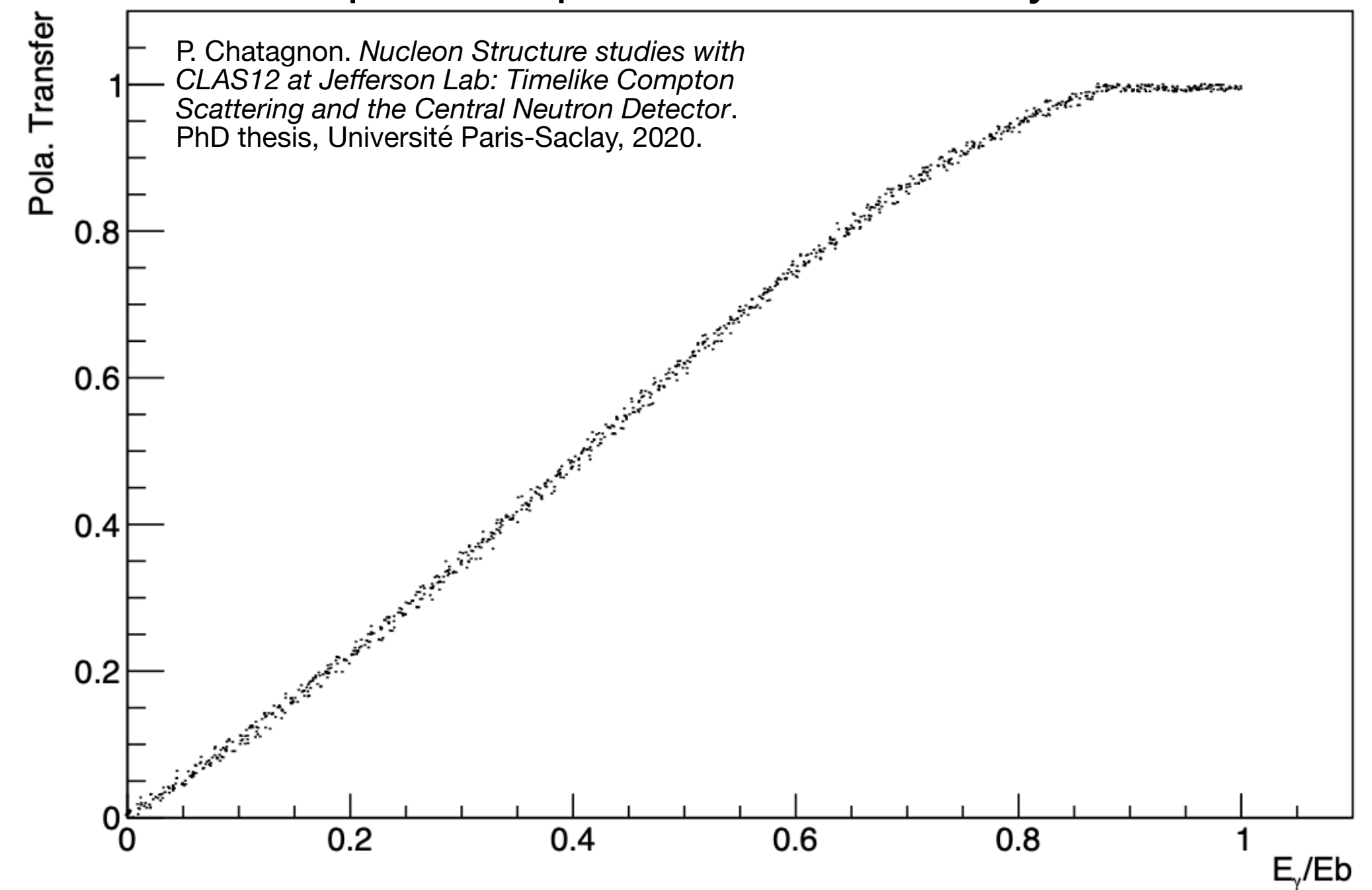


Calculating Polarization Transfer to Emitted Photons

- Photon polarization $P = SL$, where S is the beam electron helicity (± 1) and L is the polarization transfer function
- $L = k\{(E_1 + E_2)(3 + 2\Gamma) - 2E_2(1 + 4u^2\xi^2\Gamma)\}/I_0 \rightarrow$ a function of beam electron, scattered (missing) electron, and (quasi)real photon kinematics



Equivalent plot from RG-A analysis



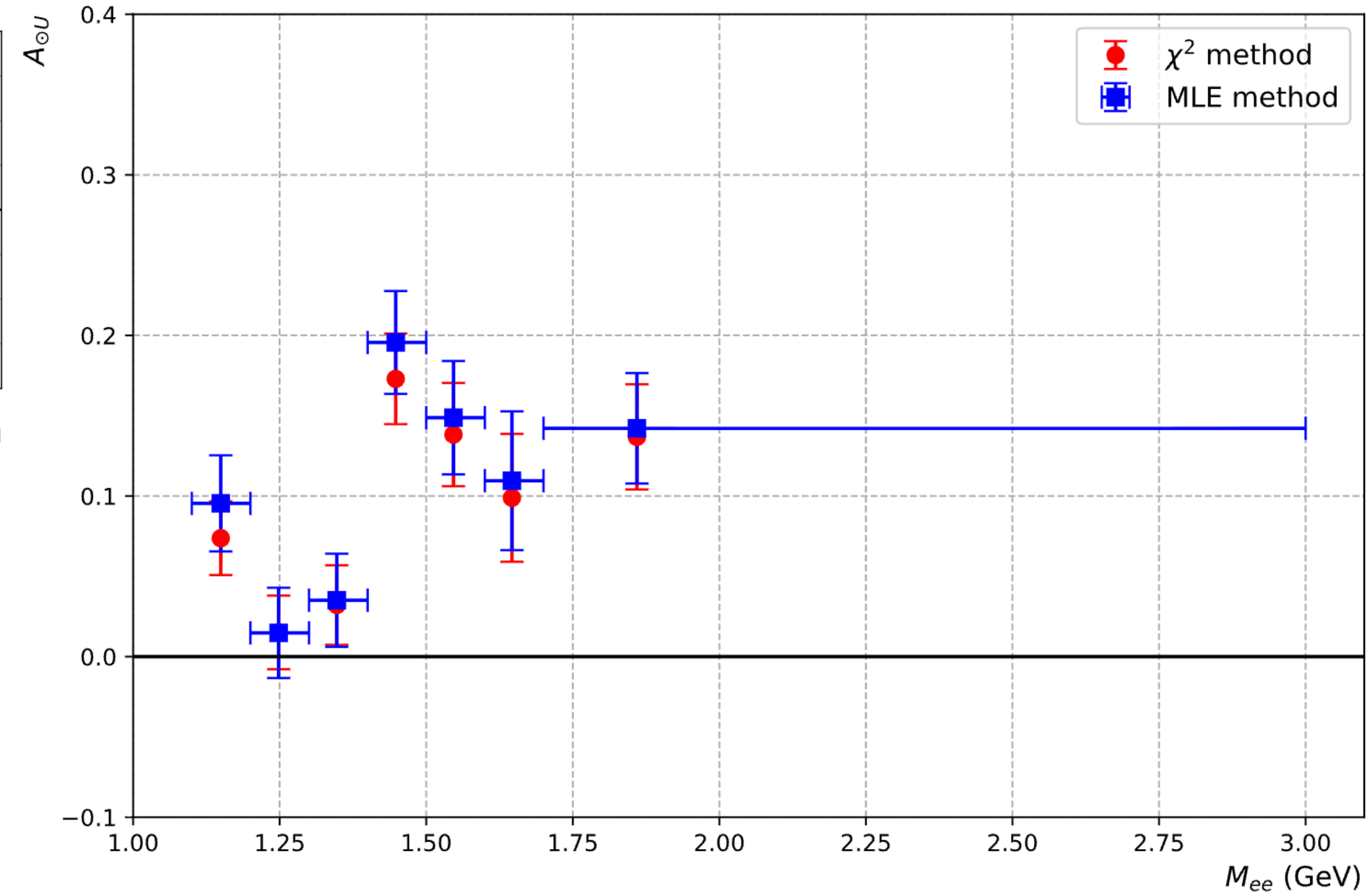
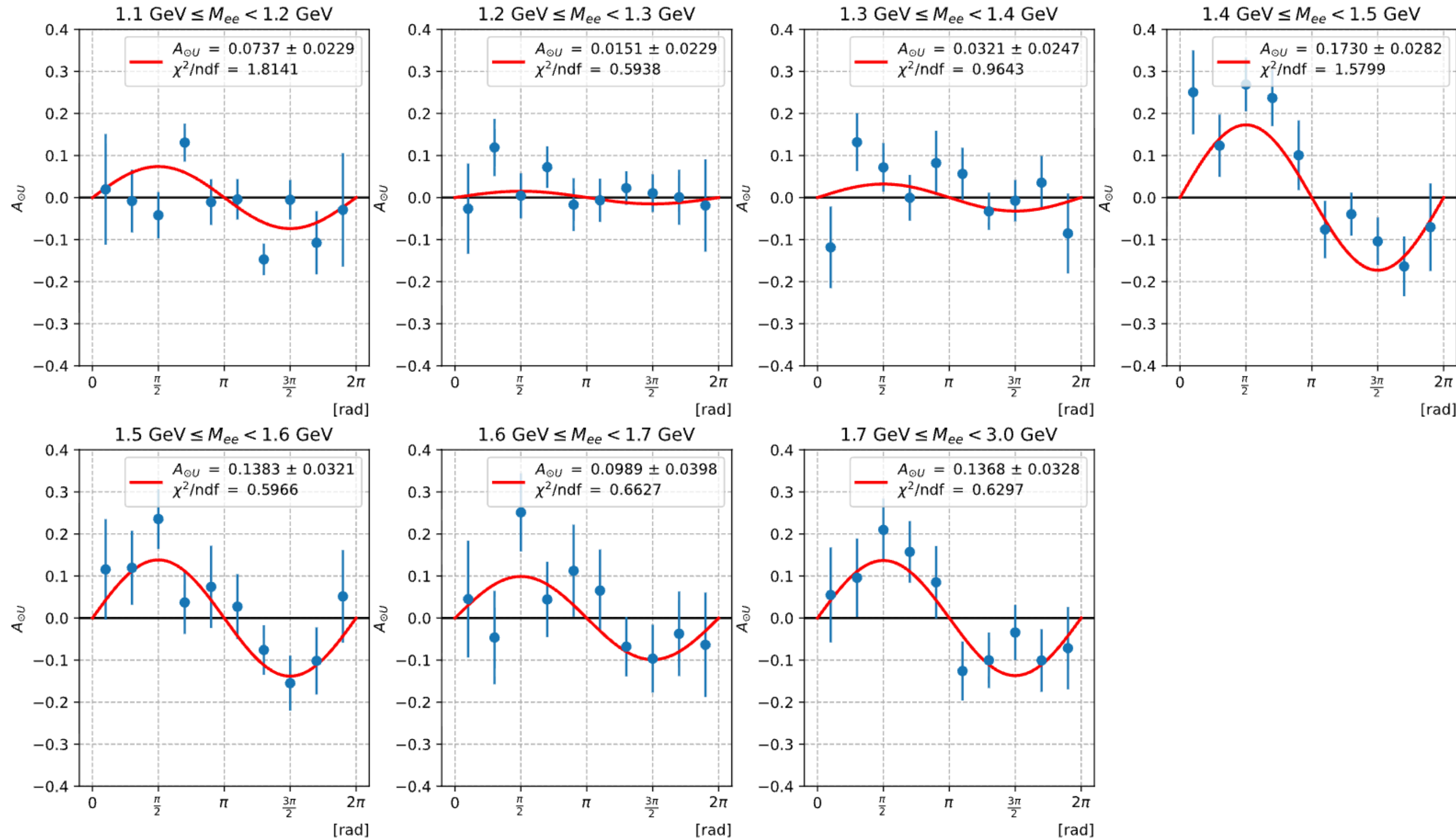
- Beyond certain E_γ/E_{beam} ratio (~ 0.90), behaviour becomes non-uniform, following RG-A procedure of setting equal to 1; cutting on $0.35 \leq E_\gamma/E_{beam} < 1.0$

Photon Polarization Asymmetry — 1D Binning in M_{ee}

$M_{ee} \in [1.1 \text{ GeV}, 1.2 \text{ GeV}, 1.3 \text{ GeV}, 1.4 \text{ GeV}, 1.5 \text{ GeV}, 1.6 \text{ GeV}, 1.7 \text{ GeV}, 3.0 \text{ GeV})$

χ^2 (binned in ϕ)

Comparing χ^2 and MLE

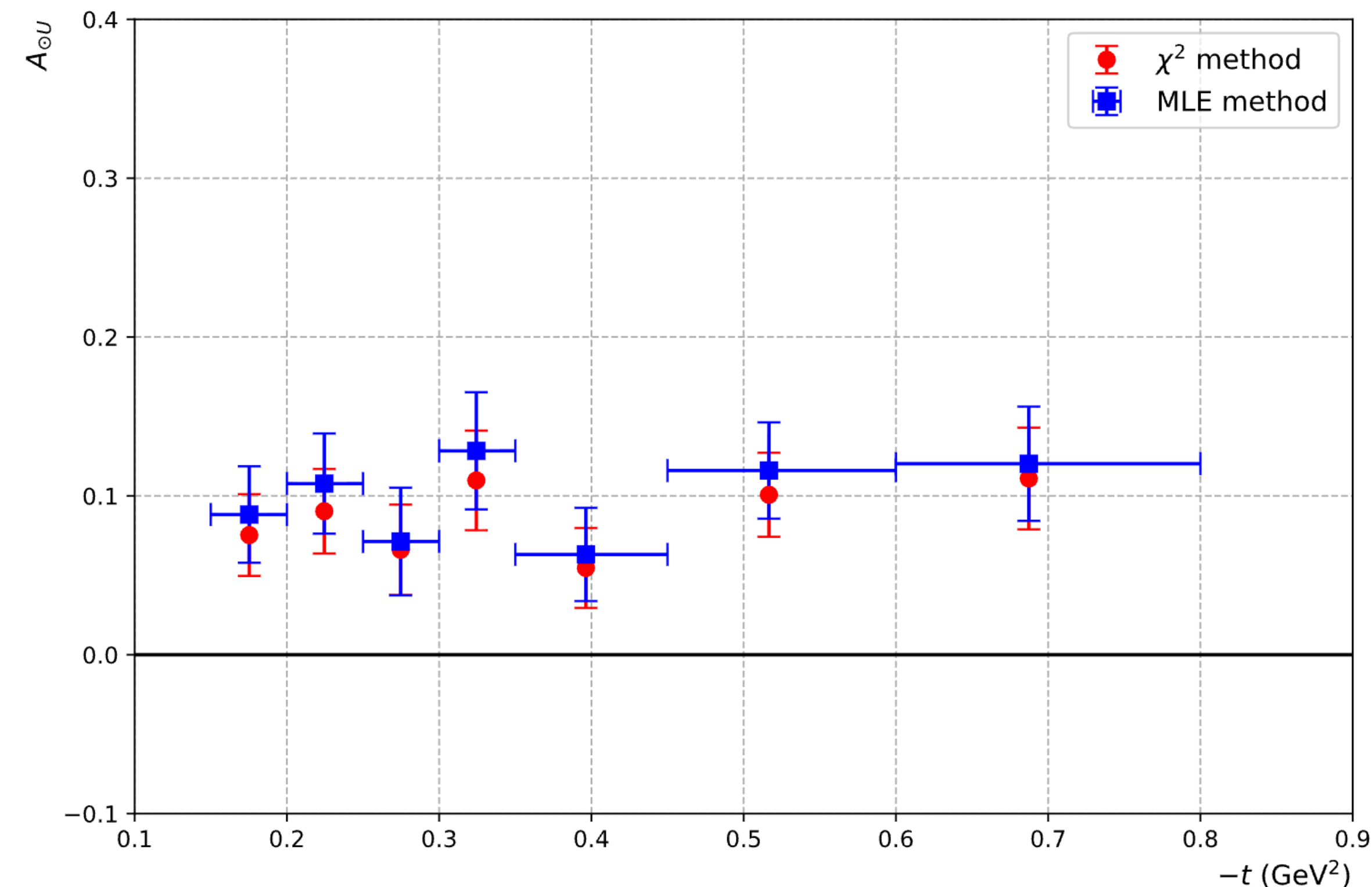
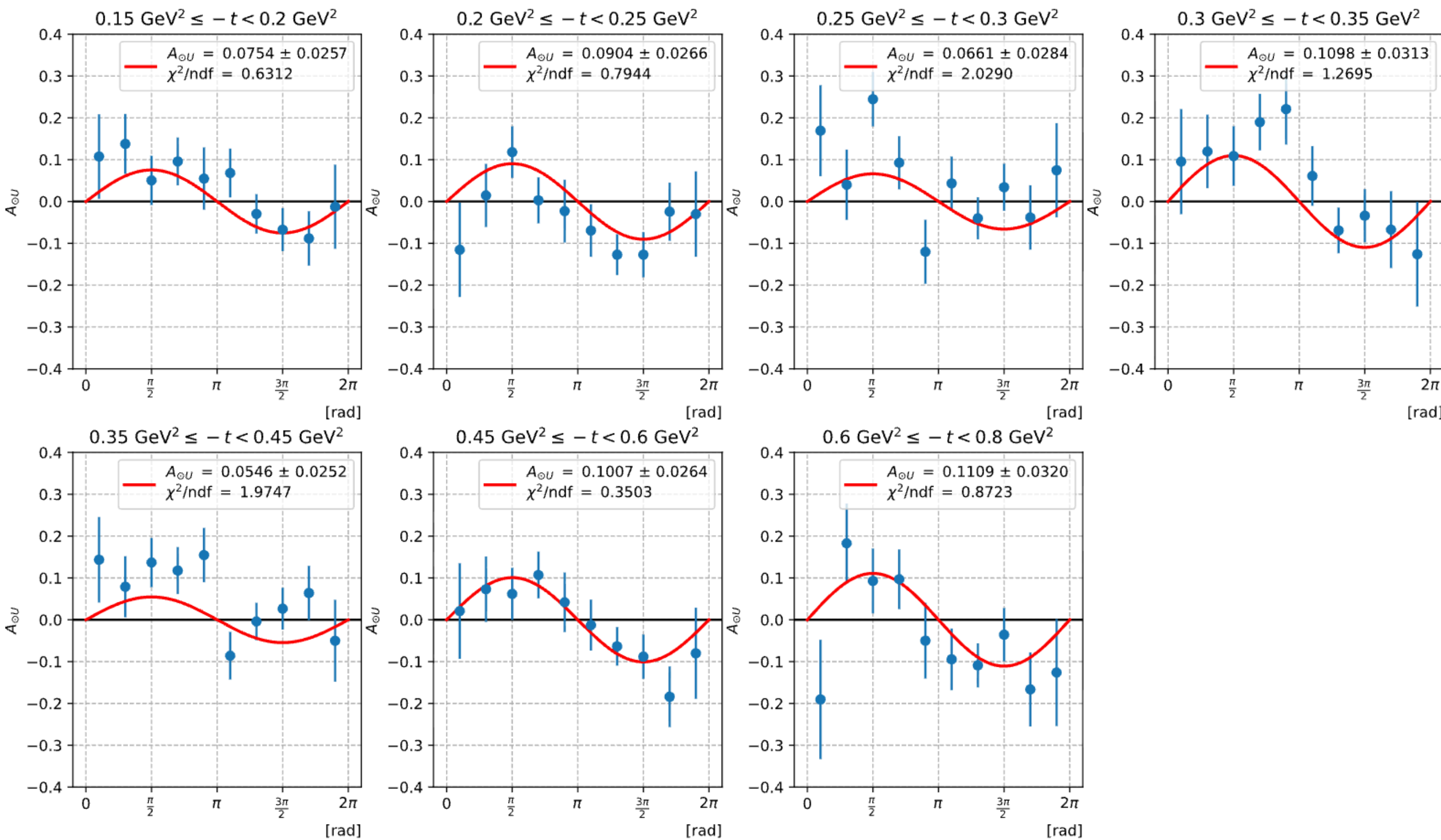


Photon Polarization Asymmetry — 1D Binning in $-t$

$-t \in [0.15 \text{ GeV}^2, 0.20 \text{ GeV}^2, 0.25 \text{ GeV}^2, 0.30 \text{ GeV}^2, 0.35 \text{ GeV}^2, 0.45 \text{ GeV}^2, 0.60 \text{ GeV}^2, 0.80 \text{ GeV}^2)$

χ^2 (binned in ϕ)

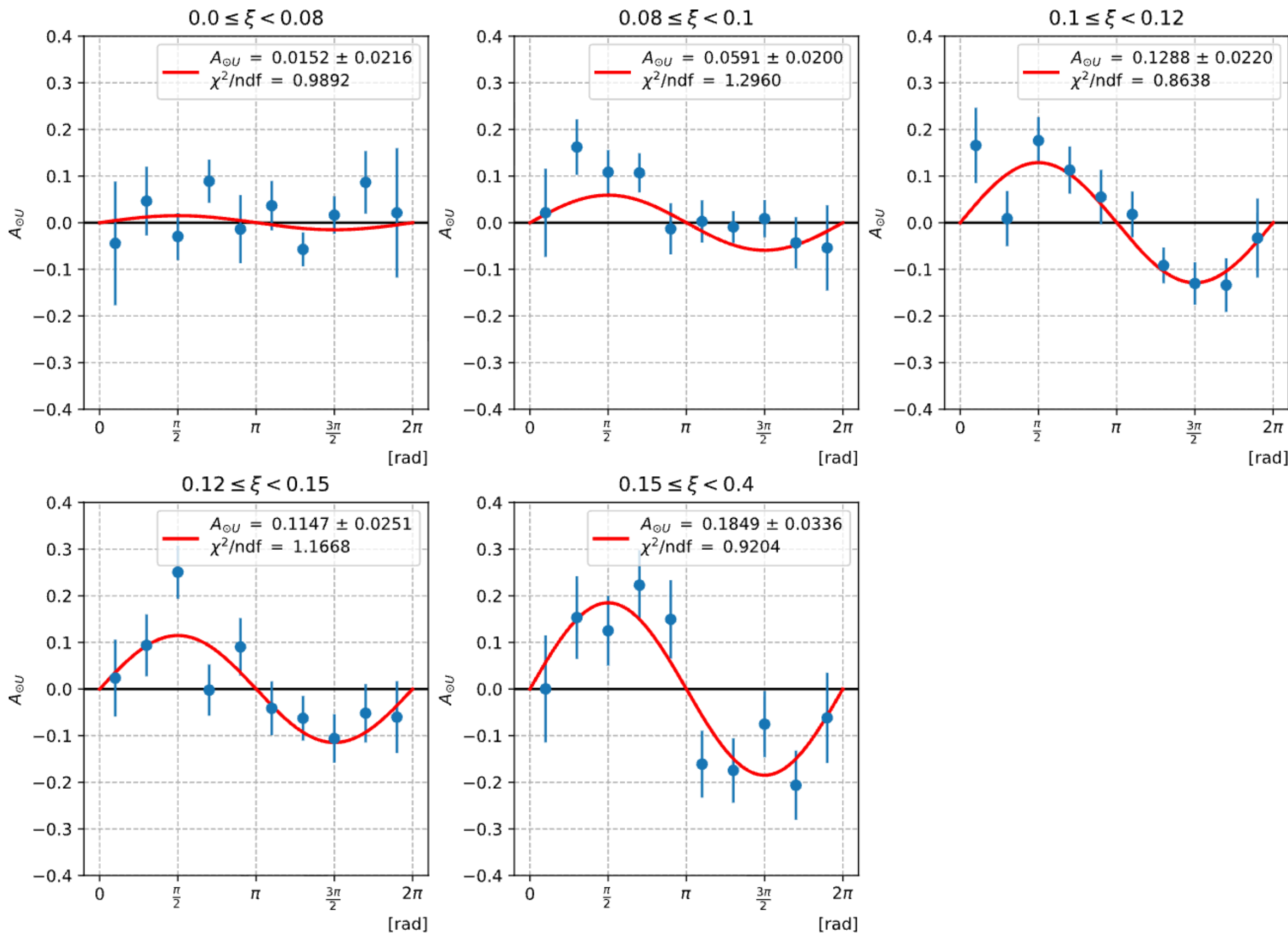
Comparing χ^2 and MLE



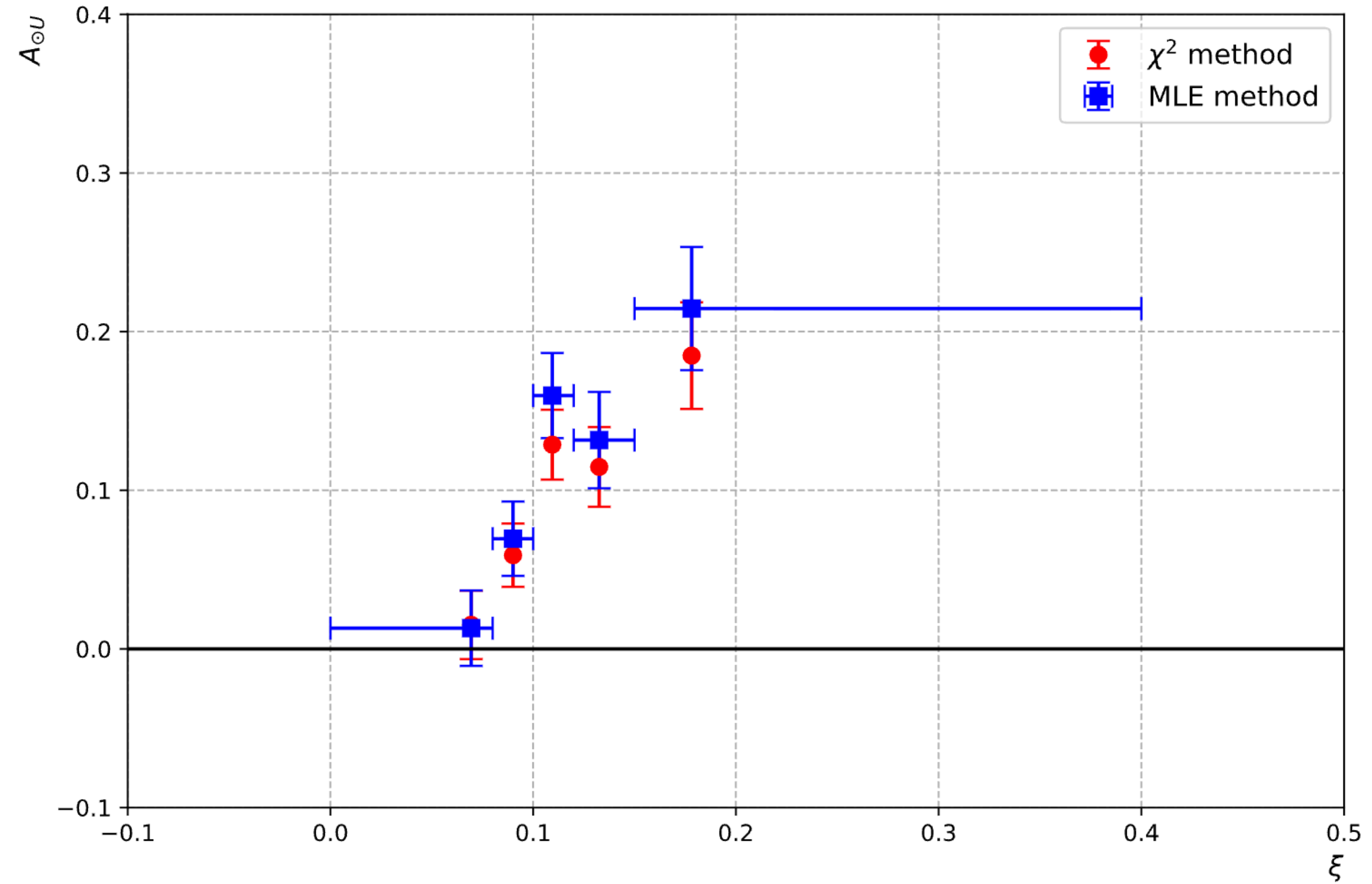
Photon Polarization Asymmetry — 1D Binning in ξ

$\xi \in [0.0, 0.08, 0.10, 0.12, 0.15, 0.4)$

χ^2 (binned in ϕ)

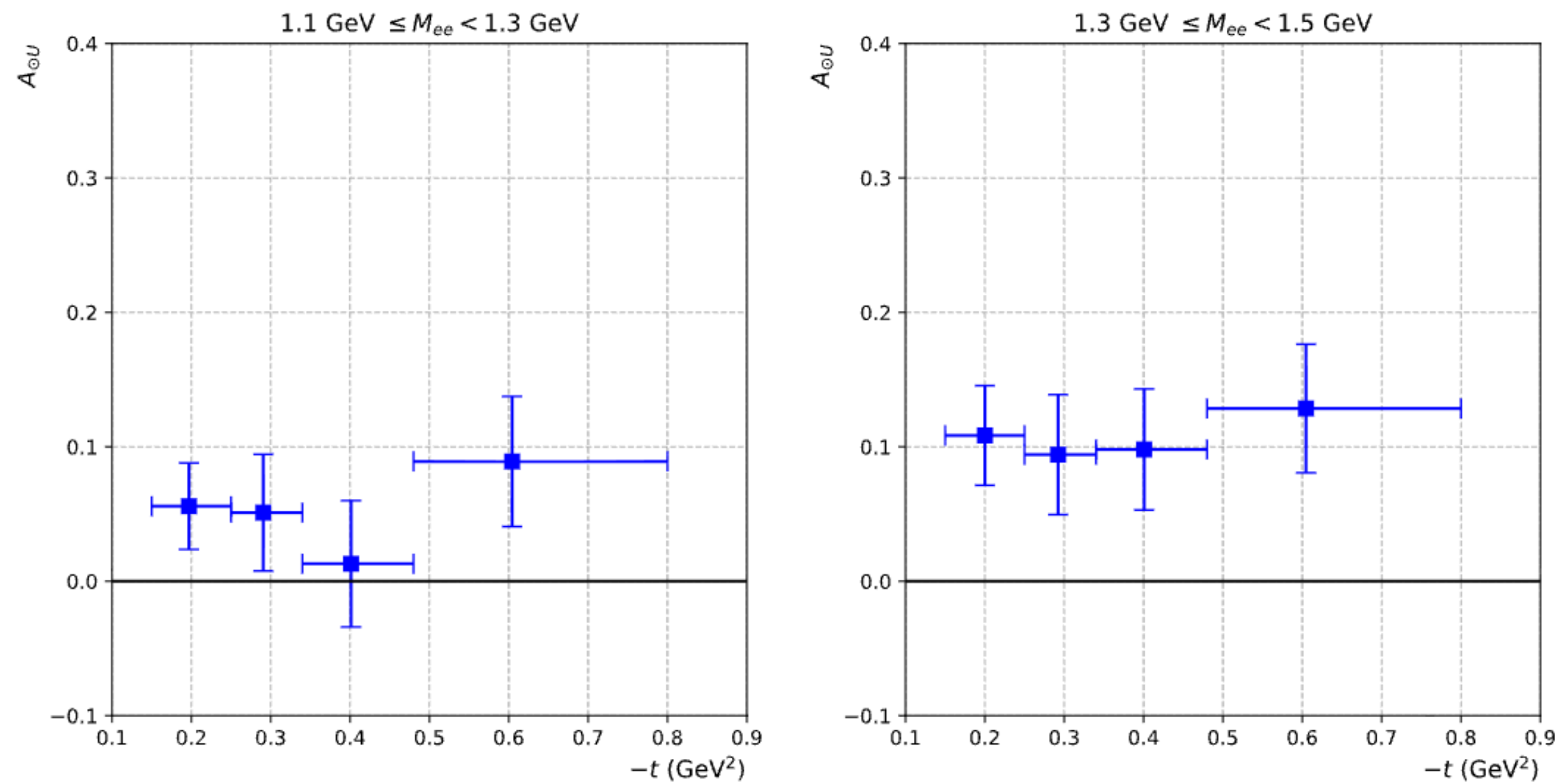


Comparing χ^2 and MLE

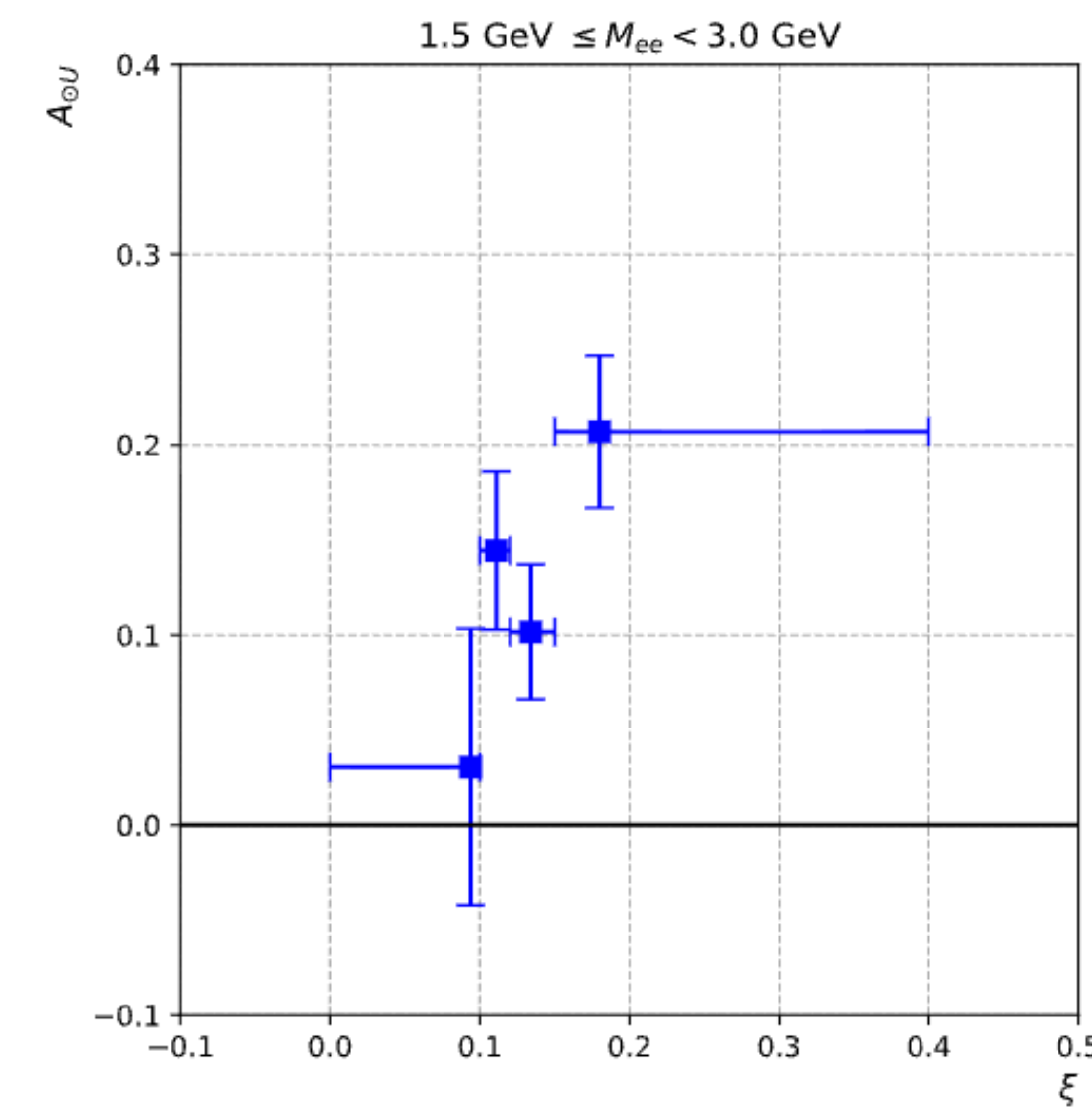
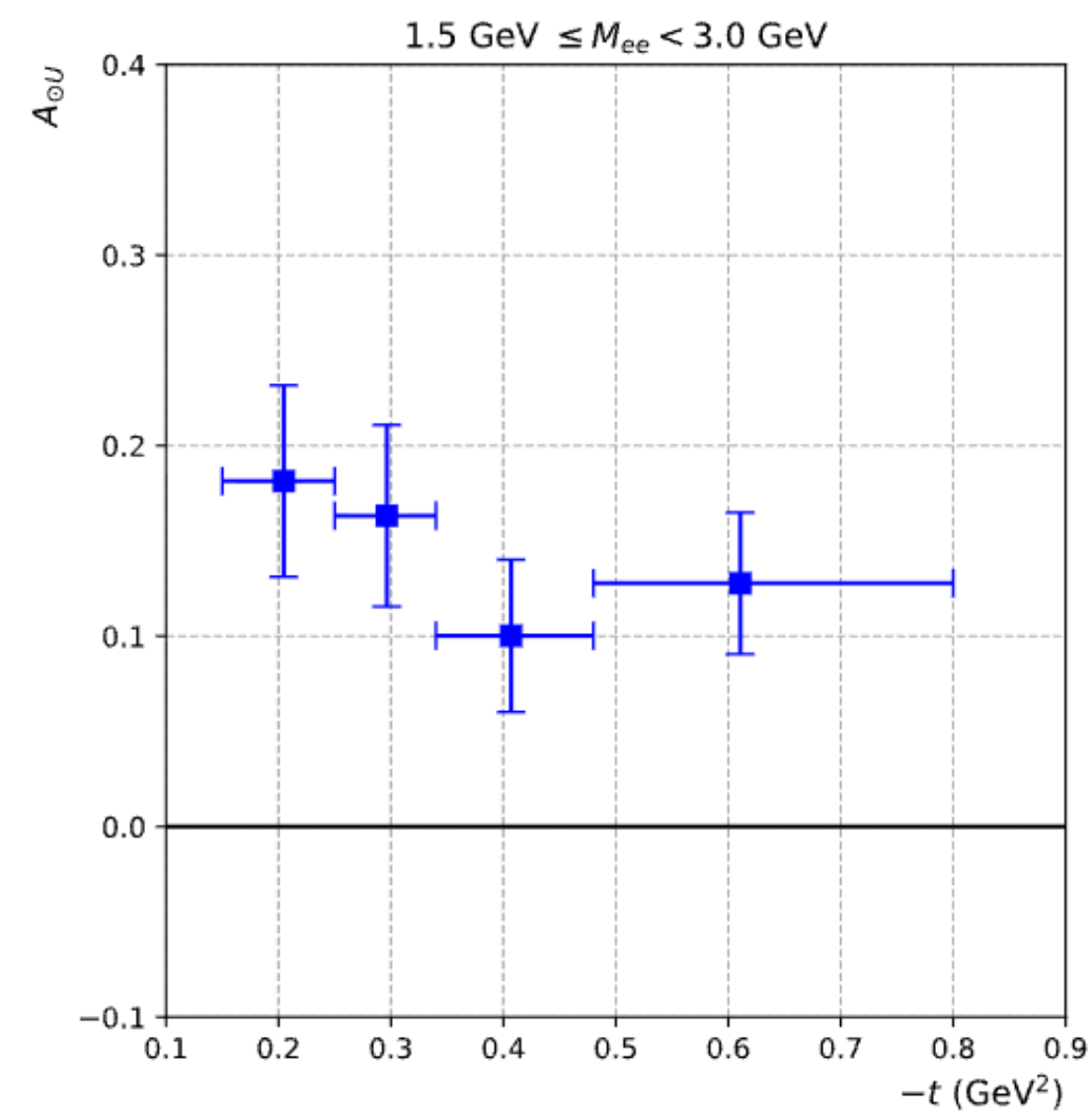
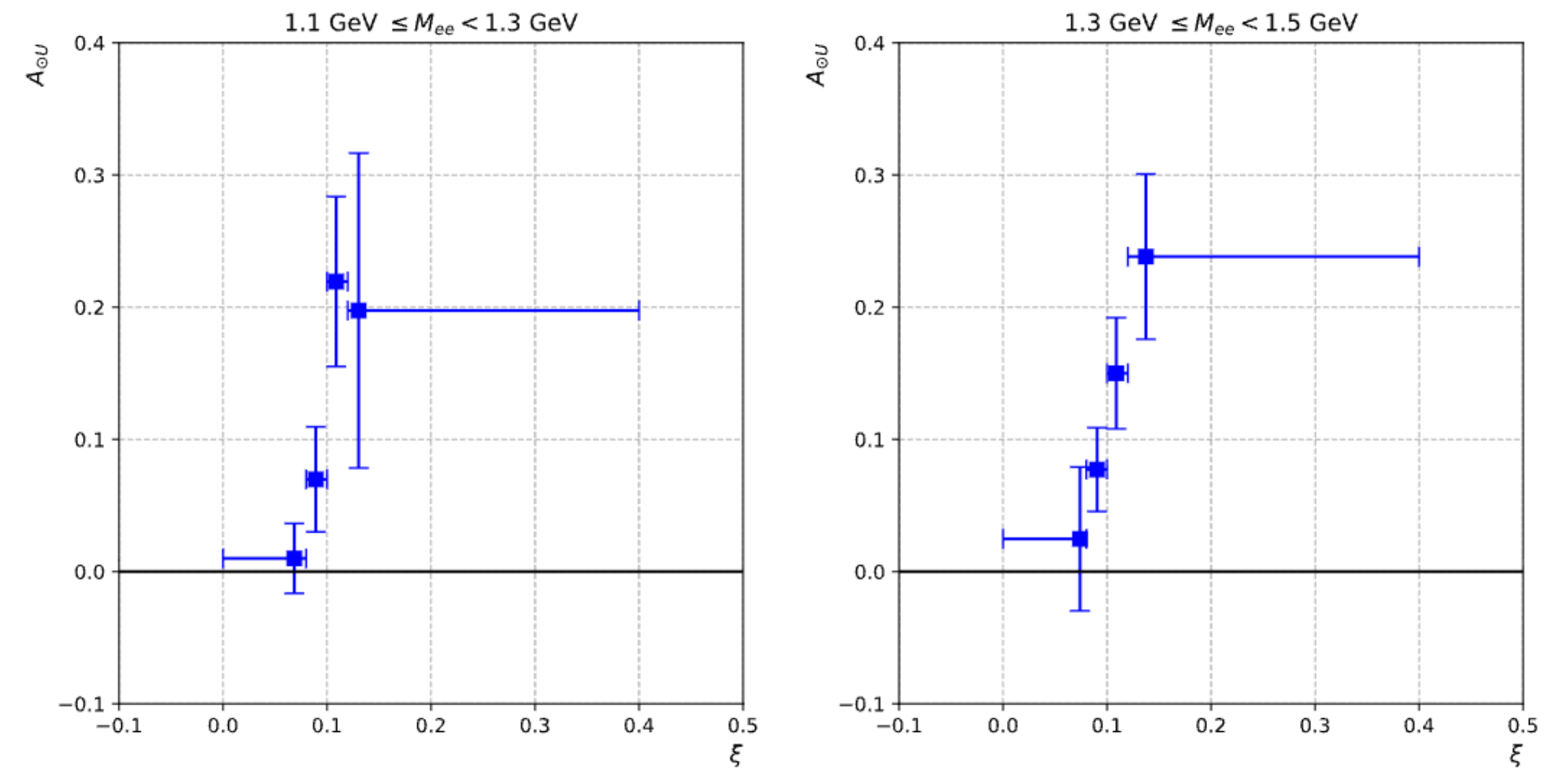


Photon Polarization Asymmetry — 2D Binning in $(M_{ee}, -t)$ and (M_{ee}, ξ)

$(M_{ee}, -t)$

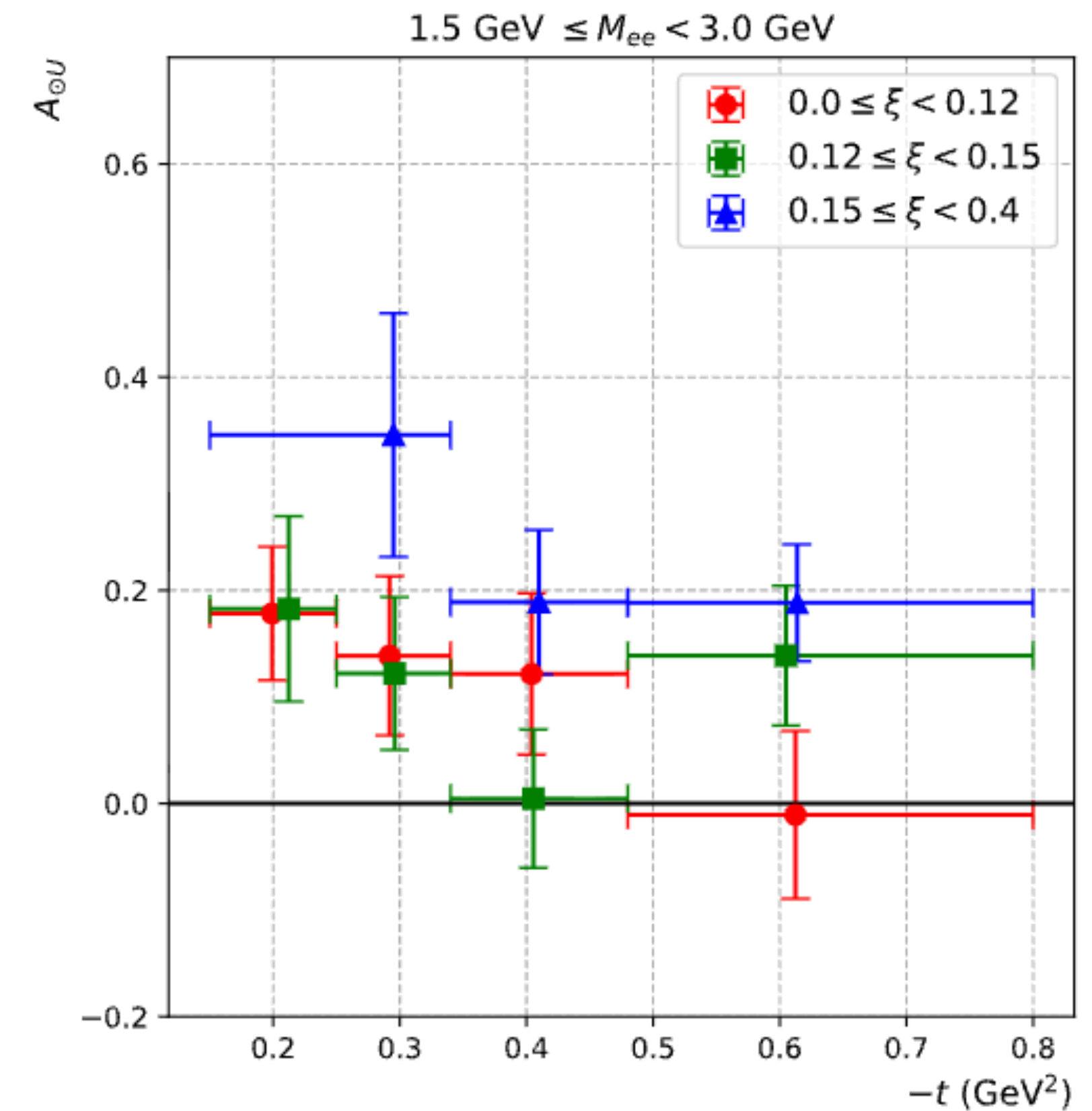
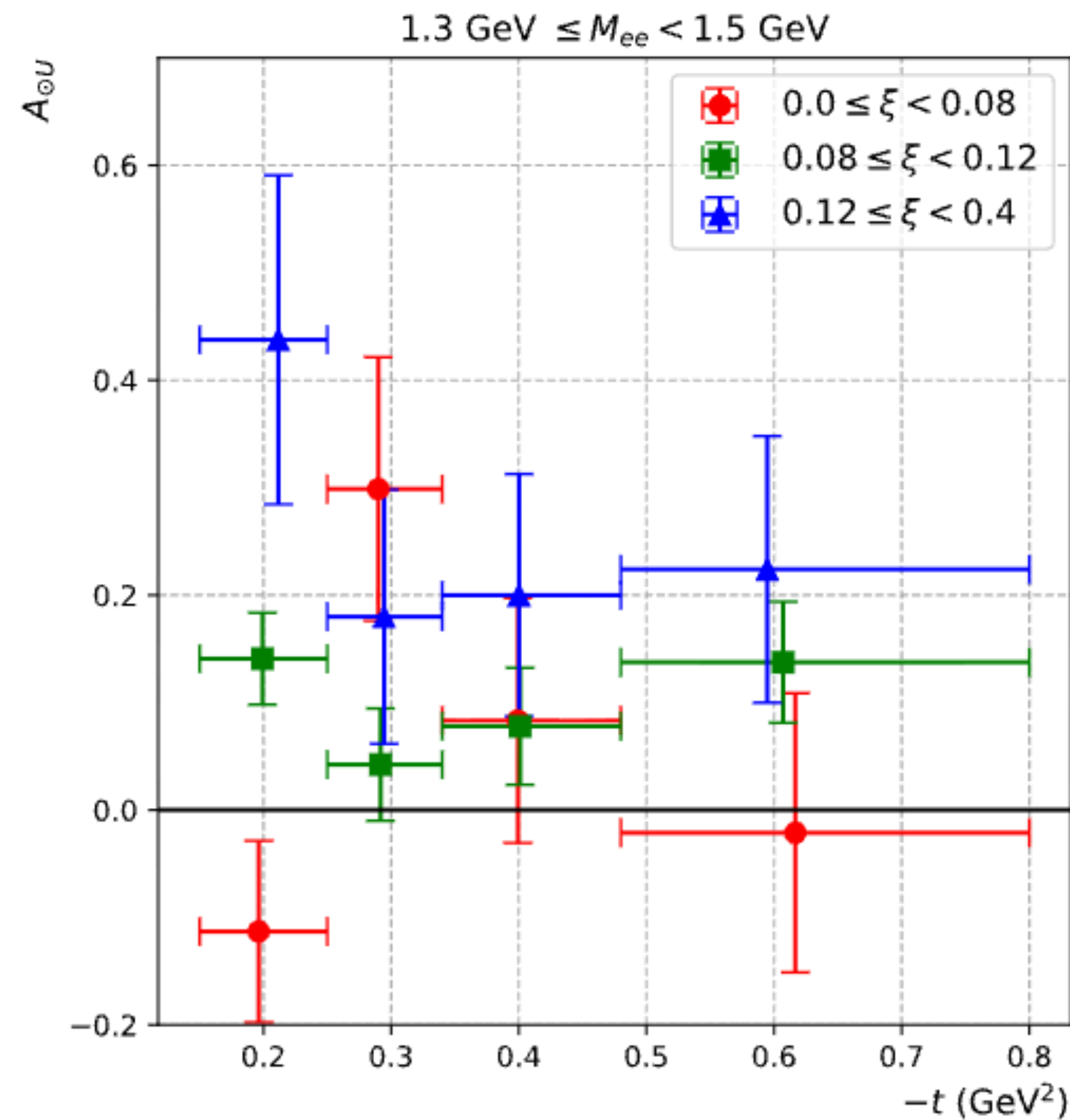
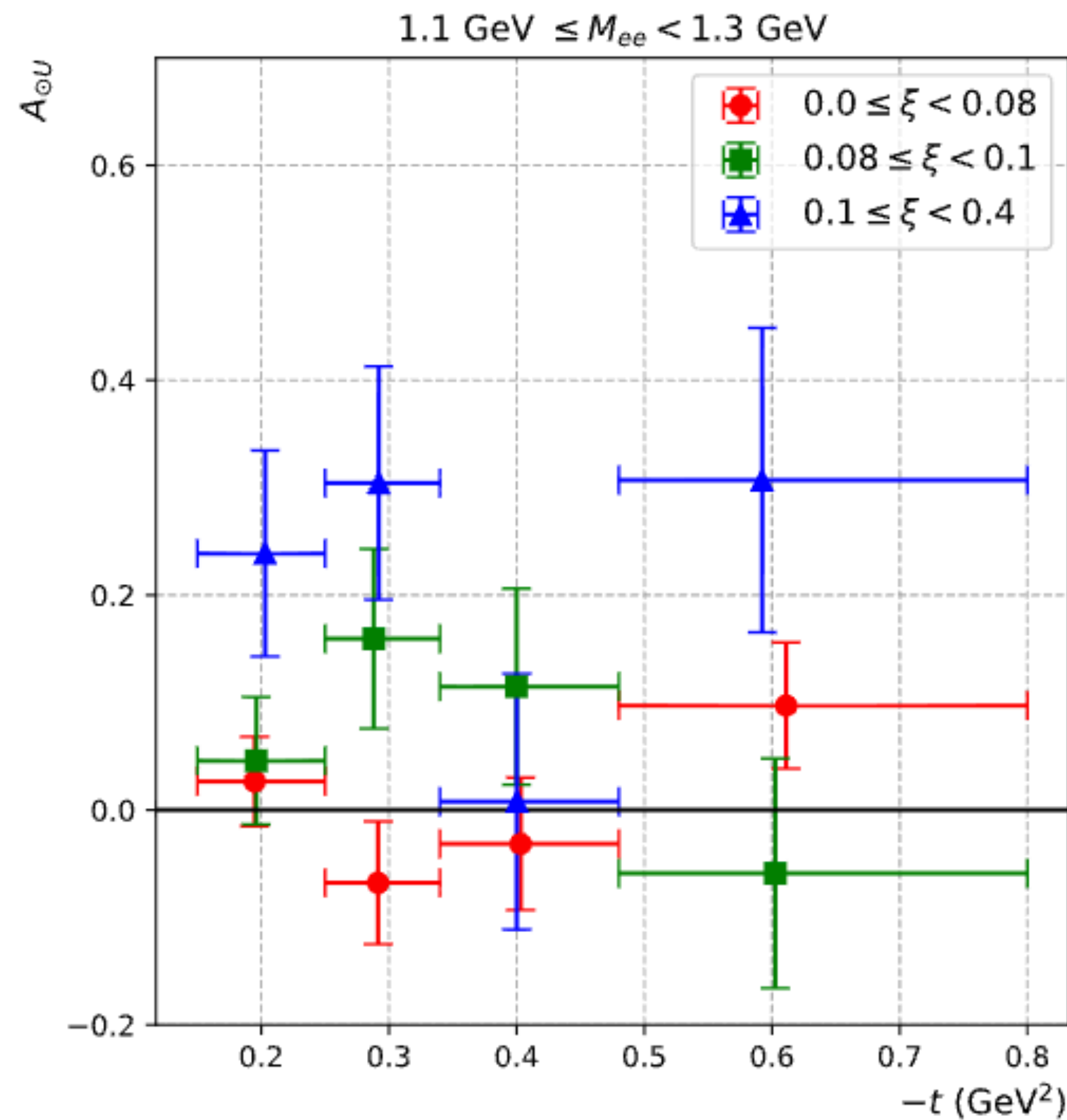


(M_{ee}, ξ)



Fitting done using both χ^2 and MLE methods, with just MLE results displayed to minimize confusion as good agreement between fitting methods (as shown in 1D cases).

Photon Polarization Asymmetry — 3D Binning



- Fits from 3D binning overall make sense and has reasonable statistical uncertainty
- Across binning choices, more bins could probably be added but hesitant to do this because QADB, quality cuts will reduce statistics

Forward-Backward Asymmetry

$$A_{FB} = \frac{N_F - N_B}{N_F + N_B} \text{ where } N_{F/B} = \sum_{events \in F/B} \frac{1}{Acc \cdot BV_{F/B}} \text{ and } E_{F/B}^2 = \sum_{events \in F/B} \left(\frac{1}{Acc \cdot BV_{F/B}} \right)^2$$

$Acc \rightarrow$ Acceptance

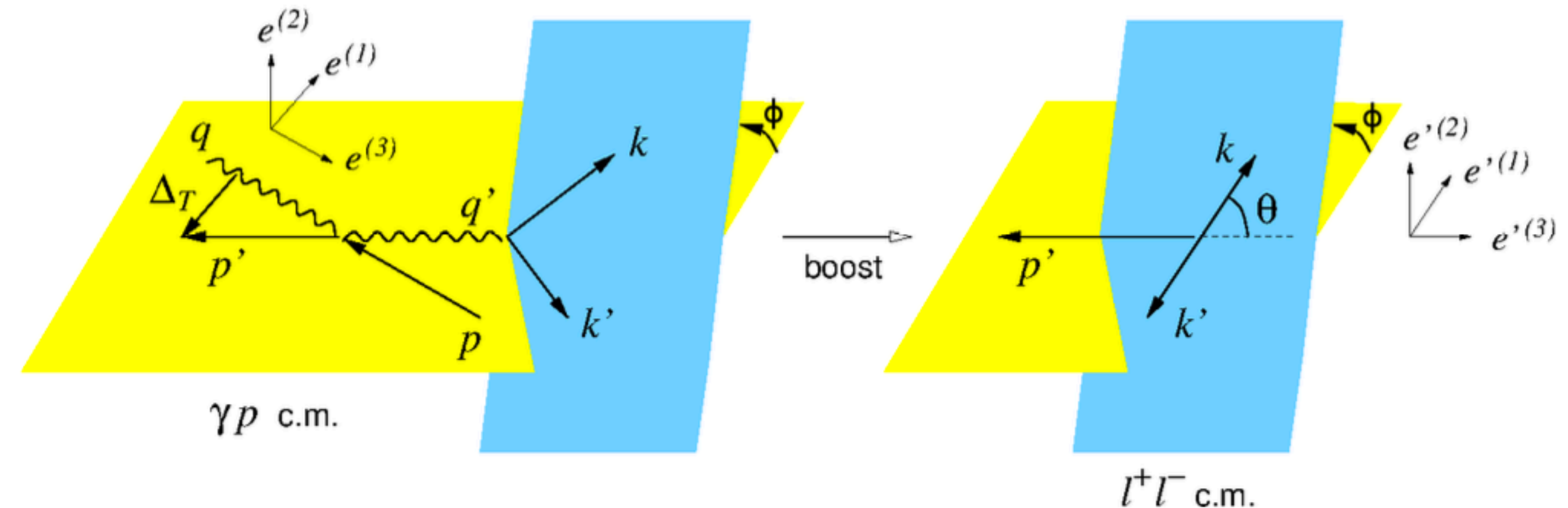
$BV_{F/B} \rightarrow$ Forward/backward bin volume correction

Forward: $-40^\circ \leq \phi < 40^\circ, 50^\circ \leq \theta < 80^\circ$

Backward: $140^\circ \leq \phi < 220^\circ, 100^\circ \leq \theta < 130^\circ$

Obtained by flipping lepton assigned to k, k' when calculating COM angles. $\phi \rightarrow \phi + 180^\circ$,
 $\theta \rightarrow 180^\circ - \theta$

E.R. Berger, M. Diehl, B. Pire. *Eur. Phys. J. C*, **23**(4):675689, 2002.



- Acceptance and bin volume corrections are not the identical for forward and backward bins, so they doesn't cancel in this asymmetry
- Important to have accurate simulations to determine acceptance and bin volume corrections. Currently difficult to do these studies for RG-K Sp24 because OSG configuration is still in development

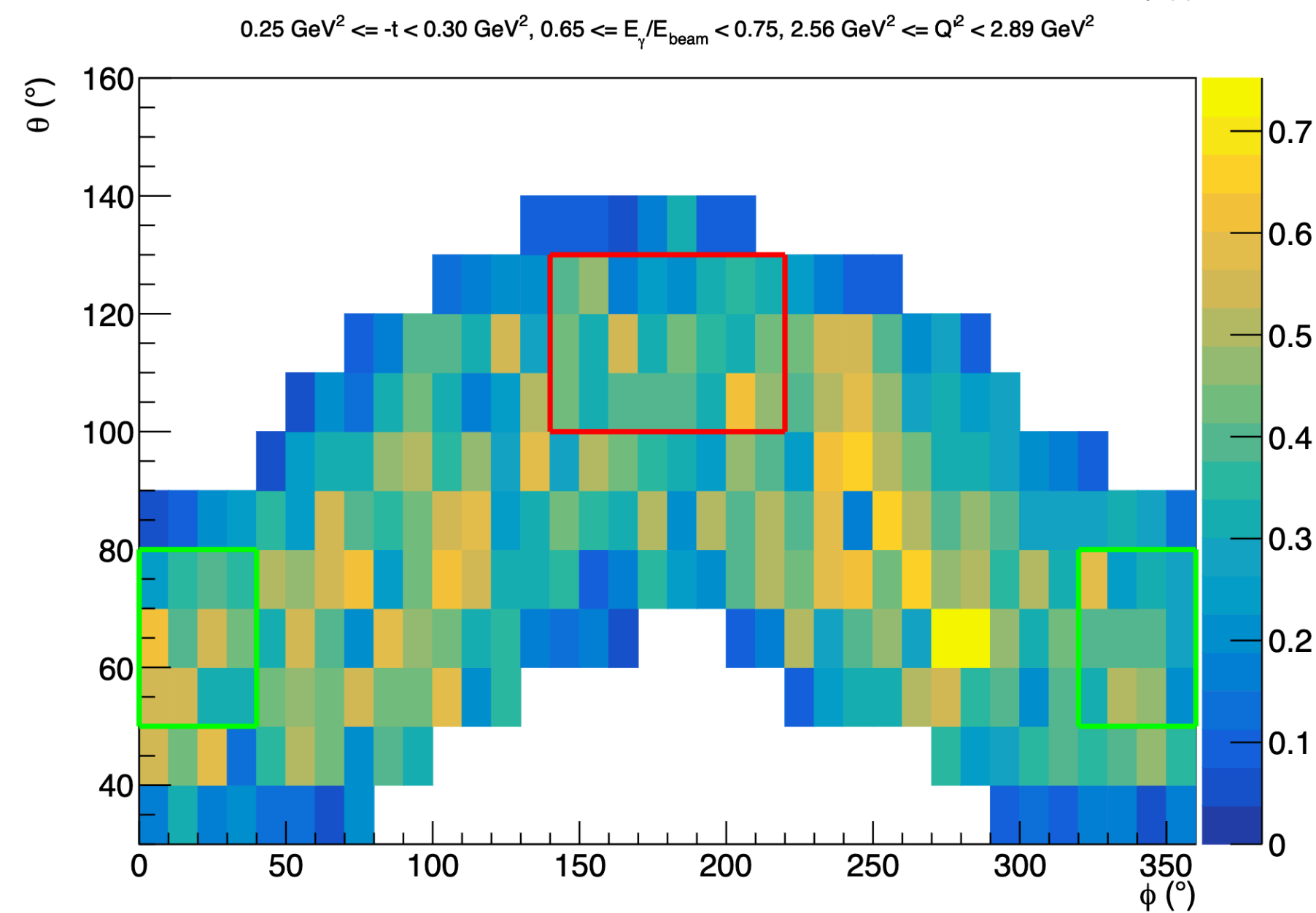
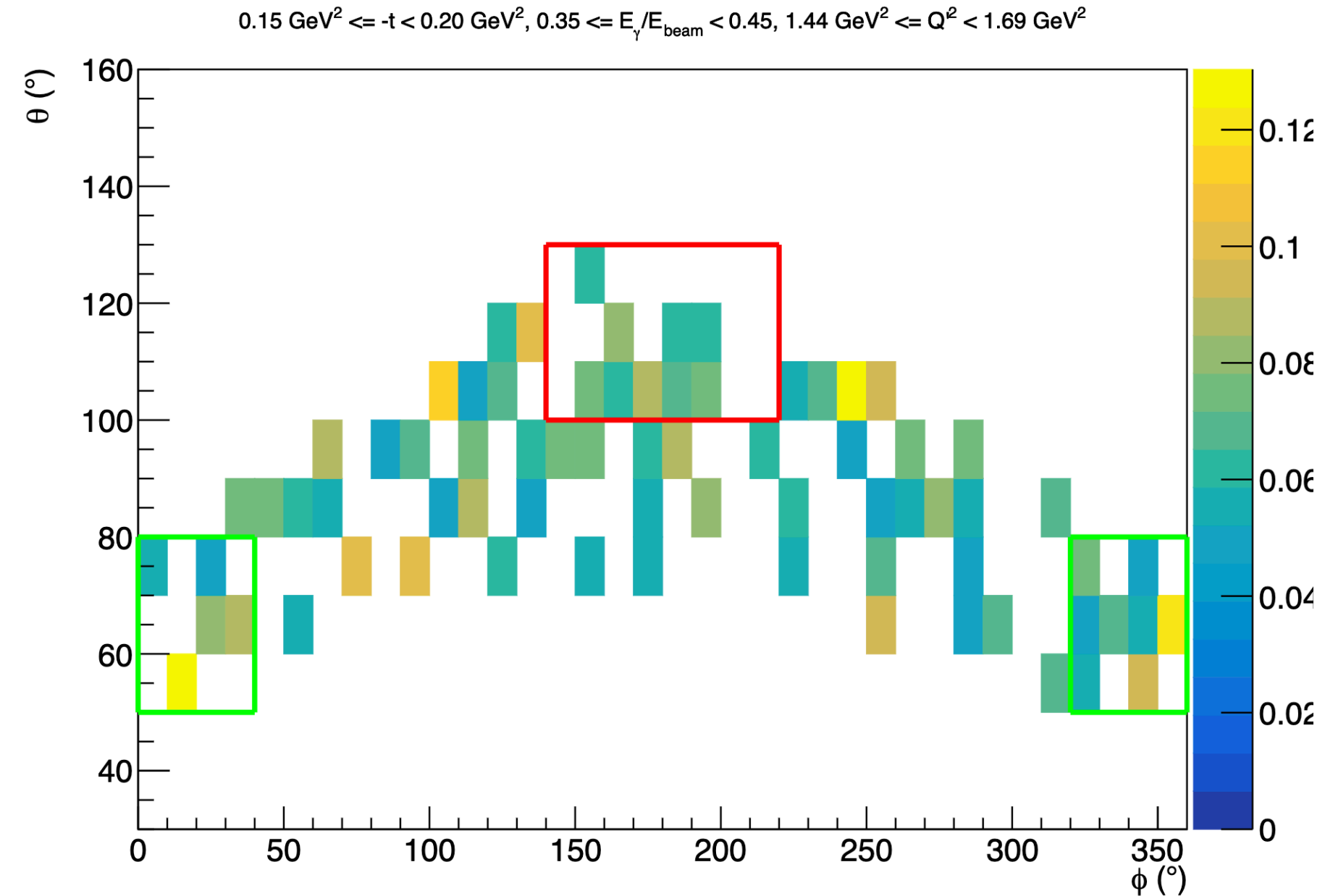
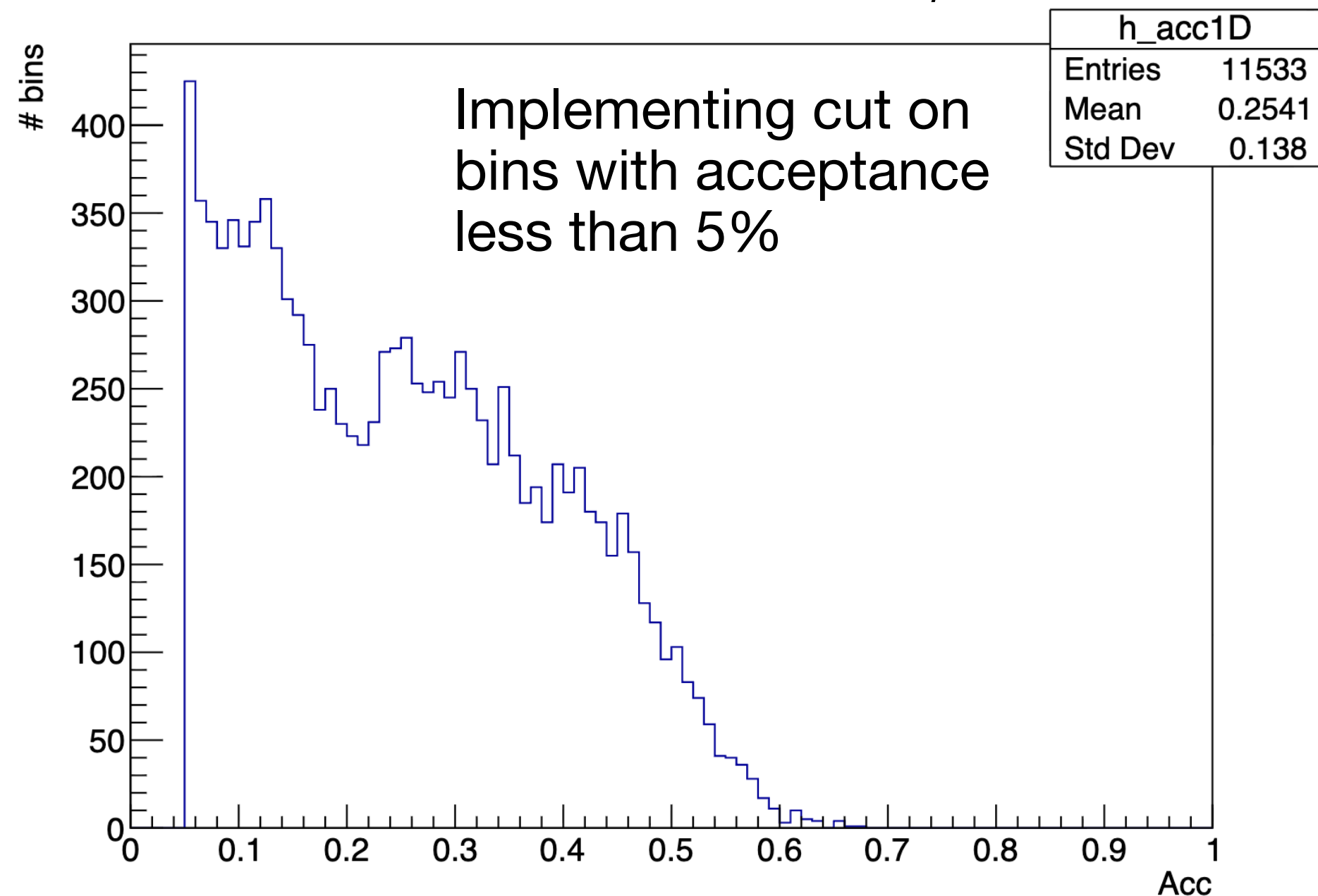
Acceptance and Bin-Volume Corrections

Using TCSGen simulation at 8.477 GeV beam energy but passed through Fa18 FTOff (6.535 GeV) configuration as stand-in while waiting for RG-K Sp24 OSG configurations

$$Acc(-t, E_\gamma/E_{beam}, Q^2, \theta, \phi) = \frac{N_{(-t, E_\gamma/E_{beam}, Q^2, \theta, \phi)}^{rec}}{N_{(-t, E_\gamma/E_{beam}, Q^2, \theta, \phi)}^{gen}}$$

$$N_{(-t, E_\gamma/E_{beam}, Q^2, \theta, \phi)}^{gen/rec} = \sum_{(-t, E_\gamma/E_{beam}, Q^2, \theta, \phi)} weight$$

$$BV_{F/B}(-t, E_\gamma/E_b, Q^2) = \frac{\sum_{\theta, \phi} b_{F/B|N \neq 0}}{\sum_{\theta, \phi} b_{F/B}}$$



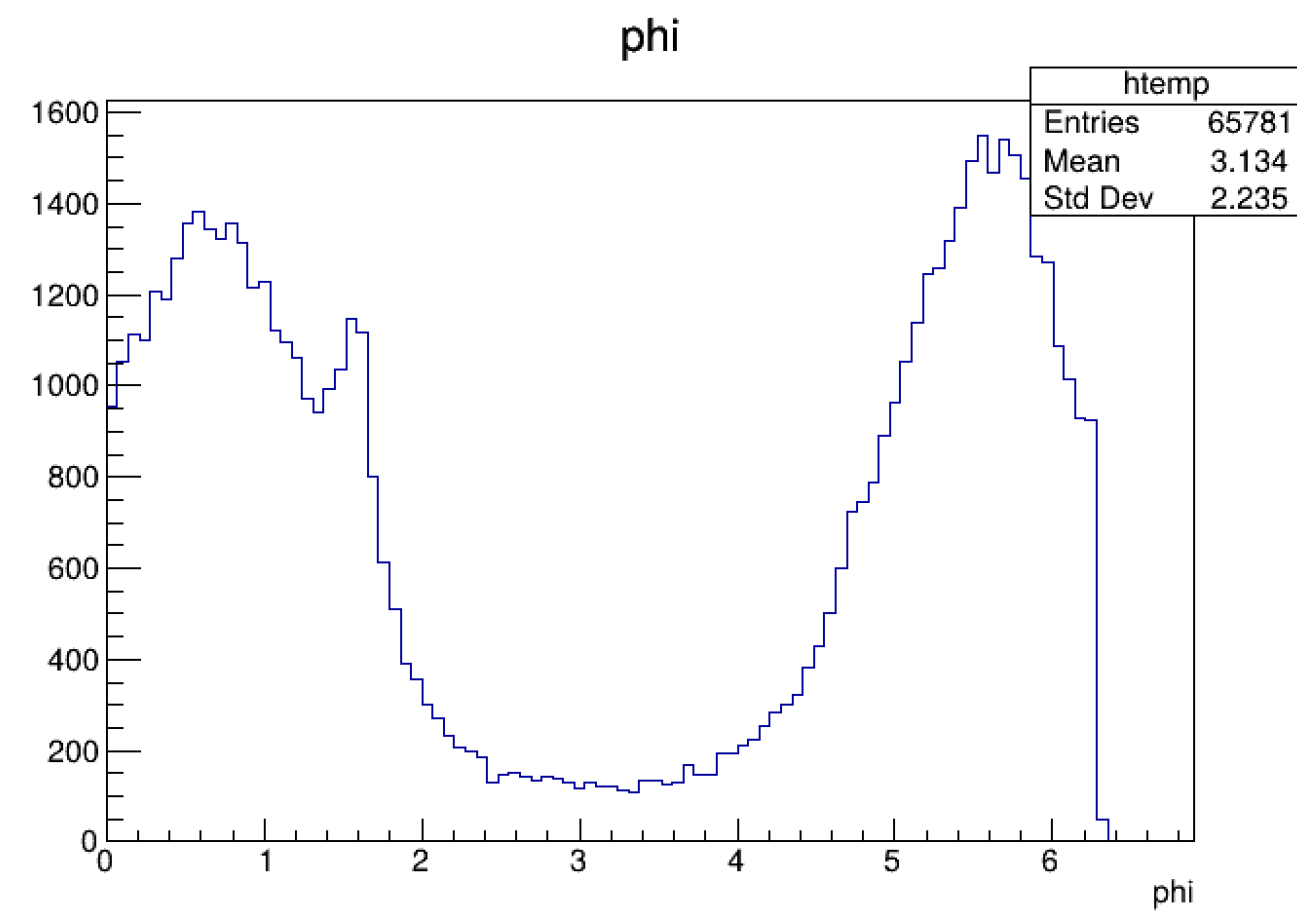
- Bin volume correction, $BV_{F/B}$, is a ratio of number of non-empty (in MC) θ, ϕ bins to total number of θ, ϕ bins in a given forward or backward bin in $-t, E_\gamma/E_b, Q^2$
- Needed for A_{FB} as acceptance is not identical for forward and backward bins

← Examples of MC θ, ϕ acceptance in different kinematic bins

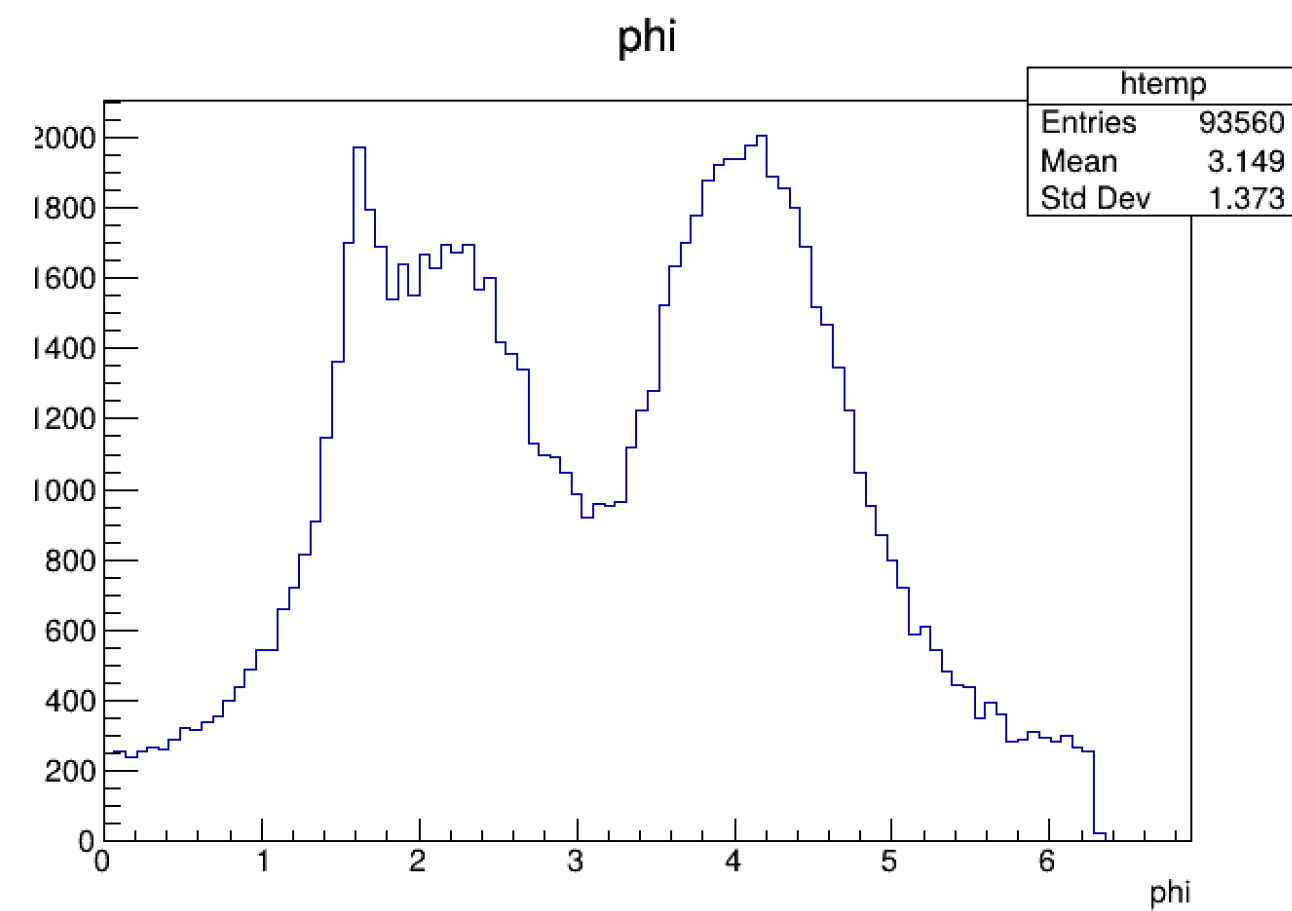
Forward-Backward Asymmetry Cross Check with RG-A

Acceptance of ϕ and θ vary considerably with torus configuration, which has significant effects on the size and shape A_{FB} . A new definition of forward and backward bins may be needed for the outbending configurations.

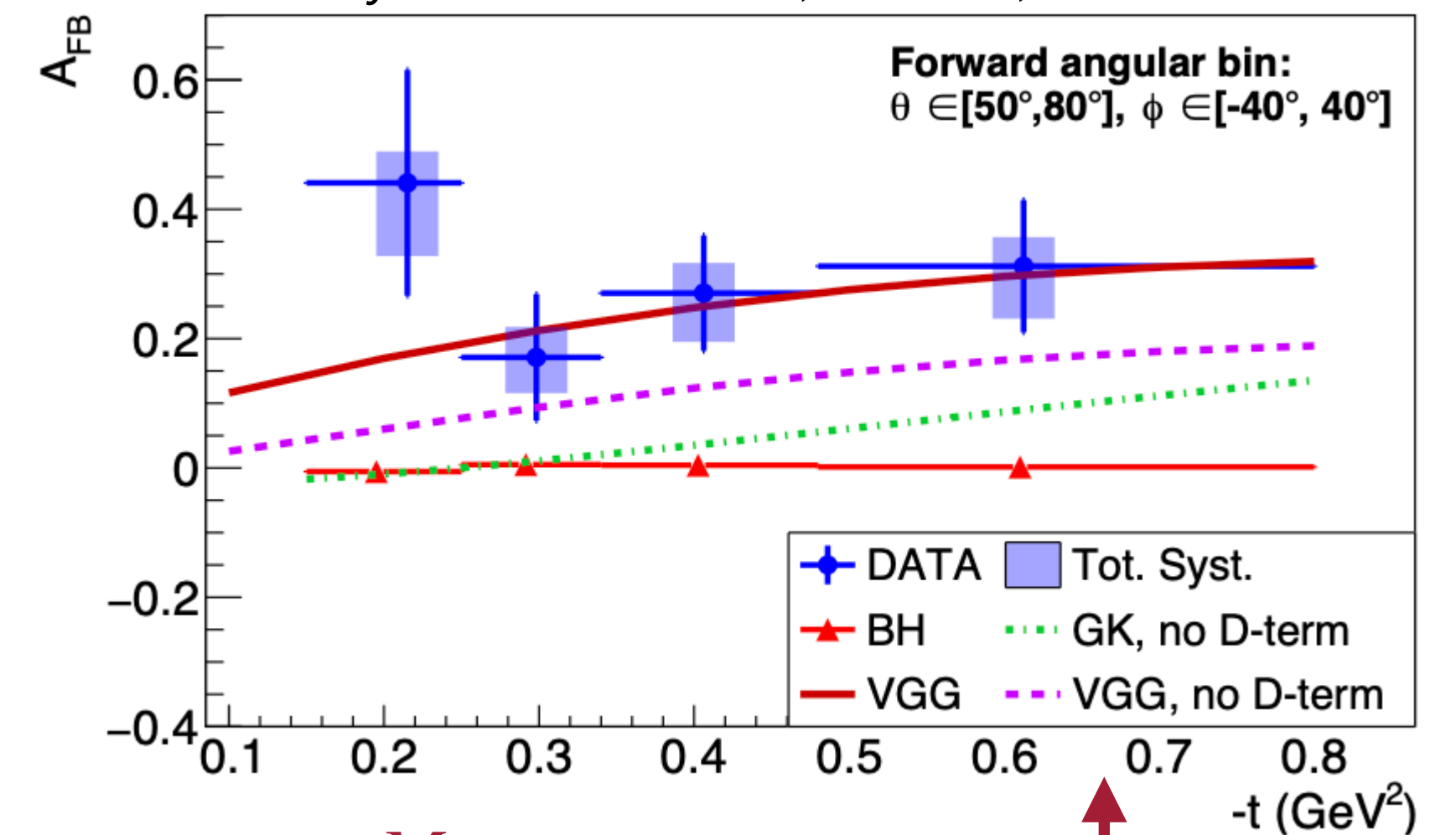
P. Chatagnon et al. (CLAS Collaboration),
Phys. Rev. Lett. 127, 262501, 2021



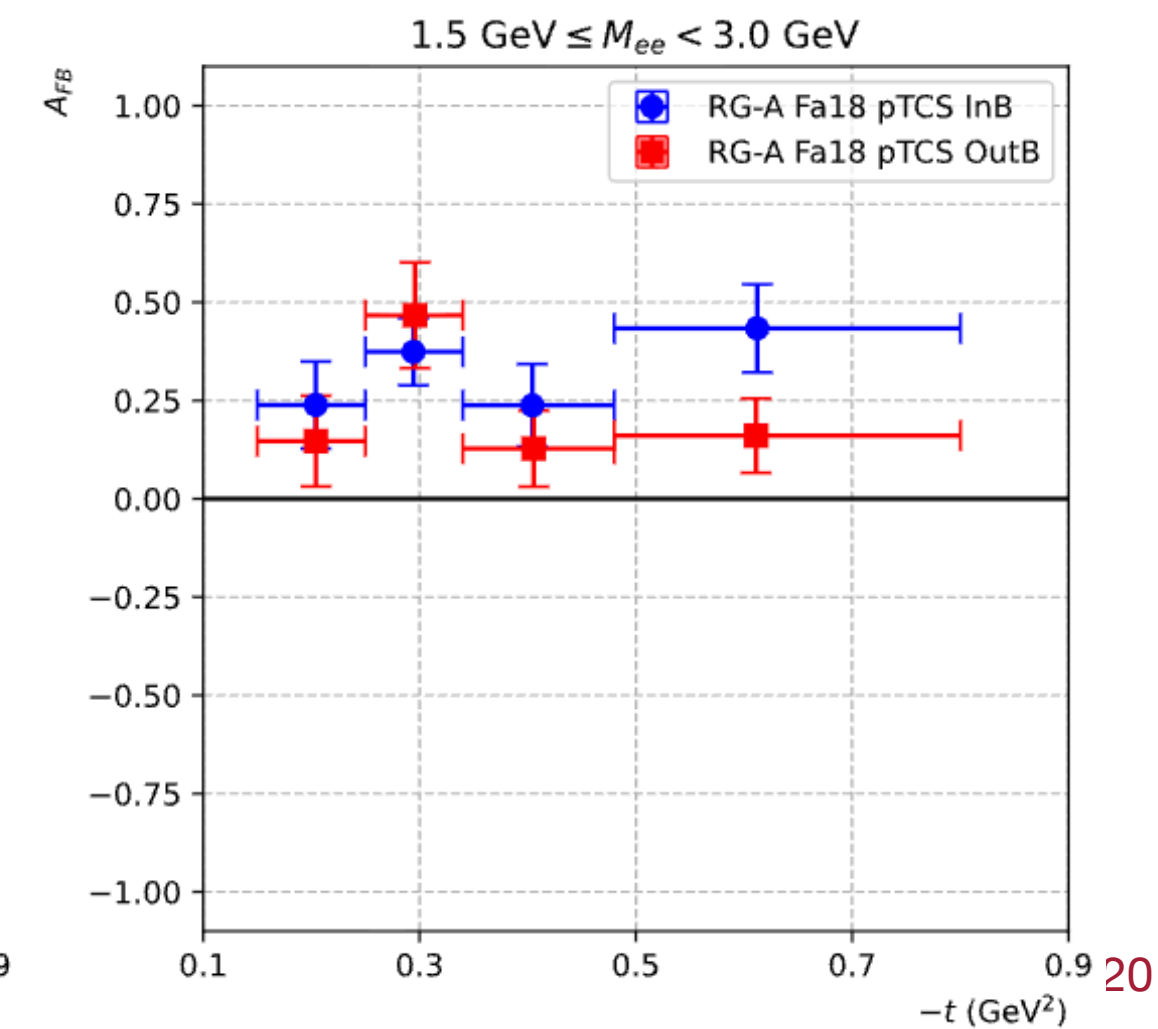
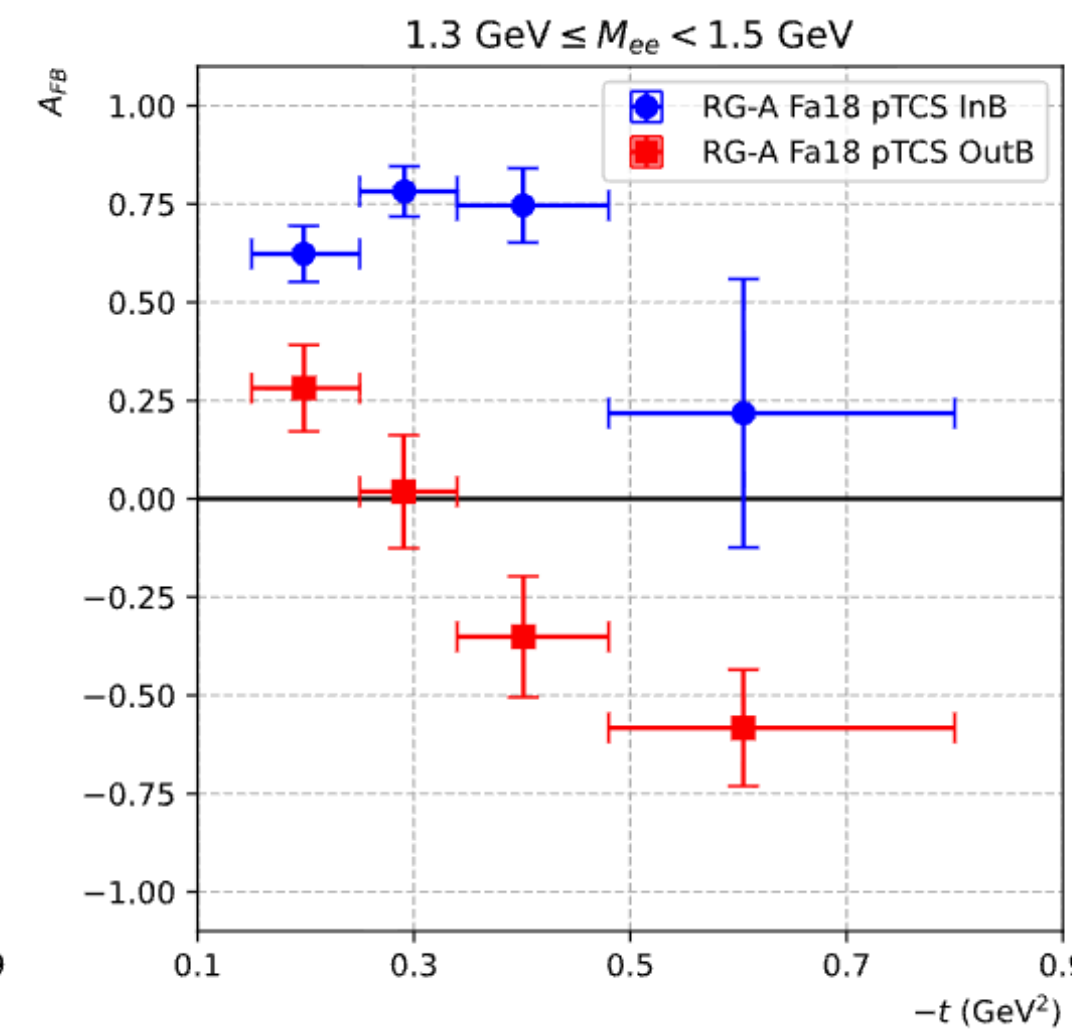
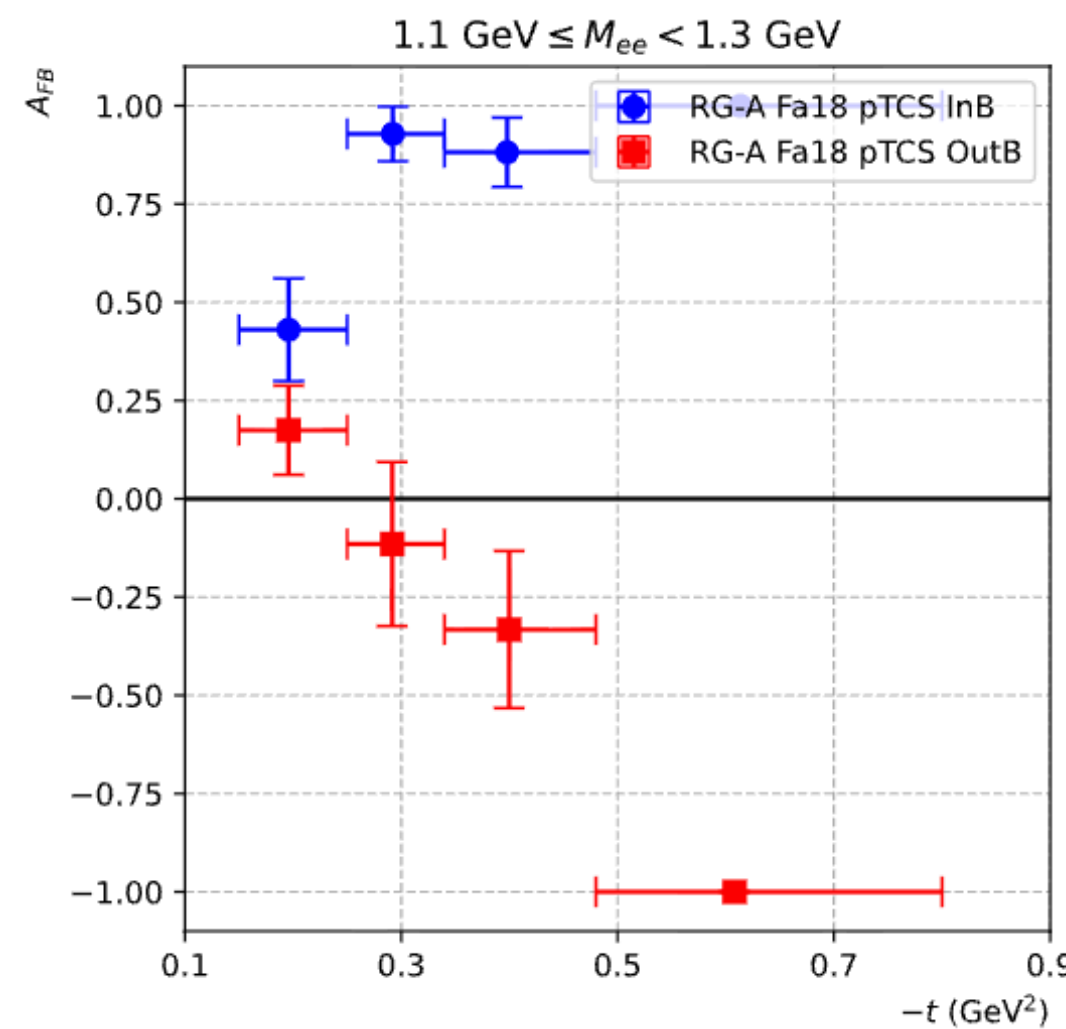
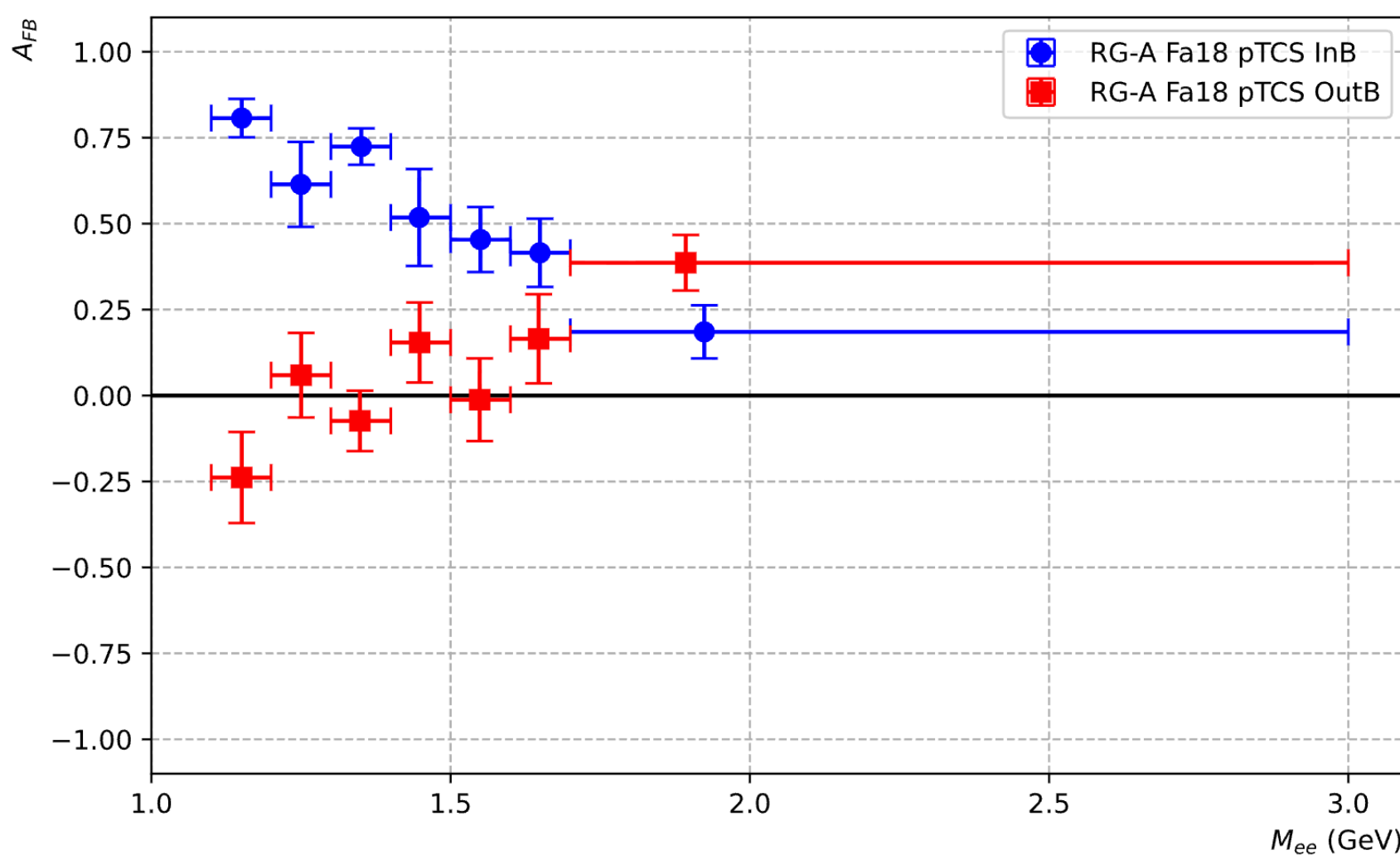
Fa18 Inb



Fa18 Outb

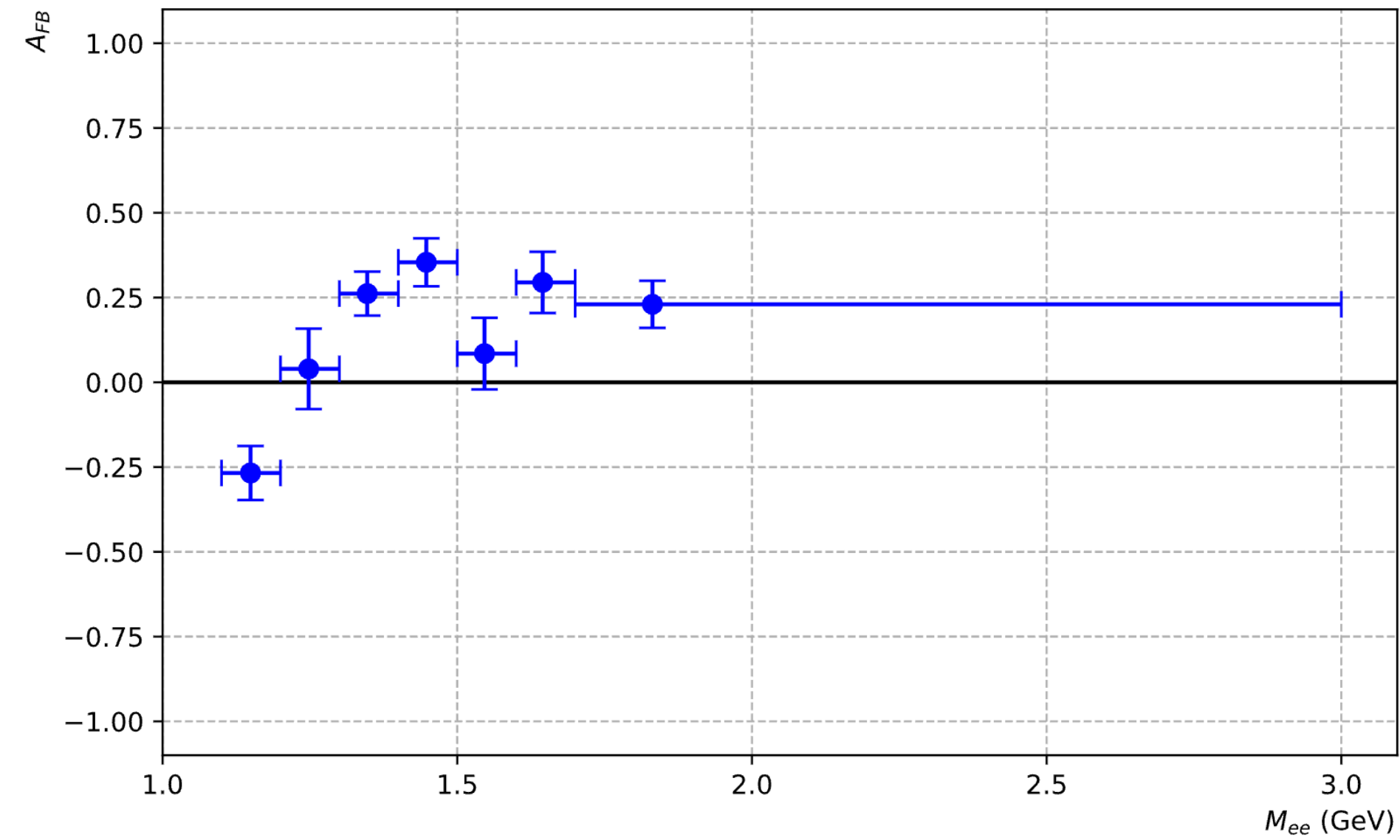


Similar M_{ee} regions, published
RG-A $\langle M_{ee} \rangle = 1.81$ GeV

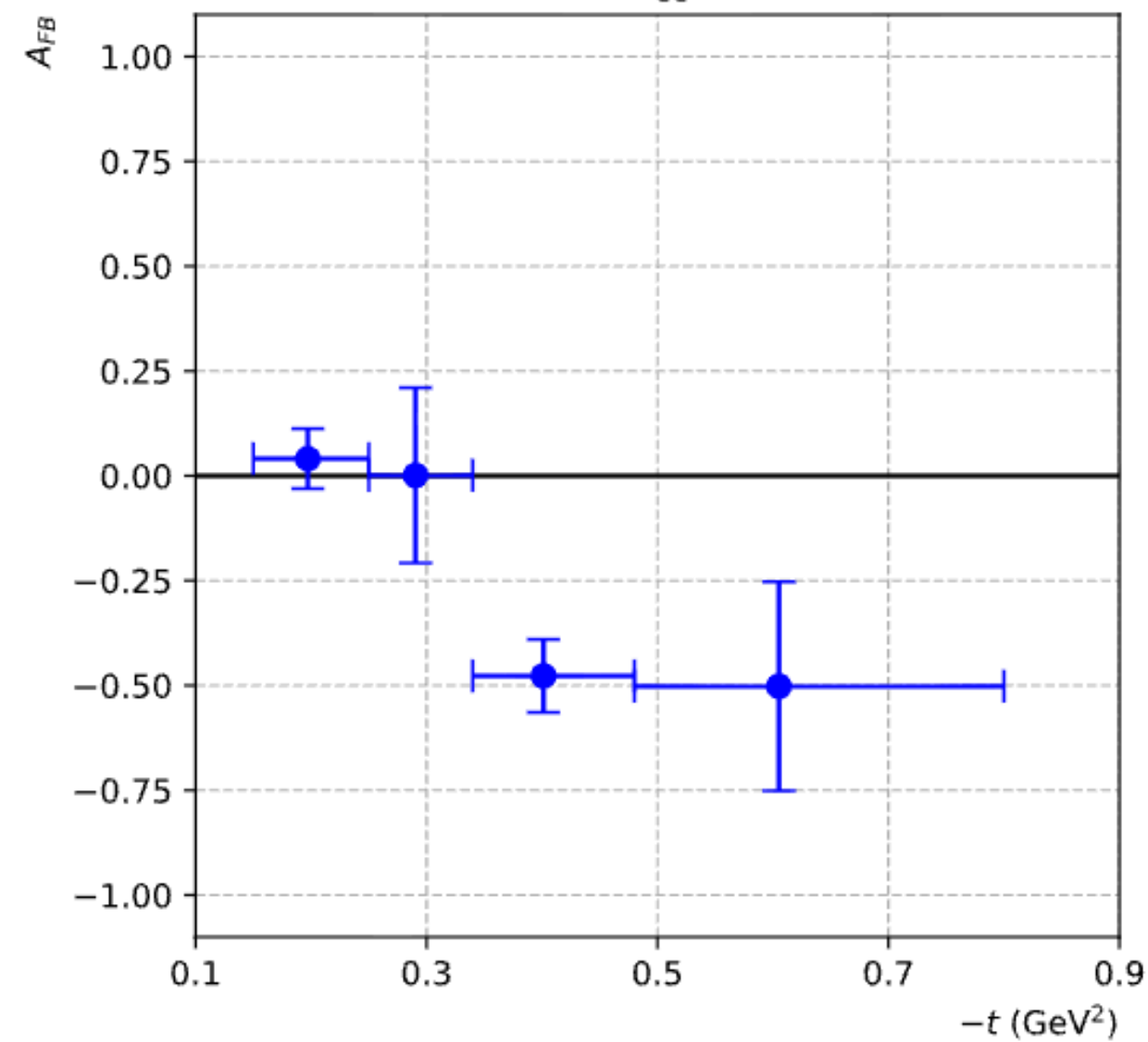


Very Preliminary RG-K Extraction Forward-Backward Asymmetry

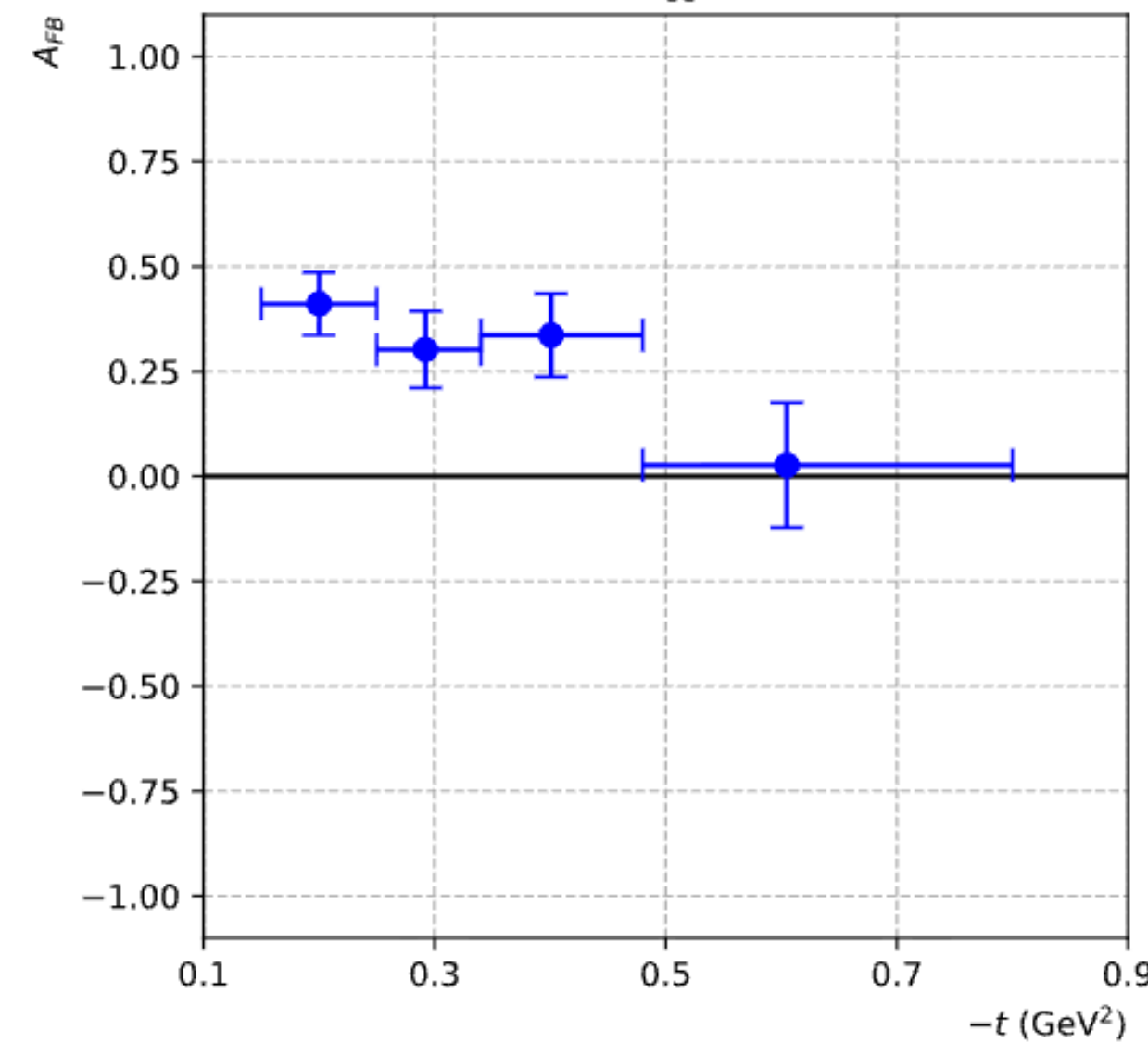
RG-K Sp24 pTCS 8.477 GeV



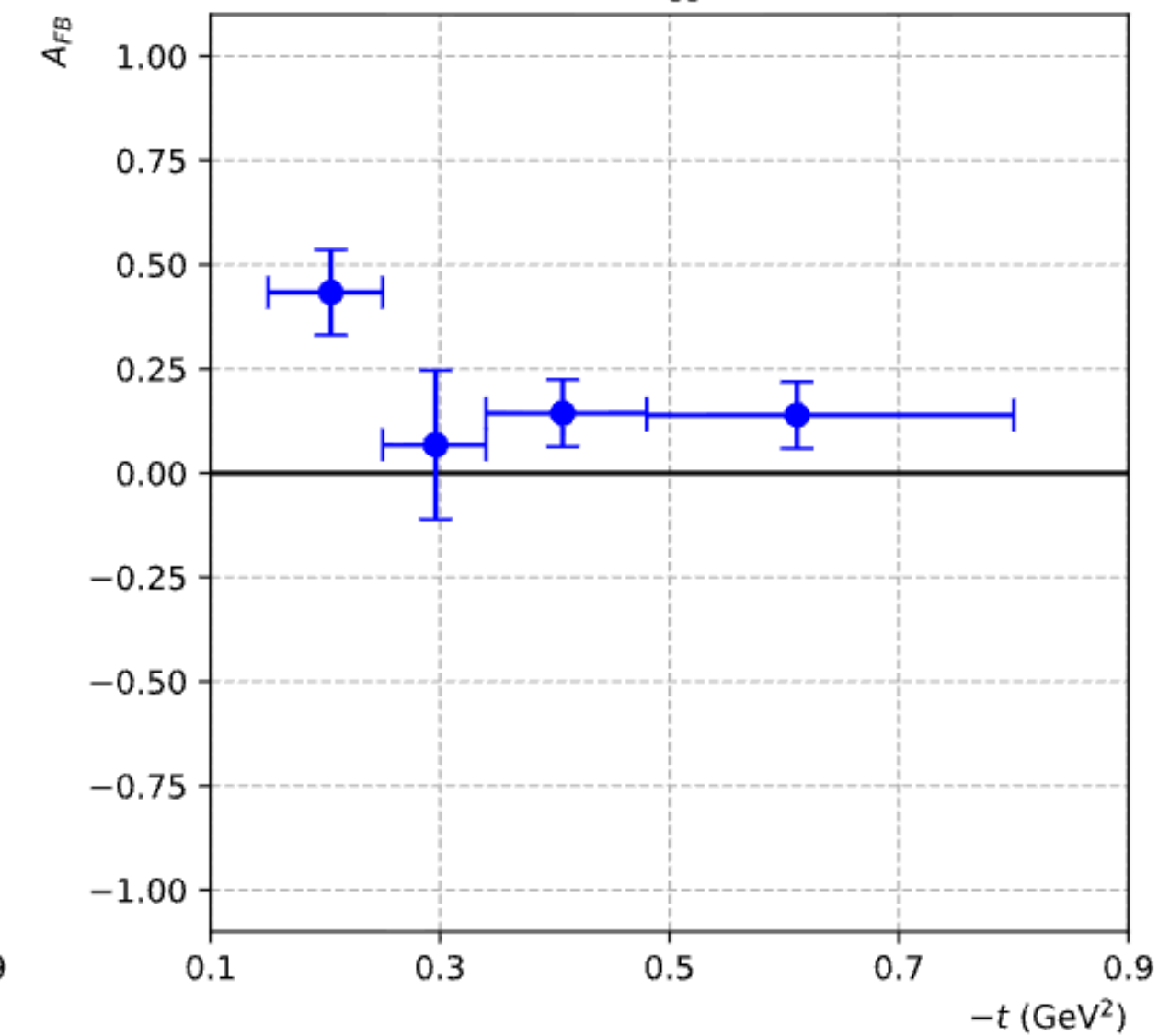
$1.1 \text{ GeV} \leq M_{ee} < 1.3 \text{ GeV}$



RG-K Sp24 pTCS 8.477 GeV
 $1.3 \text{ GeV} \leq M_{ee} < 1.5 \text{ GeV}$



$1.5 \text{ GeV} \leq M_{ee} < 3.0 \text{ GeV}$



Conclusions and Next Steps

- ✓ RG-K Sp24 data now available for analysis and shows encouraging preliminary TCS results
 - ▶ Statistics enable higher precision measurements of TCS observables, particularly at lower range in M_{ee}
 - ▶ Multidimensional extractions of photon polarization asymmetry using multiple fitting techniques are developed
 - ▶ Preliminary look at forward-backward asymmetry is promising although not yet fully developed for outbending configuration, will be improved with updated simulations
- **Plan to draft CAA following collaboration meeting to submit for review and request of approval**

Thank you, questions?

Backup Slides

Obtaining GPD Dependence of TCS σ_{INT}

$$\frac{d^4\sigma_{INT}}{dQ'^2 dt d\Omega} = A \frac{1 + \cos^2\theta}{\sin\theta} \{ \cos\phi \text{Re}\tilde{M}^{--} - \nu \sin\phi \text{Im}\tilde{M}^{--} \}$$

↓

$$\tilde{M}^{--} = F_1 \mathcal{H} - \xi (F_1 + F_2) \tilde{\mathcal{H}} - \frac{t}{4m_p^2} F_2 \mathcal{E}$$

↓

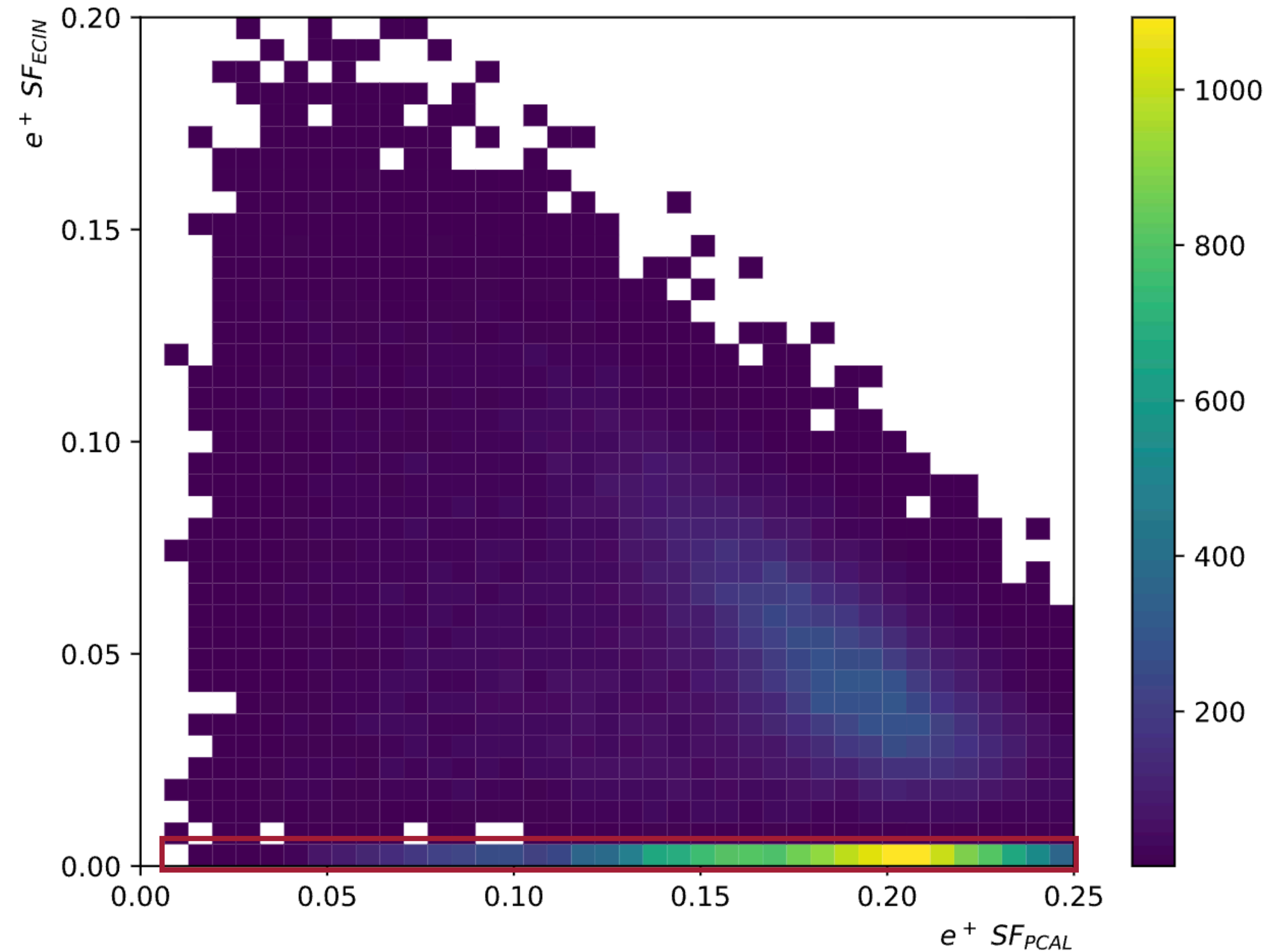
$$\text{Re}\mathcal{H}(\xi, t) + i\text{Im}\mathcal{H}(\xi, t) = \int_{-1}^1 dx H(x, \xi, t) \left(\frac{1}{\xi - x + i\epsilon} - \frac{1}{\xi + x + i\epsilon} \right)$$

&

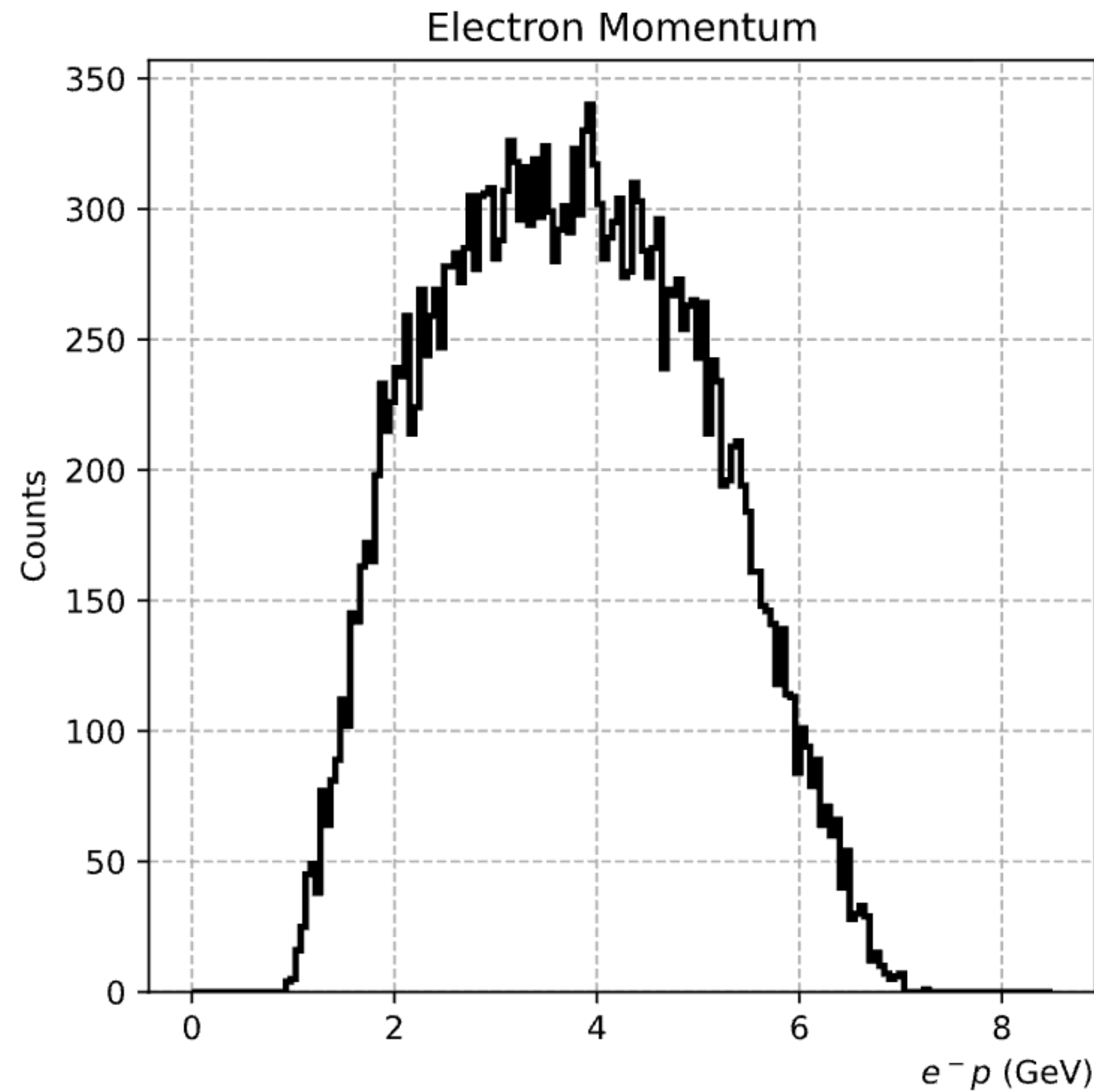
$$\text{Re}\mathcal{H}(\xi, t) \stackrel{L.O.}{=} D(t) + \mathcal{P} \int_0^1 dx \left(\frac{1}{\xi - x} - \frac{1}{\xi + x} \right) \text{Im}\mathcal{H}(\xi, t)$$

High Frequency Strip Removal

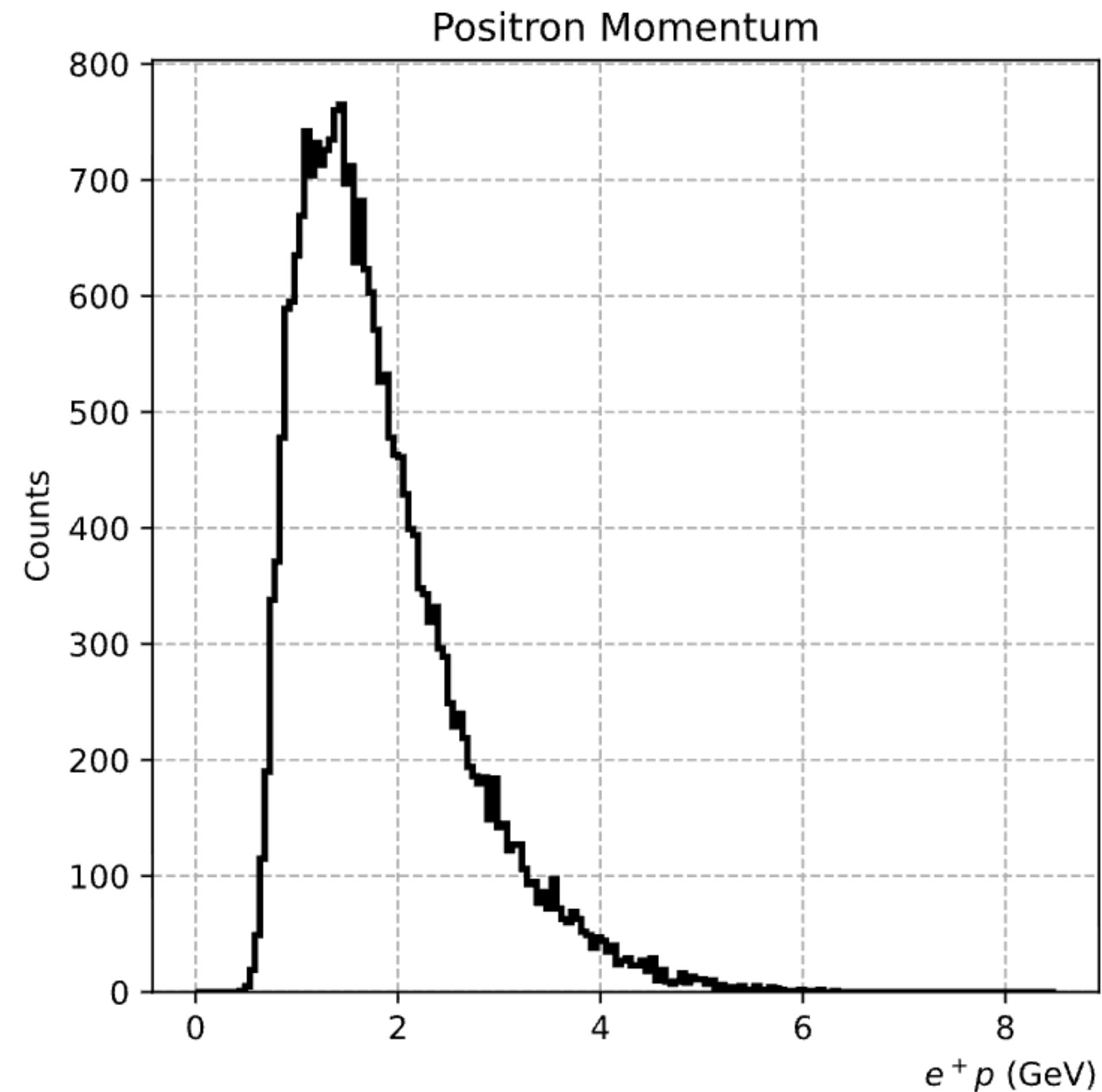
- High frequency region at low ECIN positron partial sampling fraction, these seem to be events that deposit high amounts of energy in PCAL but no energy in outer layers of the ECAL
 - We decided to also enforce $p_{PCAL}^{e^\pm} > 0.1$, $p_{ECIN}^{e^\pm} > 0$, to avoid these high frequency regions



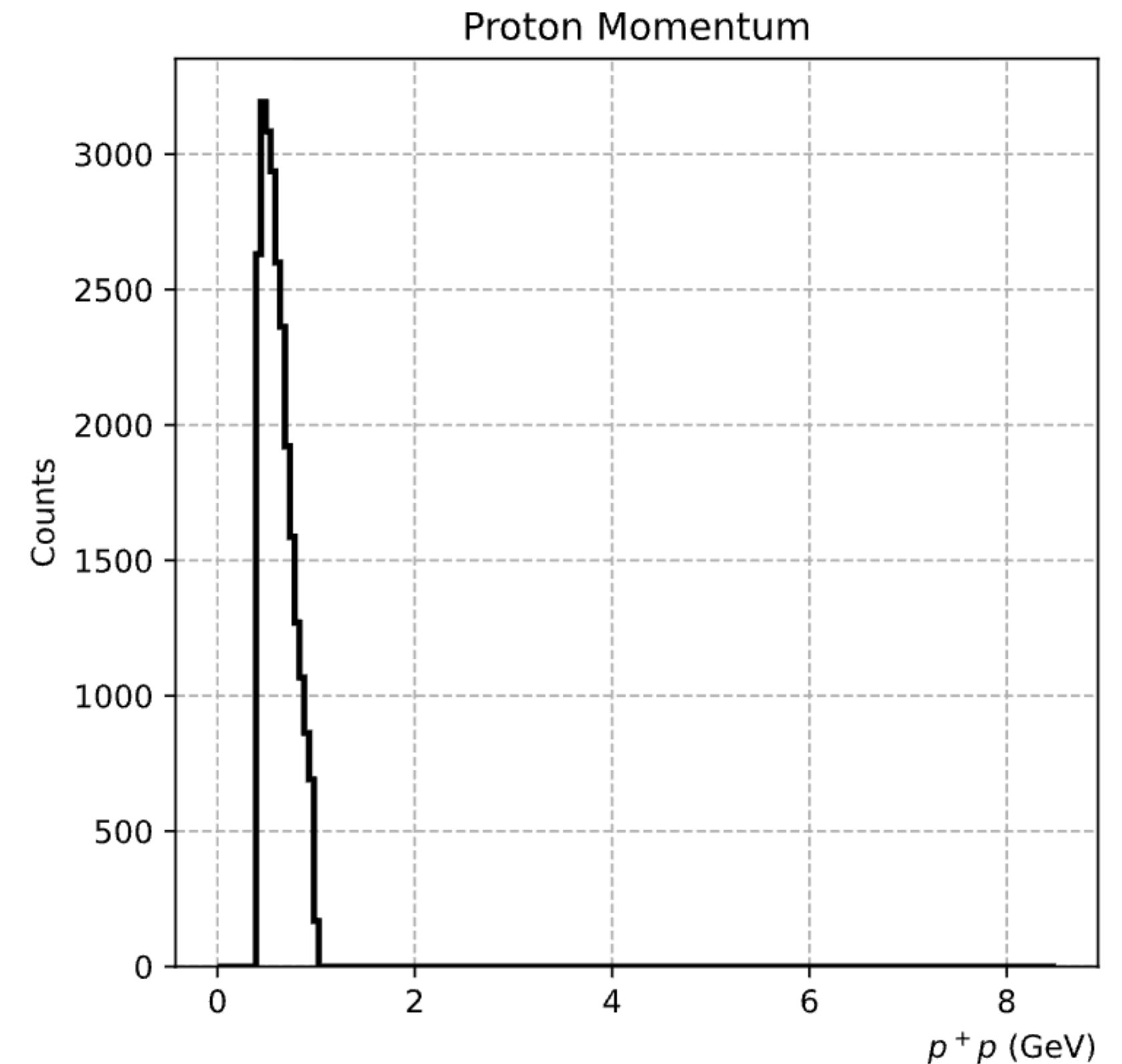
Kinematic Distributions After Cuts — Momentum Distributions



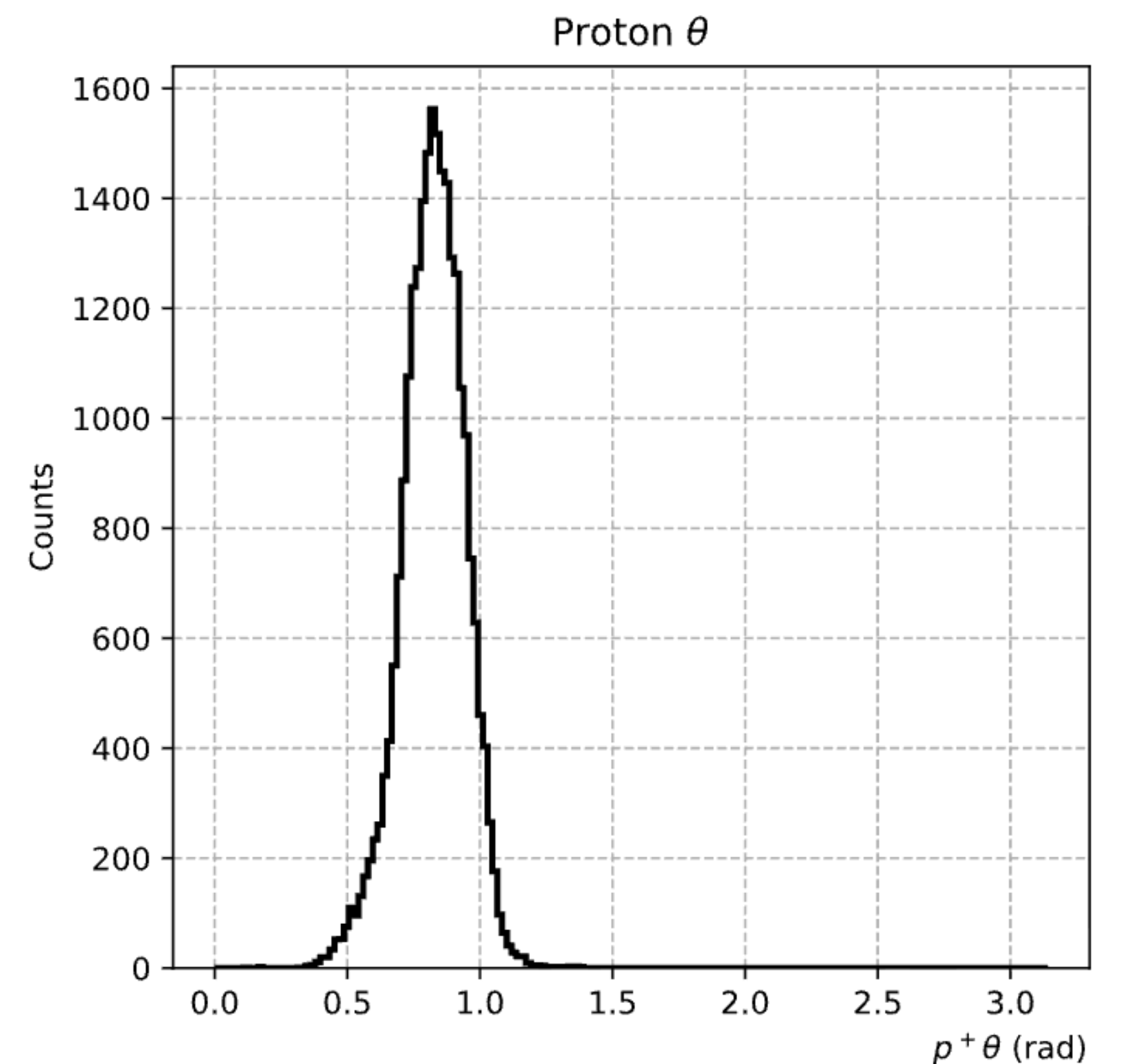
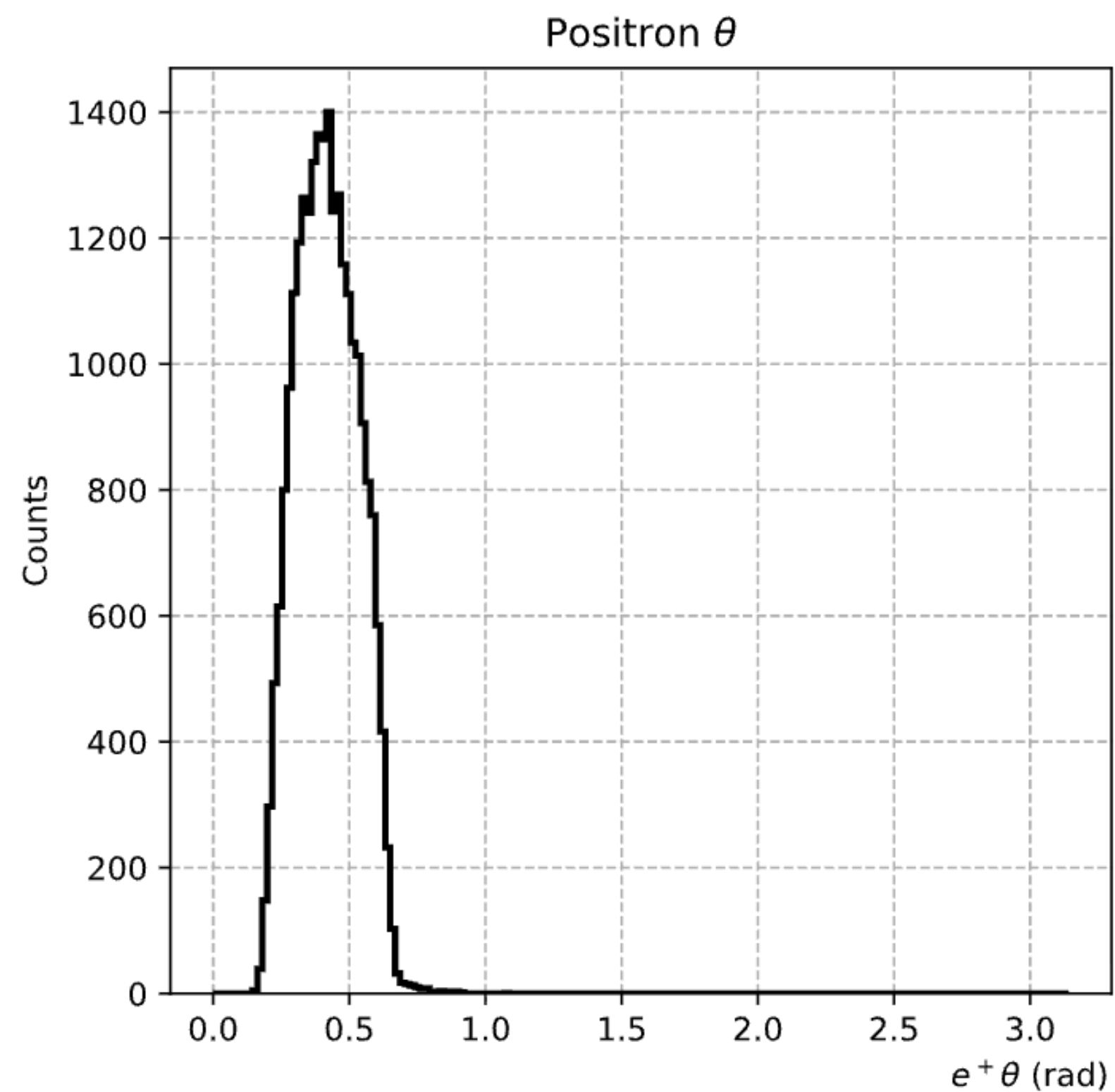
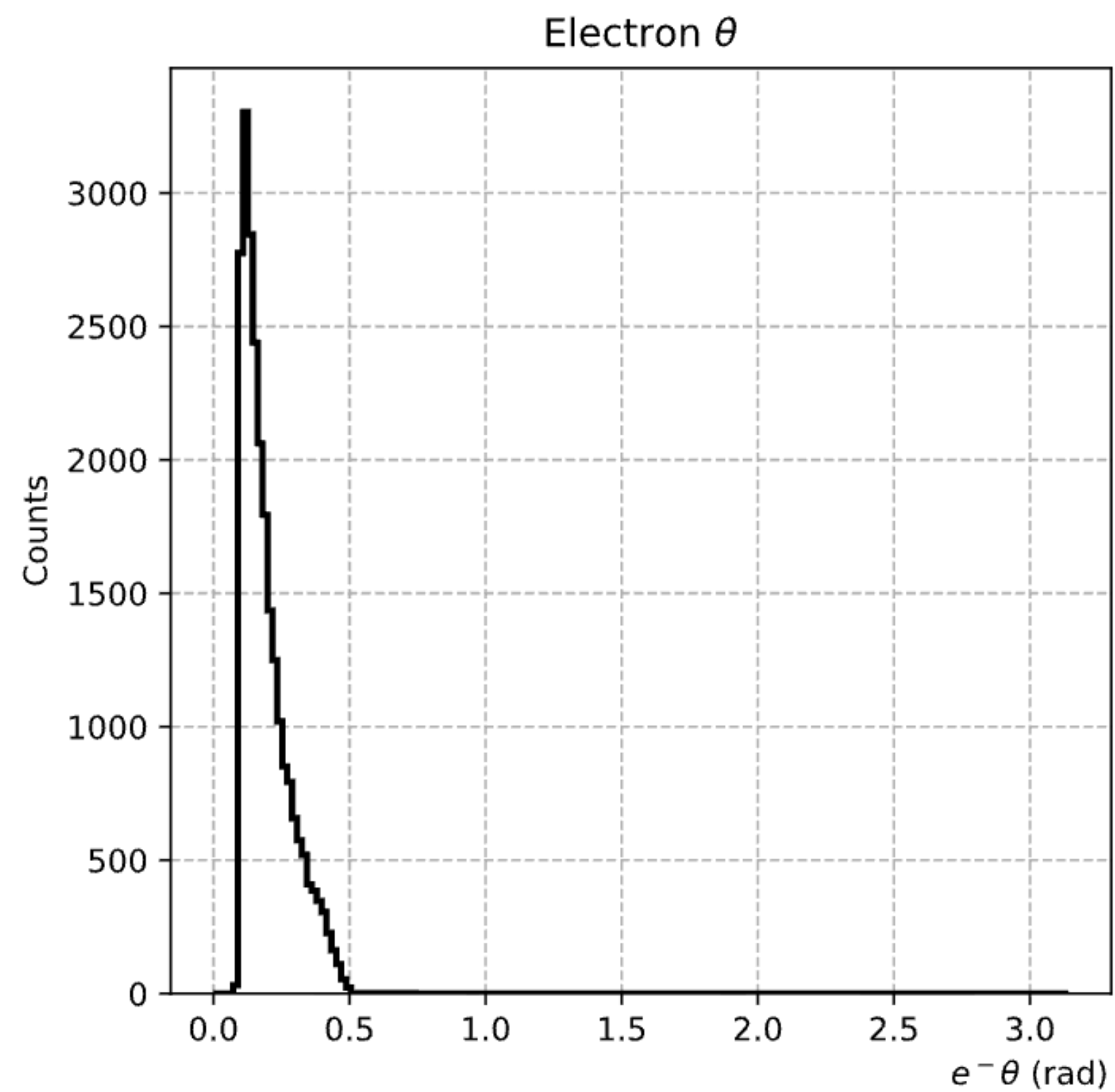
e^- momentum distribution symmetric (not amplification in region beyond HTCC efficiency) after cuts all applied.



e^+ momentum distribution predominantly within HTCC thresholds after cuts all applied.

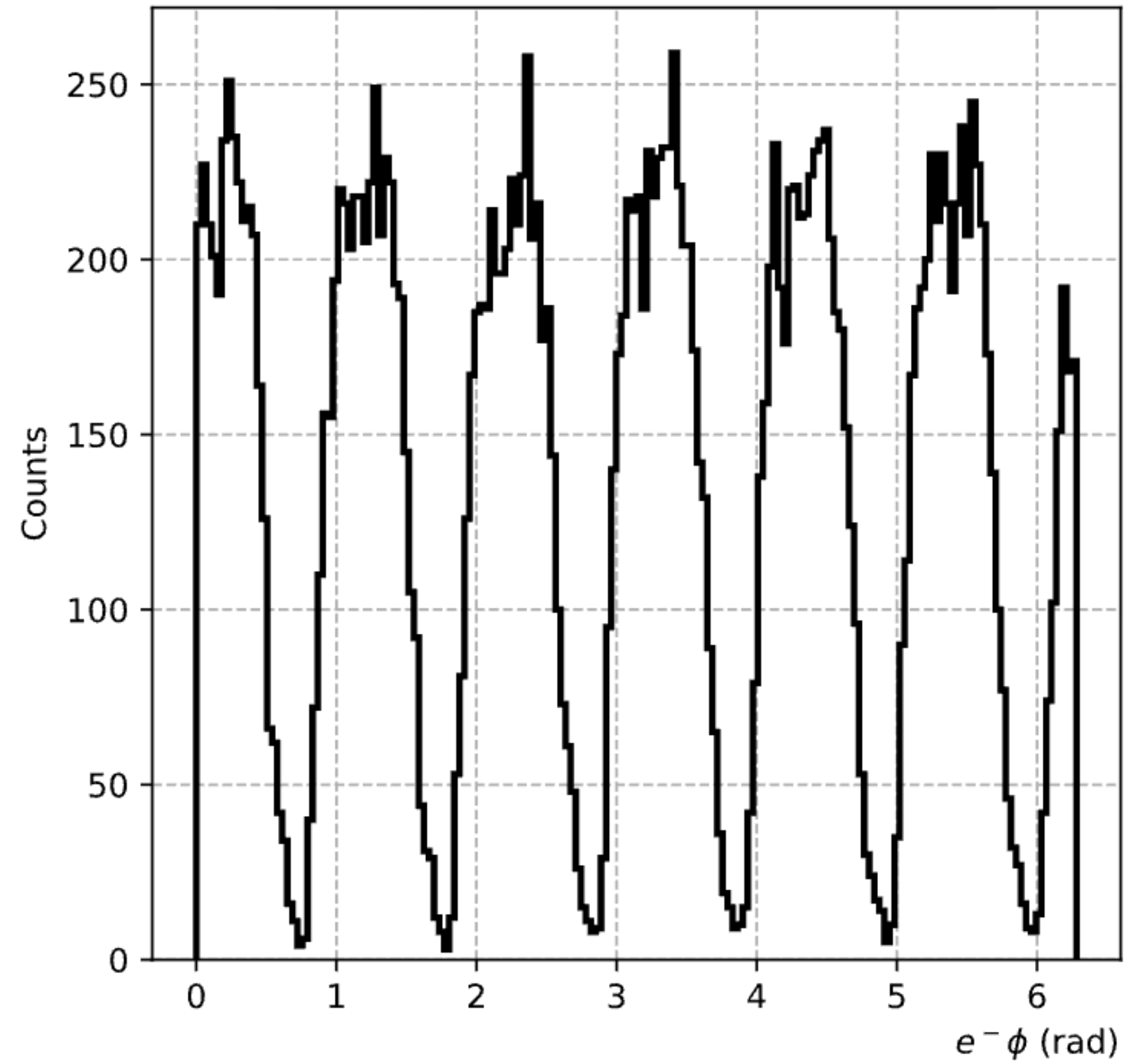


Kinematic Distributions After Cuts — Lab θ Distributions

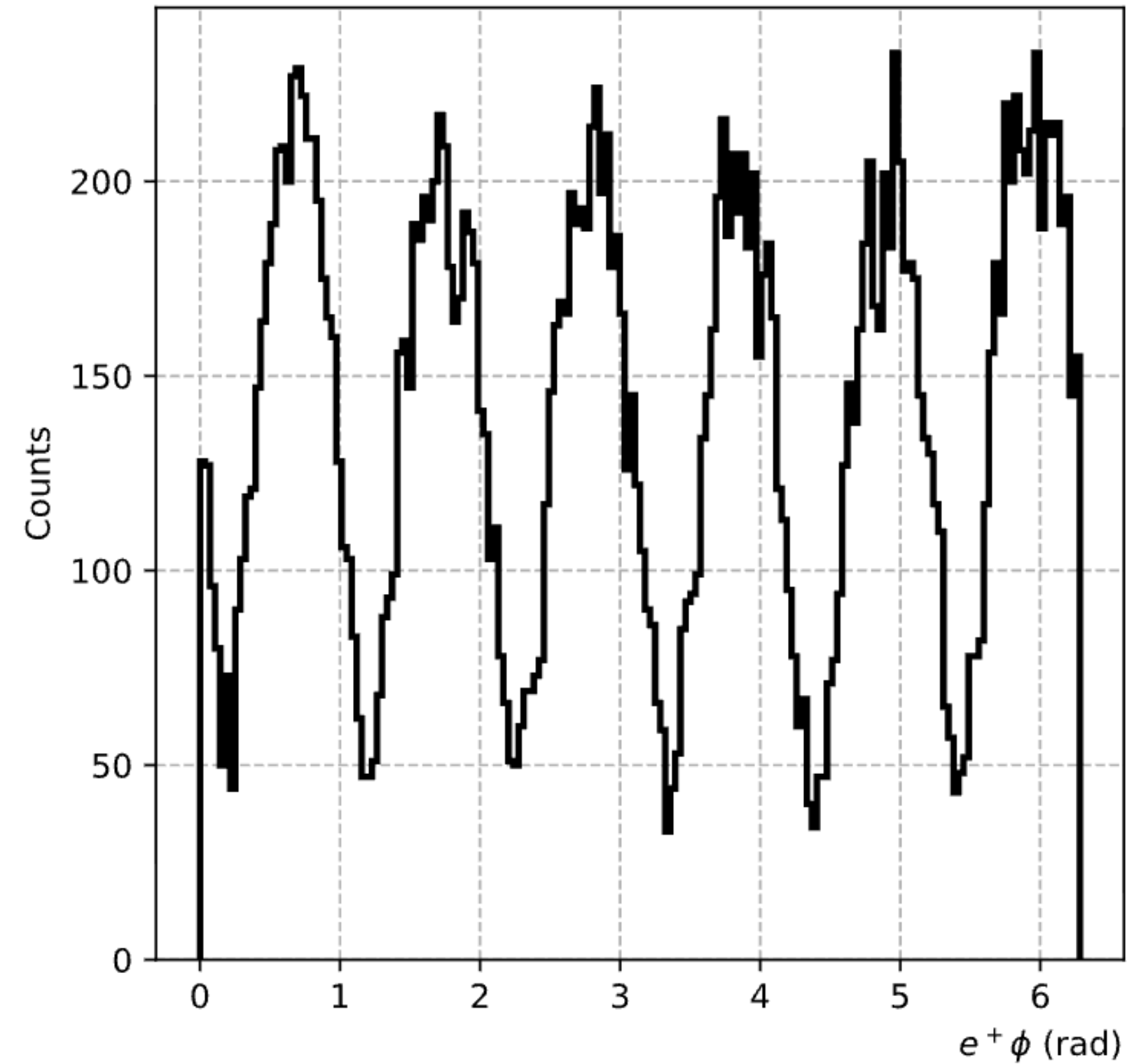


Kinematic Distributions After Cuts — Lab ϕ Distributions

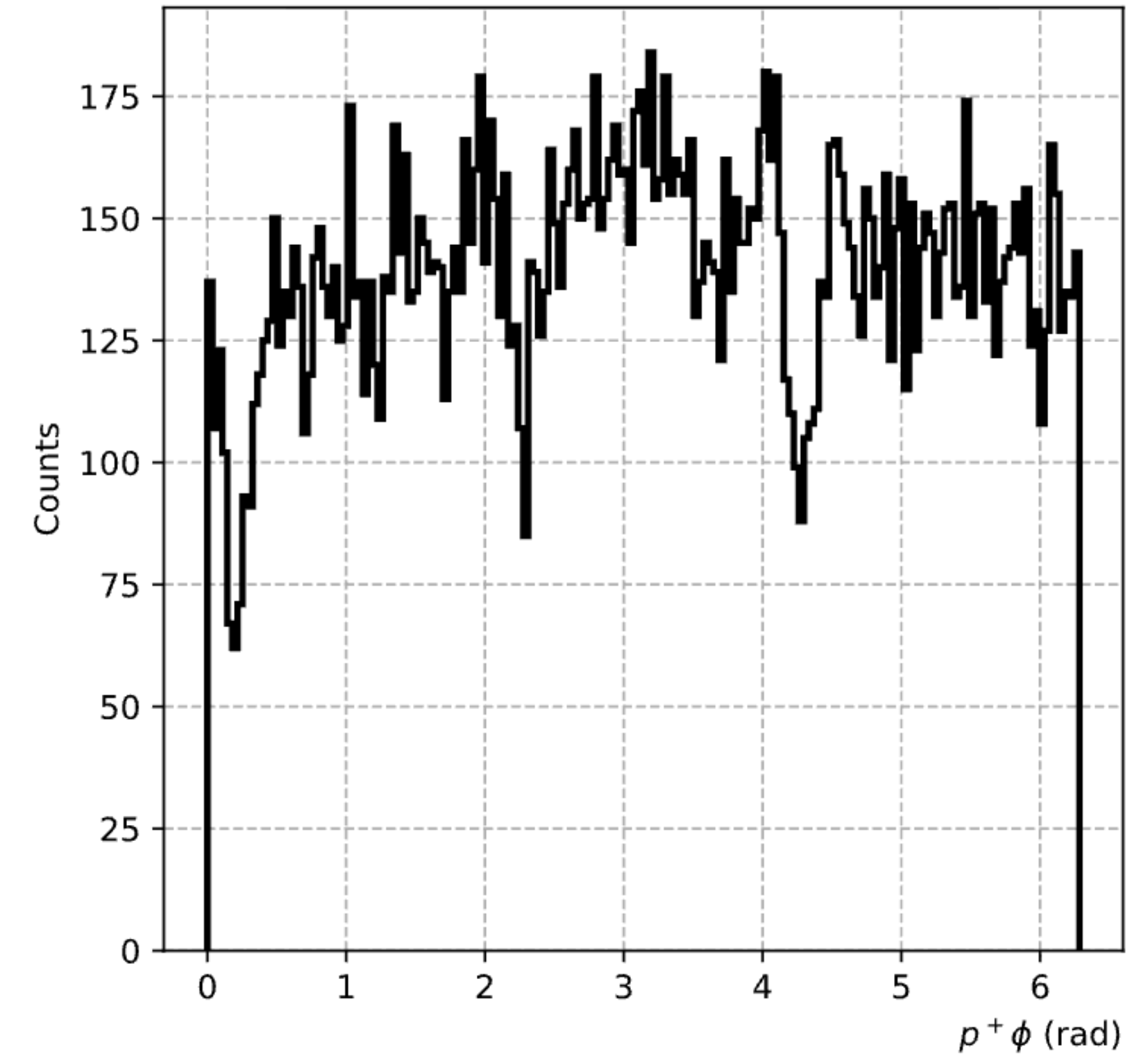
Electron ϕ



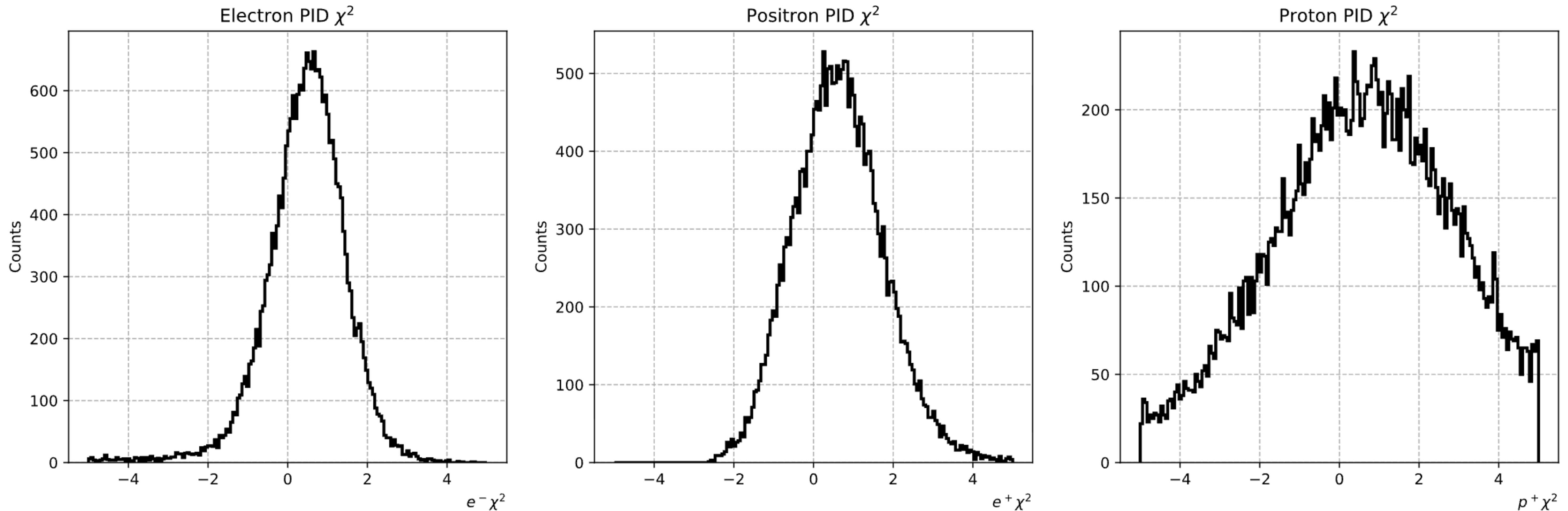
Positron ϕ



Proton ϕ

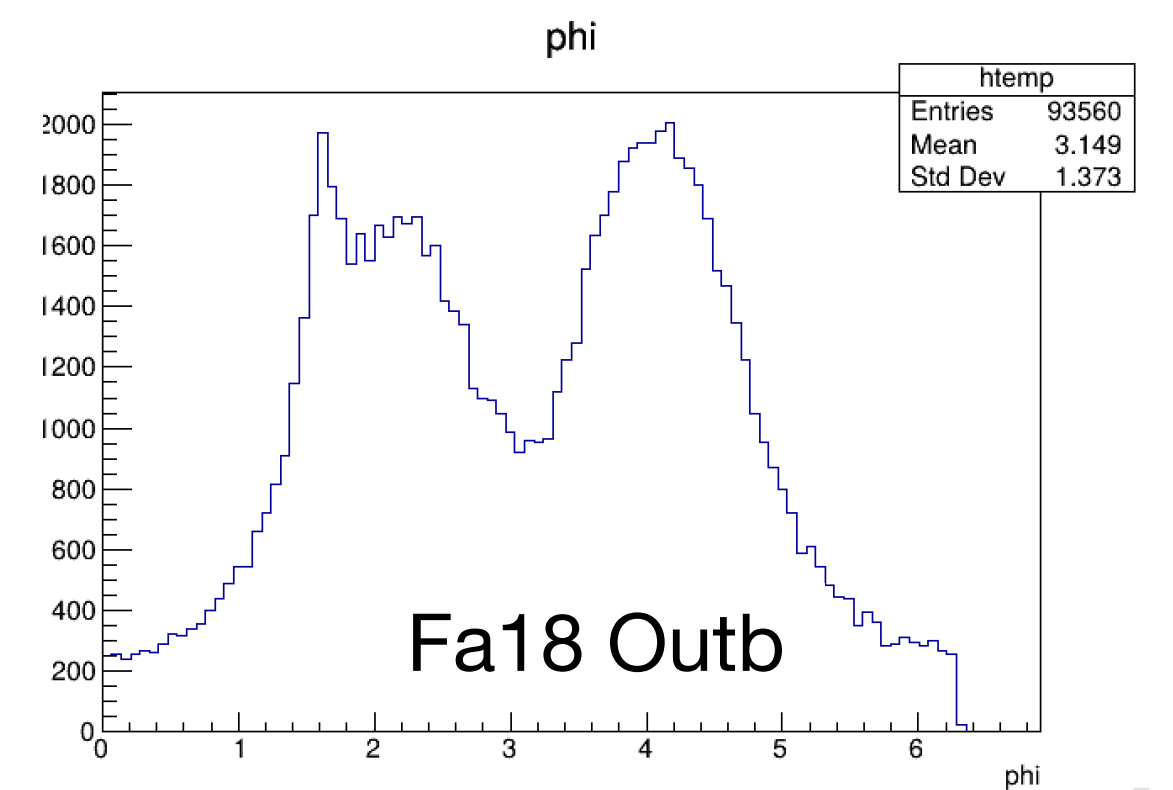
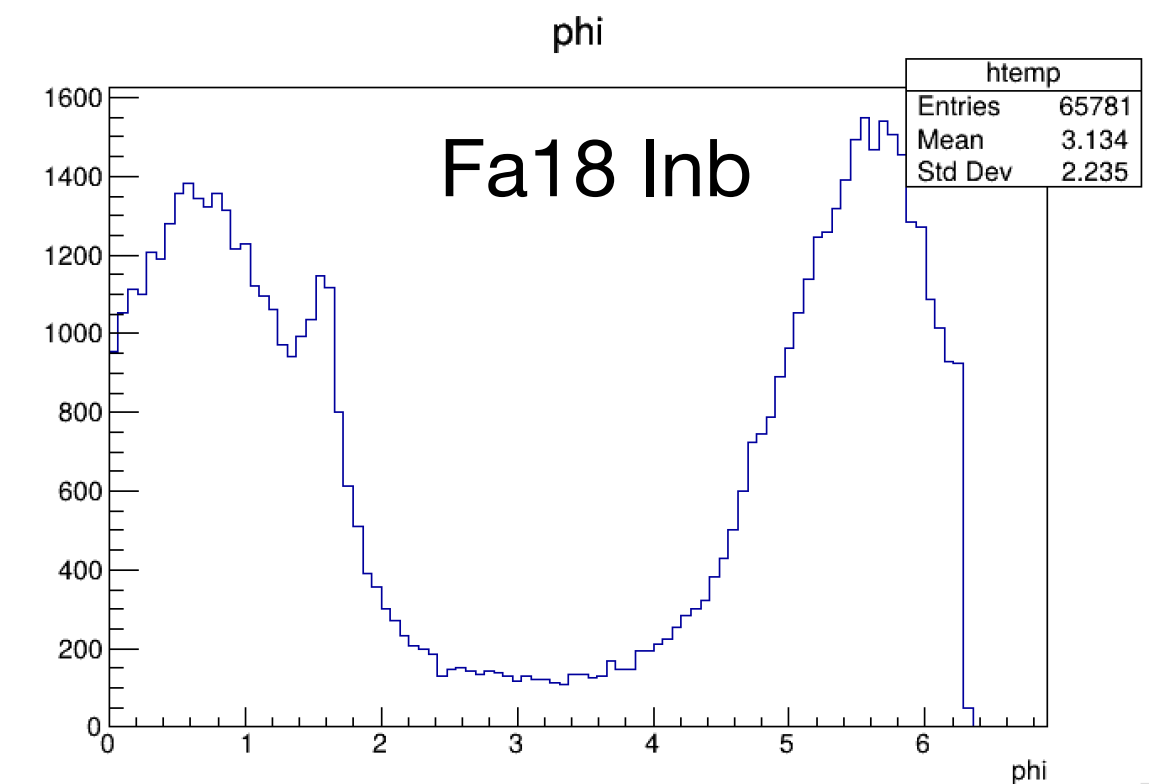
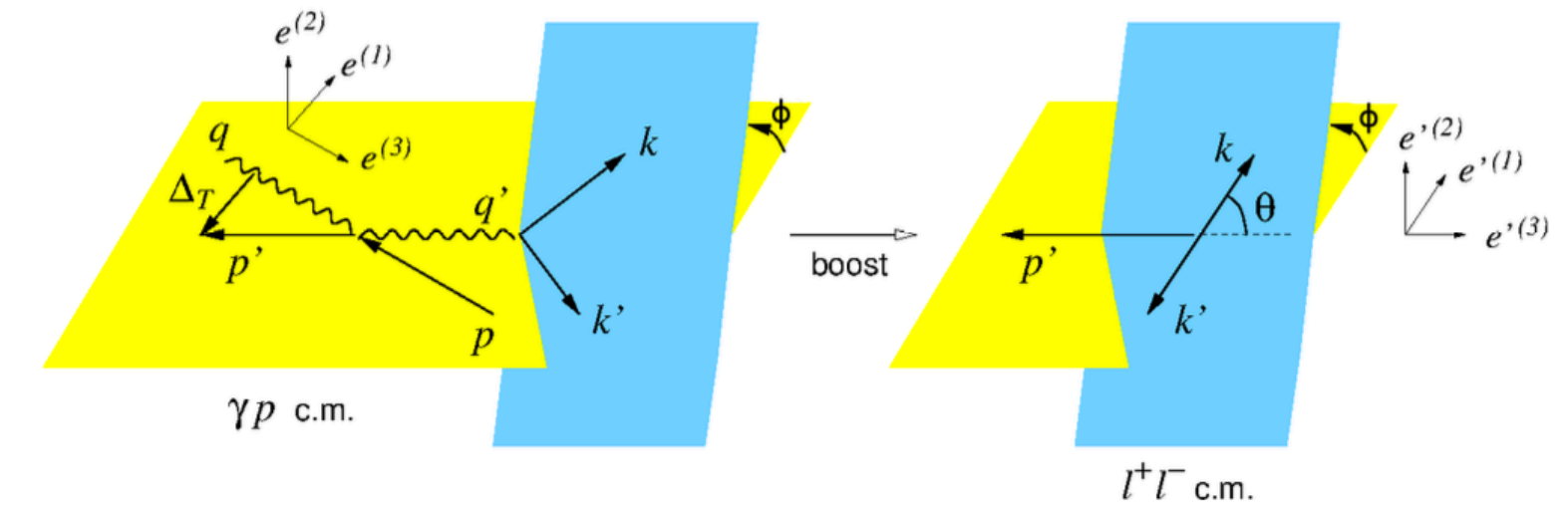
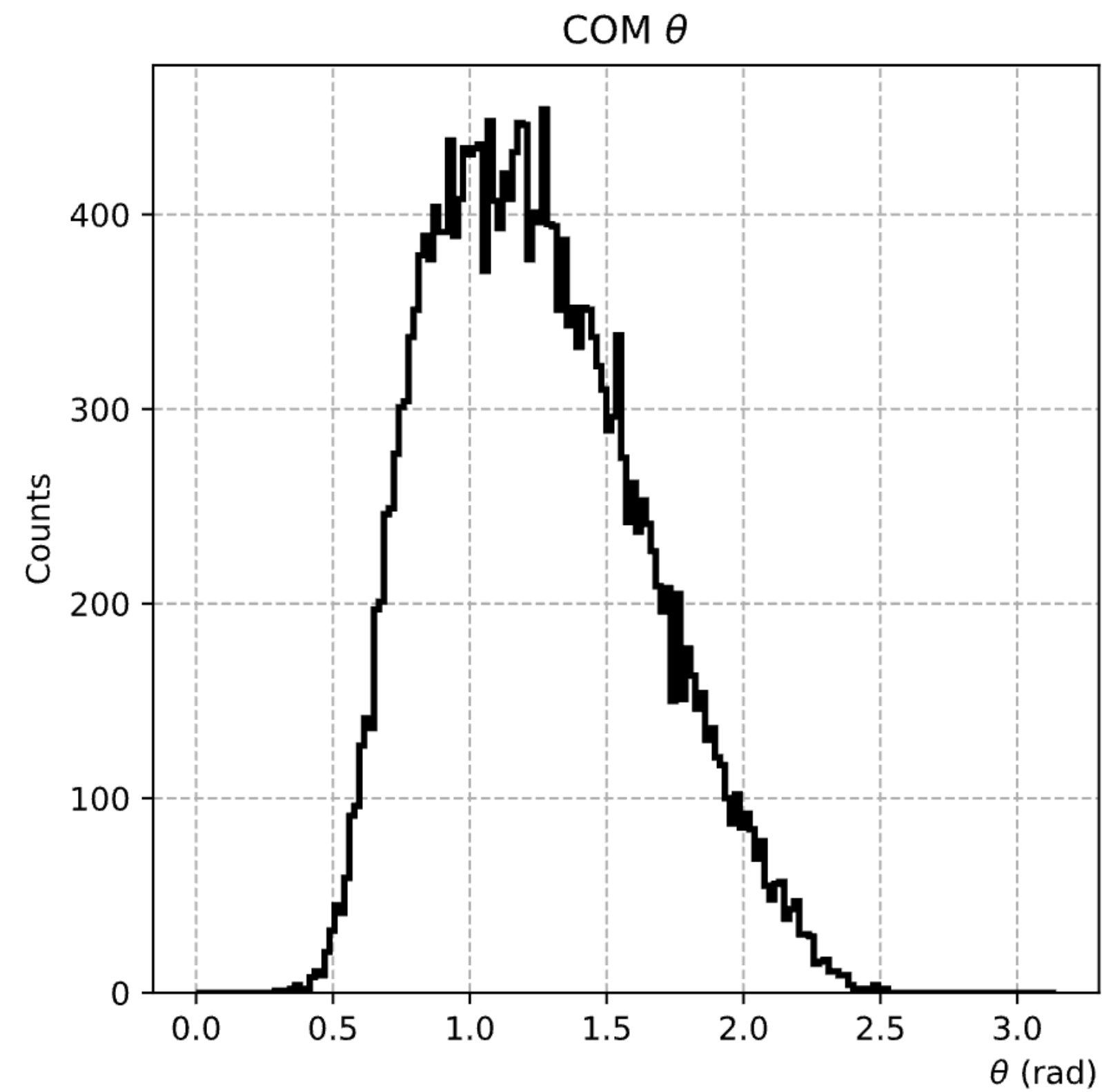
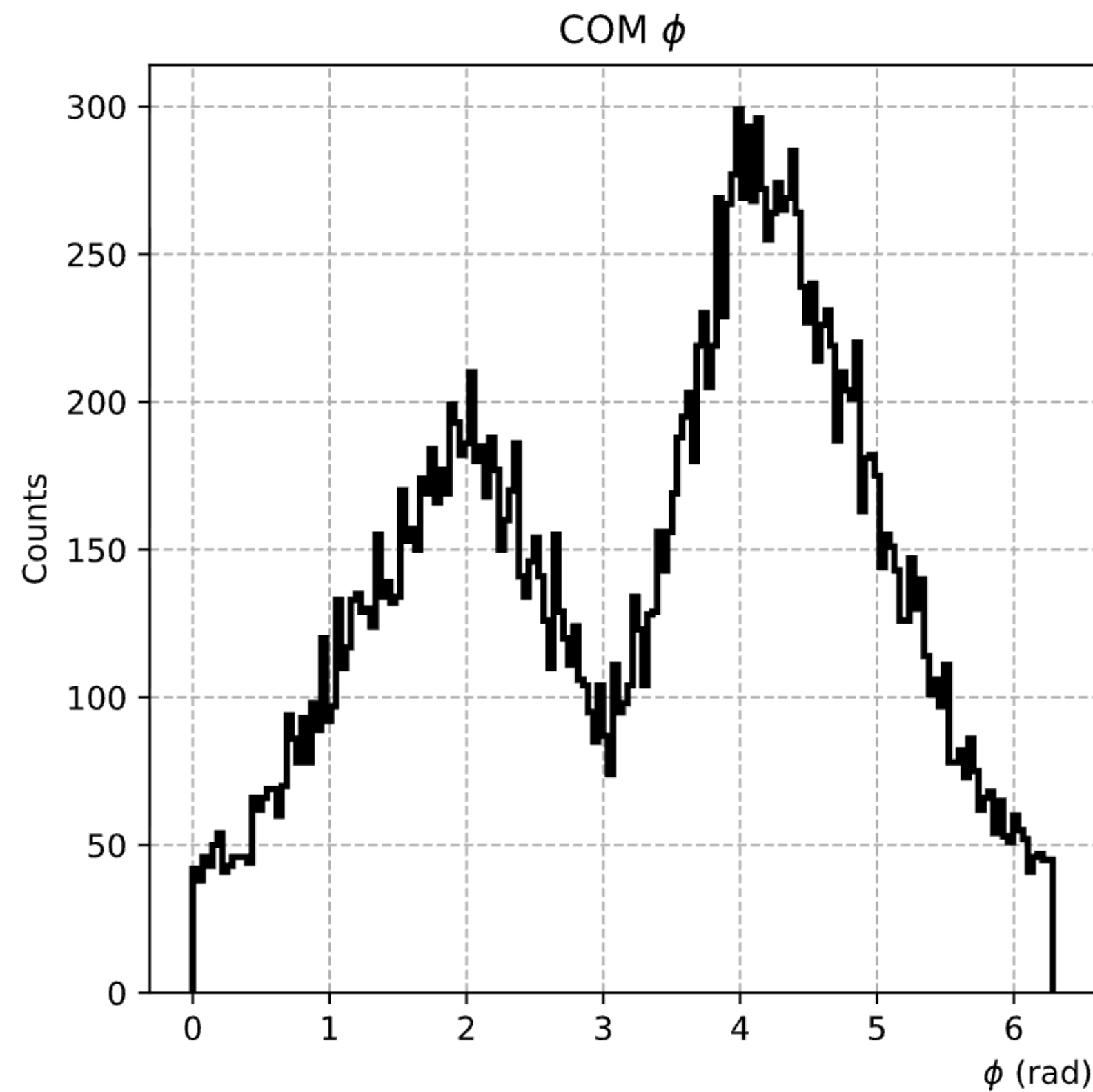


Kinematic Distributions After Cuts — PID χ^2 Distributions



Visually, all χ^2 distributions have a distribution that is centred greater than one. Also not much evidence of pion contamination in either e^\pm distribution (amplified left-hand tail in PID χ^2).

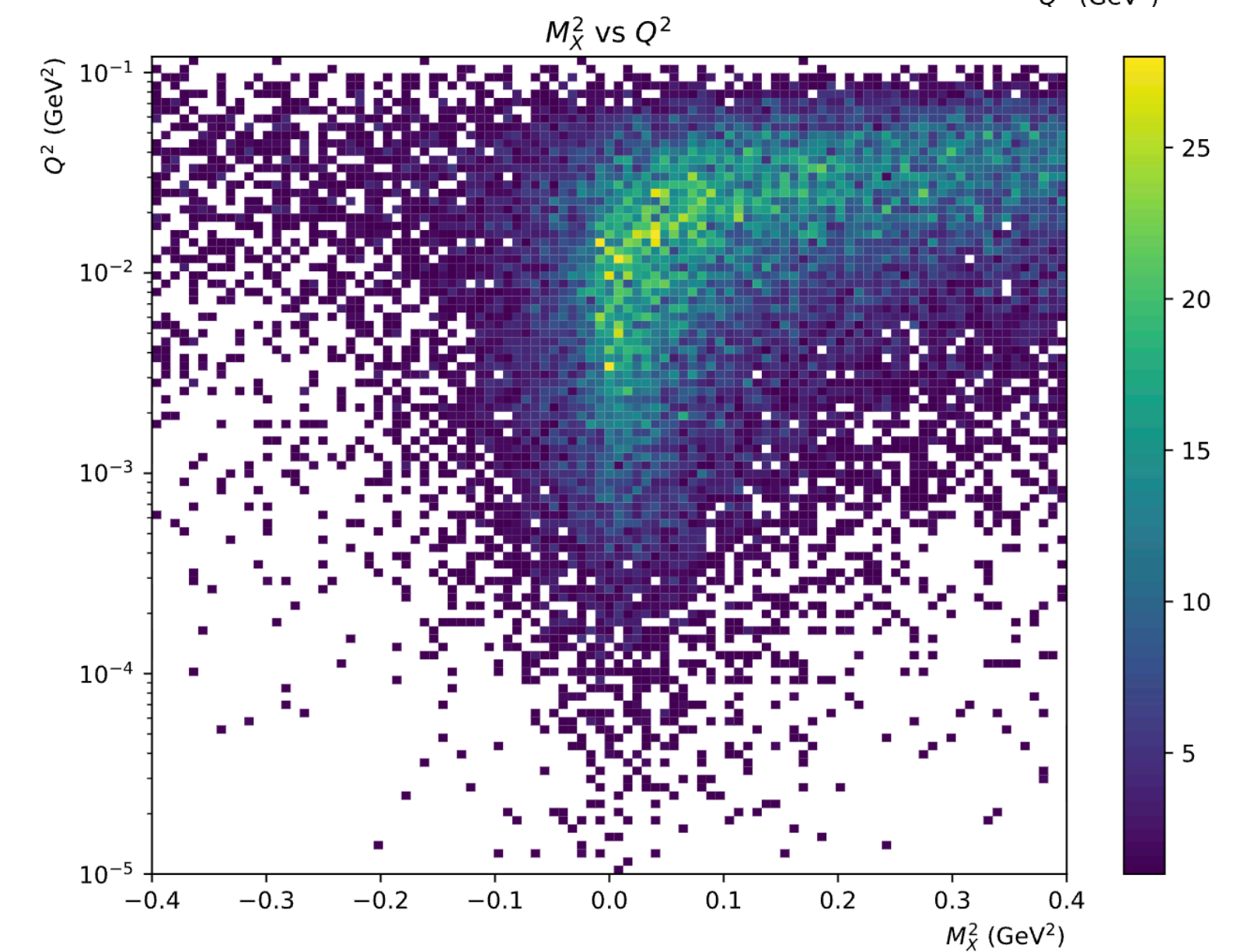
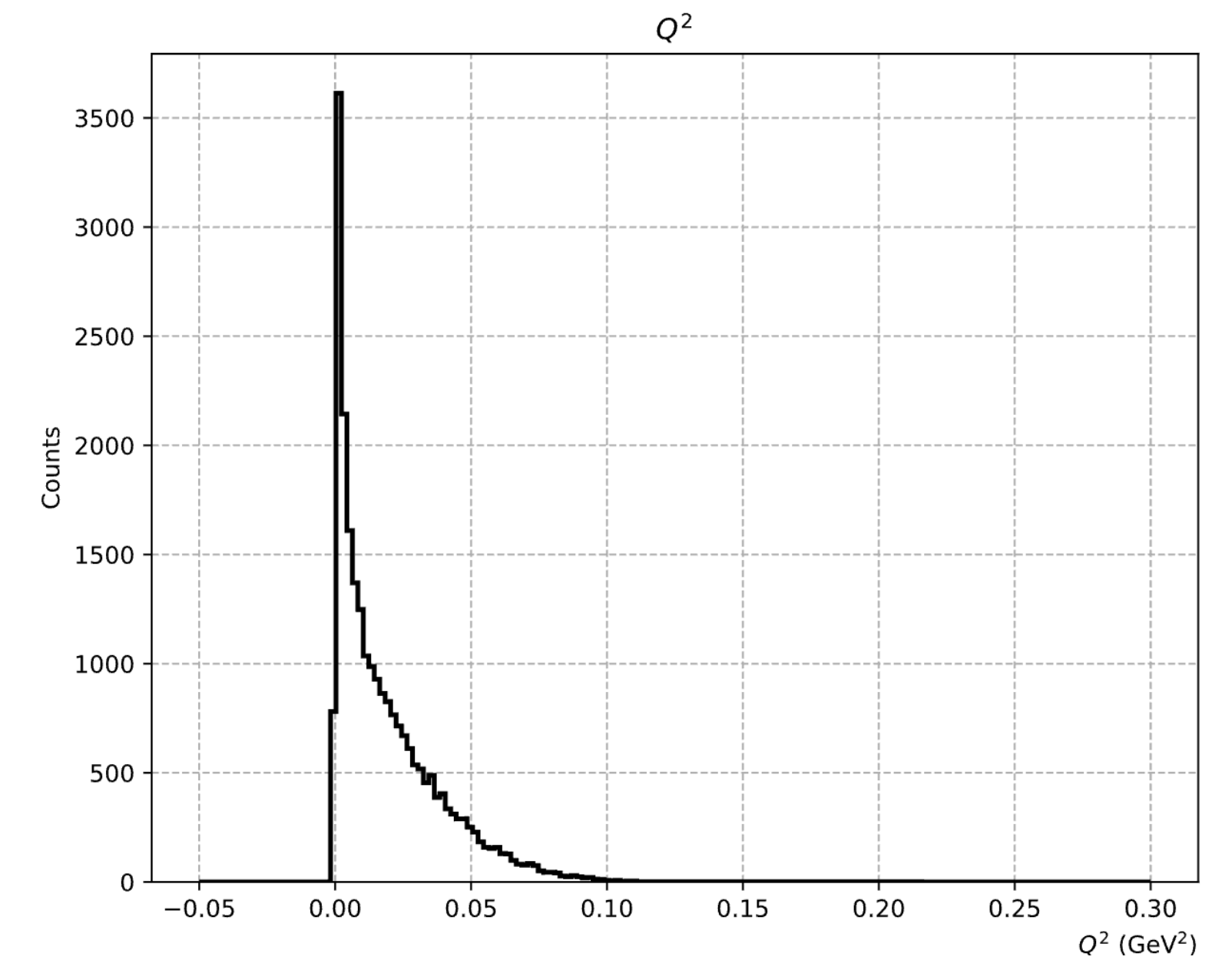
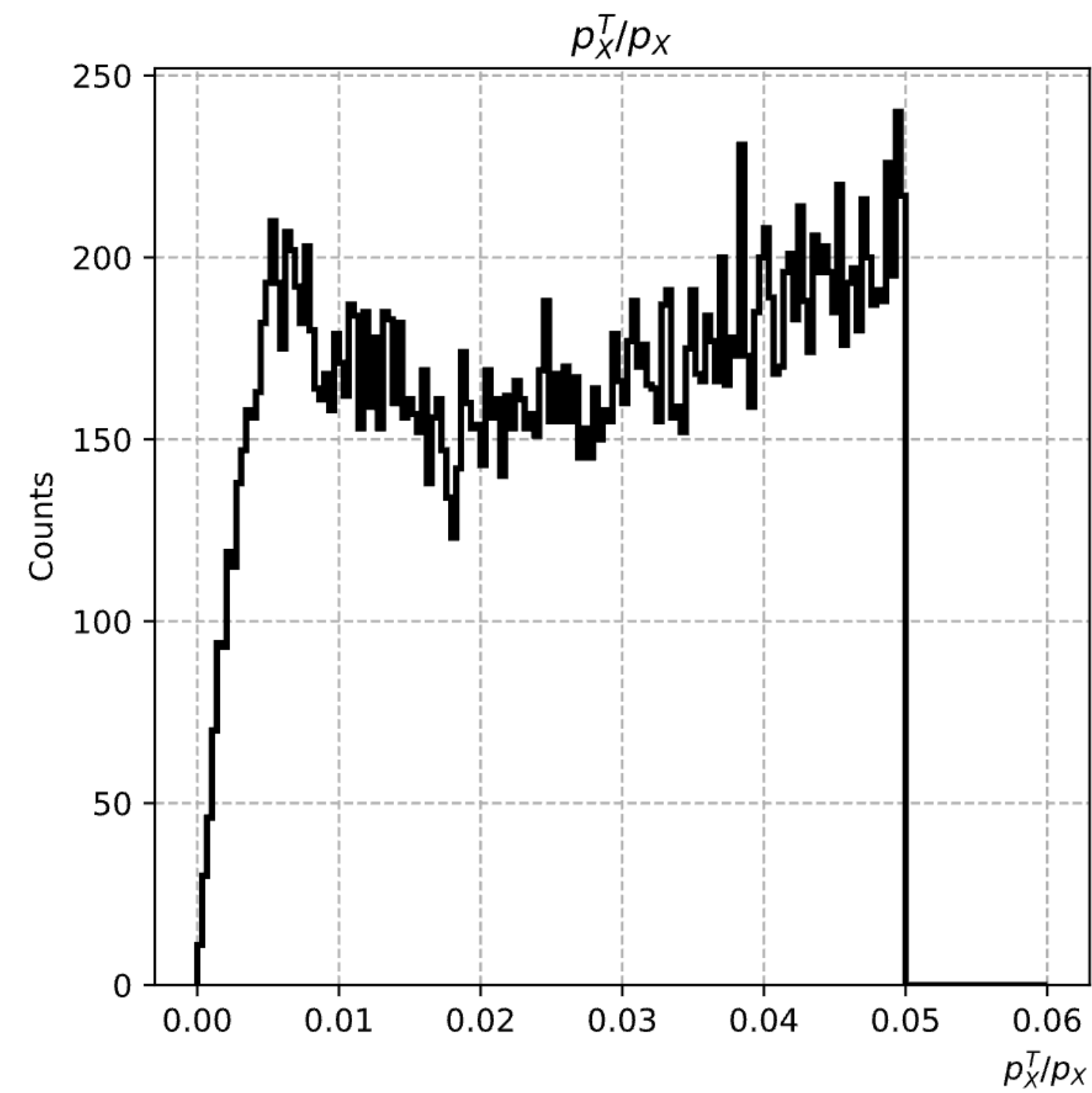
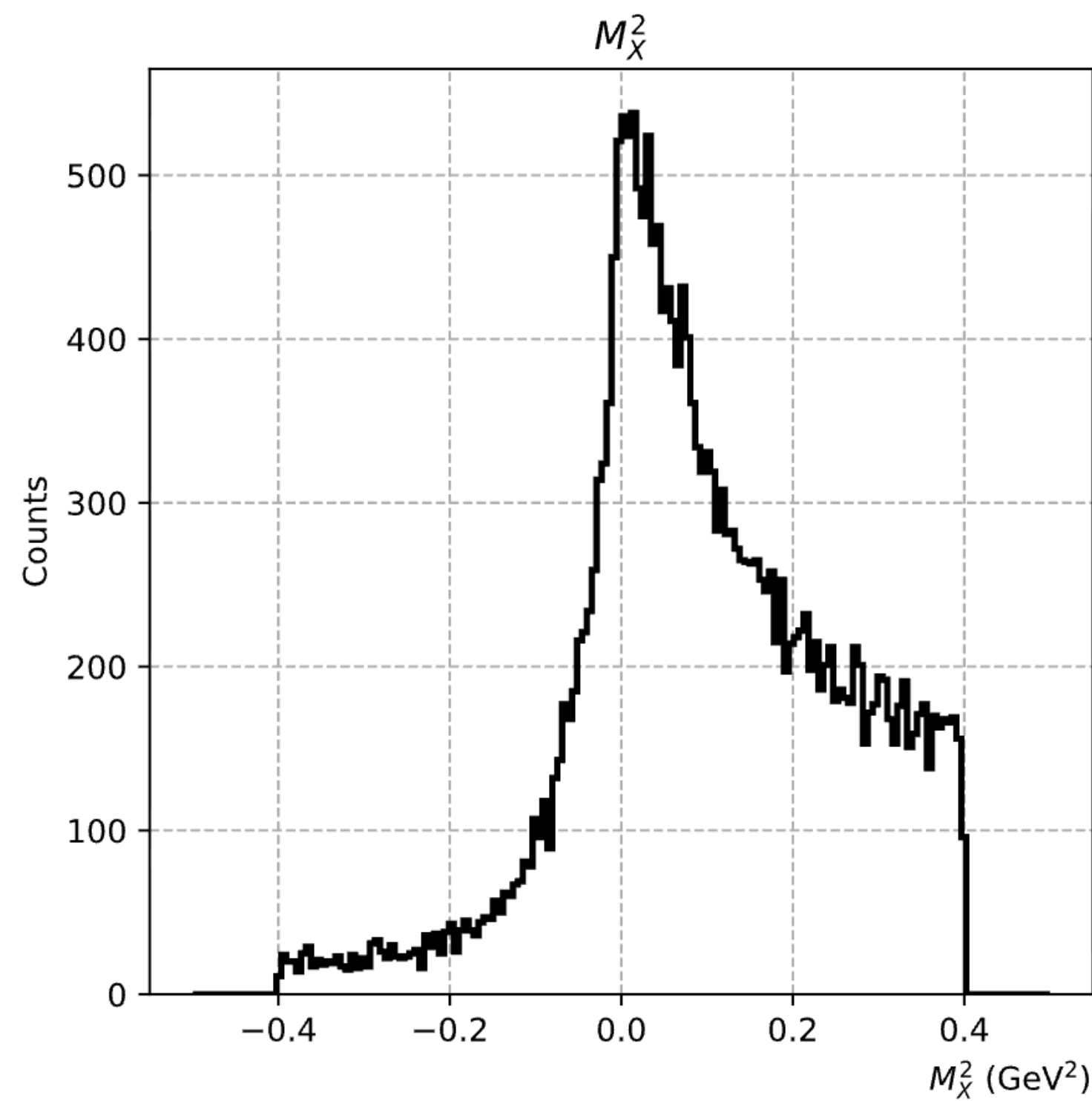
Kinematic Distributions After Cuts – COM ϕ and θ Distributions



Distribution of ϕ varies depending on if data is inbending or outbending, see Fa18 examples.

Kinematic Distributions After Cuts — Exclusivity Distributions

Additional cuts remove a lot of the background previously seen in the exclusivity distributions.



Calculating (quasi) real photon polarization

- *Photon polarization*, $P = SL$, where S is the *beam electron helicity* (± 1) and L is the *polarization transfer function*
- Define *polarization transfer function*

$$L = k\{(E_1 + E_2)(3 + 2\Gamma) - 2E_2(1 + 4u^2\xi^2\Gamma)\}/I_0$$
 - $E_1 \rightarrow$ beam electron energy
 - $E_2 \rightarrow$ scattered (missing) electron energy
 - $k = E_1 - E_2 \rightarrow$ (quasi) real photon energy
- $I_0 = \{(E_1^2 + E_2^2)(3 + 2\Gamma) - 2E_1E_2(1 + 4u^2\xi^2\Gamma)\}$
- $\xi = 1/(1 + u^2)$ (not ξ of GPDs)
- $u = E_1 \sin \theta_\gamma$
- Define *Coulomb screening factor*

$$\Gamma = \mathcal{F}(\delta/\xi) - \ln \delta - 2 - f(a)$$
 - $\delta = k/2E_1E_2$
- Define the *screening effects function*

$$\mathcal{F}(\delta/\xi) = -\frac{1}{2} \sum_{i=1}^3 \alpha_i^2 \ln(1 + B_i) + \sum_{i,j=1;i \neq j}^3 \alpha_i \alpha_j \left[\frac{1 + B_j}{B_i - B_j} \ln(1 + B_i) + \frac{1}{2} \right]$$

with $\alpha_i = (0.1, 0.55, 0.35)$, $B_i = (\beta_i \xi / \delta)^2$,
 $\beta_i = (Z^{1/3}/121)b_i$, $b_i = (6.0, 1.2, 0.3)$

 - Also use notation $\Delta = (Z^{1/3}/121)(\xi/\delta)$
- Define the *Coulomb correction function*

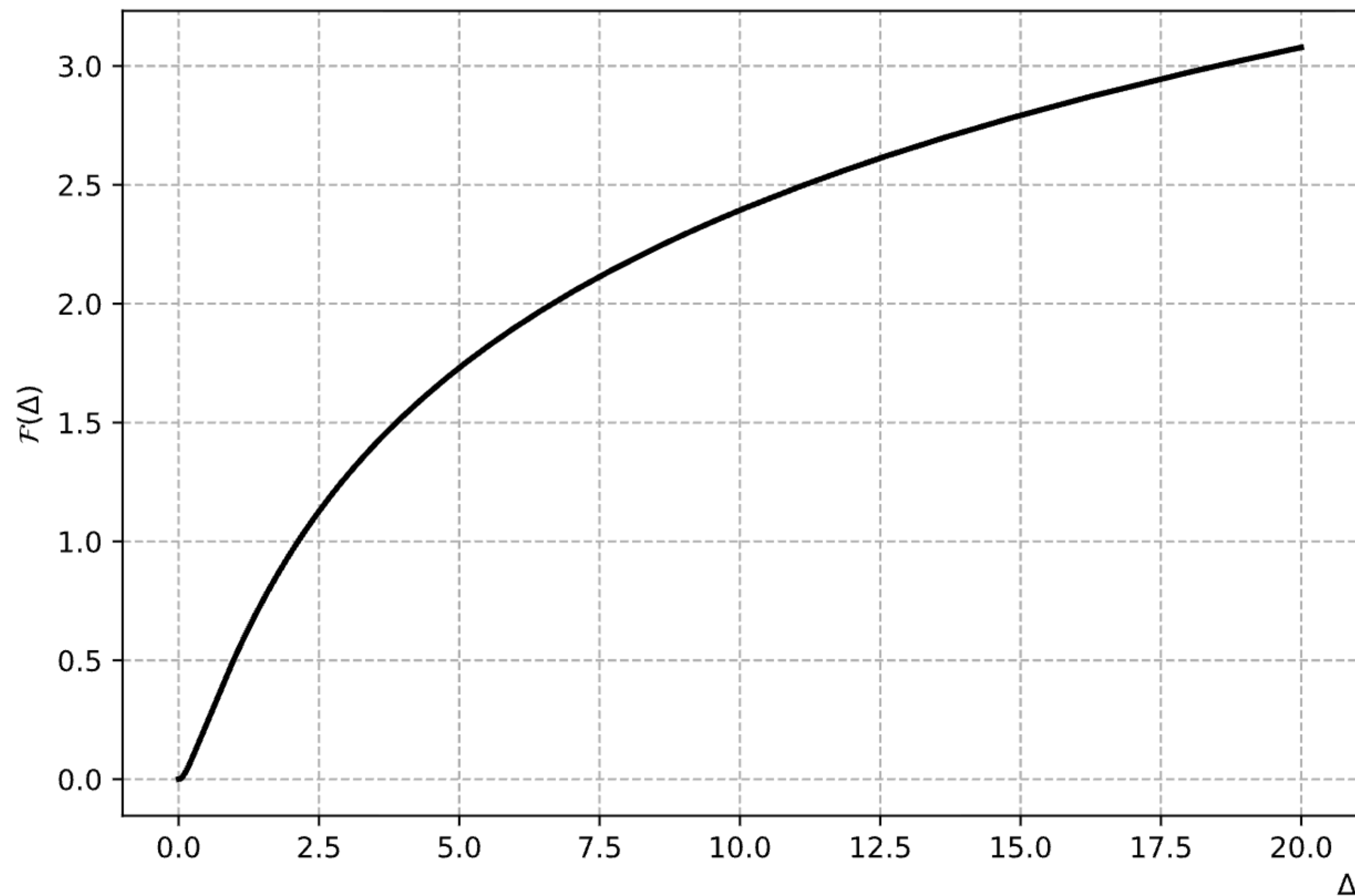
$$f(a) = a^2 \sum_{n=1}^{\infty} \frac{1}{n(n^2 + a^2)}$$

with $a = \alpha Z$ where Z is the number of protons in target material

Screening effect and Coulomb correction functions

Screening effect function

$$\mathcal{F}(\delta/\xi) = -\frac{1}{2} \sum_{i=1}^3 \alpha_i^2 \ln(1 + B_i) + \sum_{i,j=1;i \neq j}^3 \alpha_i \alpha_j \left[\frac{1 + B_j}{B_i - B_j} \ln(1 + B_i) + \frac{1}{2} \right]$$

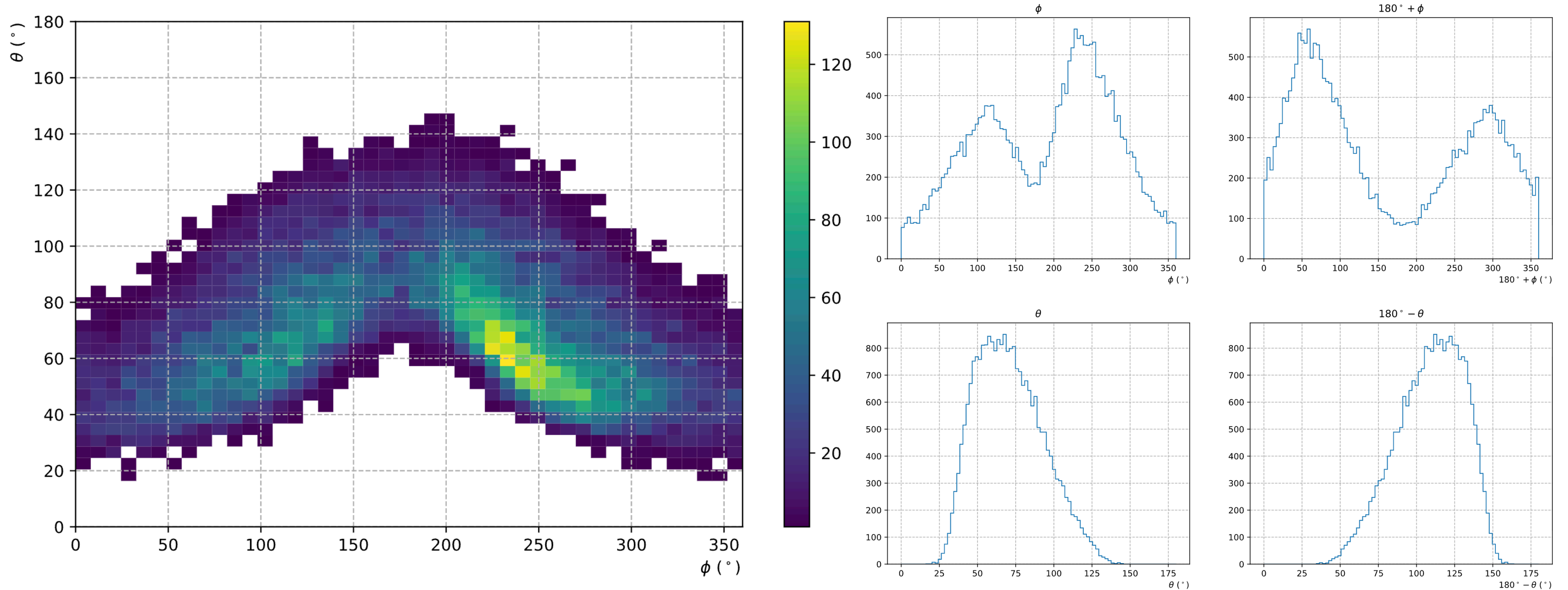


Coulomb correction function

$$f(a) = a^2 \sum_{n=1}^{\infty} \frac{1}{n(n^2 + a^2)}, \quad a = \alpha Z$$



Differences in RG-K ϕ , θ distributions



- Regions for forward and backward bin choices of inbending configuration are lower statistics using the RG-K outbending configuration data → new choices of forward and backward bins may be required
- As well, note that the distribution of ϕ versus $180^\circ + \phi$ flips for inbending versus outbending, which affects the direction of the asymmetry